THE UNIVERSITY OF ALBERTA

STRESS ANALYSIS OF ANISOTROPIC LINEARLY ELASTIC AXISYMMETRIC BODIES

by

Ⓒ PETER G. SMITH

A THESIS

SUBMITTED TO THE FACULTY OF GRADUATE STUDIES AND RESEARCH

IN PARTIAL FULFILMENT OF THE REQUIREMENTS FOR THE DEGREE

OF MASTER OF SCIENCE

DEPARTMENT OF MECHANICAL ENGINEERING

EDMONTON, ALBERTA

Spring, 1974

ABSTRACT

A finite element program utilizing an axisymmetric eight degree of freedom isoparametric quadrilateral element capable of handling both isotropic and anisotropic (assuming similar properties in tension and compression) materials was developed. The problem of a thick walled open ended cylinder subjected to internal pressure was analysed and the finite element solutions were compared to the exact analytical solutions to show convergence to the correct answer and to give an indication of the order of magnitude of errors which might be expected in other problems to which no exact solutions are known. Several problems which could have significance in orthopedics and in prosthetic design were analysed, utilizing idealized bovine femur as a material, to give an indication of the potential value of finite element analysis in these areas.

ACKNOWLEDGMENTS

The author wishes to extend his appreciation to Dr. J.G. Lenard for his suggestions, guidance, and supervision of this thesis.

Thanks are extended to Dr. W.M. Rigal for providing an insight into some problems encountered in orthopedics and to Ms. Carol Reed for typing this thesis.

Thanks are due to my wife, Robin, for her patience and understanding during the development of this thesis.

TABLE OF CONTENTS

TABLE OF CONTENTS CONTINUED

LIST OF TABLES

LIST OF FIGURES

Figure Page

NOTATION

a	cylinder inner radius
b	cylinder outer radius
$[B]$	strain-displacement matrix
$[C]$	stress-strain constitutive matrix
$DET[J]$	determinant of the Jacobian matrix
e_r	percentage error in radial stress
e_θ	percentage error in hoop stress
E	Young's modulus
E_r	Young's modulus in the radial direction
E_θ	Young's modulus in the circumferential direction
E_z	Young's modulus in the axial direction
f	general internal element displacements
F	general equivalent nodal forces
q	general distributed external loading per unit area
G	shear modulus
G_{zr}	shear modulus in the zr plane
H	cylinder height
I	interference fit
$[J]$	Jacobian matrix
$[J_{C.T.}]$	conjugate transpose of the Jacobian matrix
$[K]$	structural stiffness matrix
$[K]^e$	element stiffness matrix
N	element shape functions
N_G	element geometric shape functions

N_u	element displacement shape functions
p	cylinder internal pressure
p_z	axial force per unit area
r	radial coordinate
R	external concentrated nodal forces
u	general radial displacement
$\tilde{u}$	element internal radial displacement
$\underline{u}$	element nodal radial displacement
$\tilde{v}$	element internal axial displacement
$\underline{v}$	element nodal axial displacement
w	general axial displacement
γ_{zr}	shear strain between the planes $z\theta$ and $r\theta$
δ	general nodal displacements
$\tilde{\varepsilon}$	element internal strains
ε_r	strain in radial direction
ε_θ	strain in tangential direction
ε_z	strain in axial direction
η	local element coordinate
θ	tangential direction coordinate
ν	Poissons' ratio
$\nu_{r\theta}$	Poissons' ratio between the radial and tangential strains
ν_{zr}	Poissons' ratio between the axial and radial strains
$\nu_{z\theta}$	Poissons' ratio between the axial and tangential strains
ξ	local element coordinate
σ_o	reference stress

σ_r	radial stress
$\sigma_{r_{F.E.}}$	radial stress predicted by finite element analysis
σ_{r_o}	theoretical radial stress
σ_θ	hoop stress
$\sigma_{\theta_{F.E.}}$	hoop stress predicted by finite element analysis
$\sigma_{\theta\ max}$	maximum hoop stress
σ_{θ_o}	theoretical hoop stress
$\sigma_{\theta_{ult}}$	ultimate bone strength in the tangential direction
σ_z	axial stress
τ_o	reference shearing stress
$\tau_{r\theta}$	shear stress on the radial plane acting in the tangential direction
τ_{rz}	shear stress on the radial plane acting in the axial direction
τ_{zr}	shear stress on the axial plane acting in the radial direction
$\tau_{z\theta}$	shear stress on the axial plane acting in the tangential direction
ϕ	shape factors relating internal element properties to nodal properties
ϕ_G	geometric shape factors
ϕ_u	displacement shape factors

CHAPTER I

INTRODUCTION

1.1 BROAD SCOPE OF THESIS

Prosthetic devices are used in orthopedics to help heal some bone fractures as well as to assist mobility when the bone's load carrying capacity is diminished through disease. There are basically two components involved in prosthesis design - the element to be inserted into or attached to the bone and the bone itself. Design problems of this kind have, in the past, been solved by ad hoc methods. Only recently have systematic studies been performed to delineate the problems encountered in prosthesis design. Some of these problems are: mechanical and medical behaviour of bone-metal interface; response of live bone to various mechanical loadings; healing characteristics of bones when the fracture surface is under stress; response of prosthesis to various loads; and loads on prosthesis during walking or running. This list is far from exhaustive. The general problem of prostheses design is considered in this thesis. After a review of literature the aims of this work are stated after which the specific problems are formulated.

1.2 REVIEW OF PERTINENT LITERATURE

The need for accurate determination of stresses and strains in anisotropic bodies, particularly in bones, is increasing with the development of new and better prosthetic devices.

The earliest mention of the mechanical significance of bone form was made by Galileo (1638), but its strength and other physical properties were not extensively studied until the latter half of the nineteenth century. Since then stress and strain in bones have been studied by considering sections of bones, recording stress-strain phenomena in models of bones, analysing stress-strain phenomena in intact bones, and by mathematical analysis. A good review of these works may be found in Evans' [1] book Stress and Strain in Bones.

Recently, finite element methods have been applied to the stress analysis of human intervertebral discs by H. Kraus et al [2]. The basic theory of the finite element method is developed by Zienkiewicz [3]. This, along with some reference to the fundamentals of anisotropic elasticity described by Hearman [4] and an isoparametric constant strain triangular element (F.E.C.S.T.) developed by Dr. D. Murray of the University of Alberta, was sufficient for the development of the axisymmetric isoparametric element used in this work. Zienkiewicz states [3], and Tong and Pian show [5] that this element formulation has the necessary requirements to converge to the correct solution.

The fundamental equations of elasticity may be found in numerous texts - see, for example Wang [6], and have been applied to the isotropic open ended cylinder problem. The anisotropic solutions were developed from these equations without the assumption of isotropy. Bird et al [7] experimentally determined

the Young's moduli for bovine femur cortical bone in the radial, tangential and axial directions and gave an indication of the range of Young's moduli which may be expected in bovine femur. McElhaney [8], among other results for the dynamic response of bone, gave Poisson's Ratio of bovine femur for various rates of strain in the axial direction. Other works, including those of Dempster and Coleman [9], Evans et al [10] and [11], Amtmann [12] and Lugassy [13], gave an insight as to the complexity of structure and composition of bones and therefore of the complexity necessarily involved in the study of their mechanical behaviour.

As Fung states [14]:

"New experiments which cover a wide range of extensions in different directions are needed in order to extend our knowledge of the stress-strain relationship for biological tissues".

It might also be added that methods of utilizing this knowledge, once obtained, must also be explored.

1.3 AIMS OF THESIS

The aims of this thesis were threefold. Firstly a finite element program was to be developed for determining displacements and stresses in isotropic and anisotropic axisymmetric, linearly elastic bodies under axisymmetric loadings. This program was then to be tested on a problem for which an exact solution exists to show convergence to the correct solution and to give an estimate of the errors which could be expected for problems for which no exact

solutions exist.

Secondly, although quite generally applicable, this method was to be applied to analyse stresses in idealized long bones due to the insertion and presence of prostheses and hence to show this method as a useful aid for future prothesis design.

Thirdly, further work necessary to give improved results and to obtain a better 'tool' with which to analyse stresses in bones (or other anisotropic bodies) and help design prosthetics was to be suggested.

1.4 DEFINITION OF THE PROBLEMS TREATED

Chapter II contains a description of the formulation of the finite element and the development of the stress-strain matrix [C]. In Chapter III the results and discussion for the test problem of thick walled open ended cylinders under internal pressure are presented. The assumptions used are stated and discussed in Chapter IV, and the results and discussion for bovine femur under various loadings are given. The loadings used are internal displacement due to the insertion of an interference fit rod, with and without a shearing traction applied by the rod, and axial force applied to bone with a flat and a hemispherical cap fixed on one end. Conclusions and suggestions for further research are given in Chapter V.

The basics of the finite element method are given in Appendix I. The governing equations and open ended cylinder solutions used for comparison in the test case are developed in Appendix II. The program used is described and given in Appendix III.

CHAPTER II

GOVERNING EQUATIONS AND ELEMENT FORMULATION

2.1 GOVERNING EQUATIONS OF TORSIONLESS AXISYMMETRIC ELASTICITY

The following equations define the elastic axisymmetric problem:

(i) Strain-displacement relations:

$$\varepsilon_r = \frac{\partial u}{\partial r}, \quad \varepsilon_\theta = \frac{u}{r}, \quad \varepsilon_z = \frac{\partial w}{\partial z}, \quad \gamma_{rz} = \frac{\partial u}{\partial z} + \frac{\partial w}{\partial r} \tag{2.1}$$

(ii) Equilibrium equations in terms of stresses:

$$\frac{\partial \sigma_r}{\partial r} + \frac{\partial \tau_{rz}}{\partial z} + \frac{\sigma_r - \sigma_\theta}{r} = 0 \tag{2.2}$$

$$\frac{\partial \tau_{rz}}{\partial r} + \frac{\partial \sigma_z}{\partial z} + \frac{\tau_{rz}}{r} = 0$$

(iii) The equilibrium equations in terms of displacements (Neuber-Papkovich) [21] have been expressed as:

$$\begin{gathered} \frac{\partial^2 u}{\partial r^2} + \frac{1}{r}\frac{\partial u}{\partial r} - \frac{u}{r^2} + \frac{1}{2(1-\nu)}\frac{\partial^2 w}{\partial r \partial z} + \frac{1-2\nu}{2(1-\nu)}\frac{\partial^2 u}{\partial z^2} = 0 \\ \frac{\partial^2 w}{\partial z^2} + \frac{1-2\nu}{2(1-\nu)}\left(\frac{\partial^2 w}{\partial r^2} + \frac{1}{r}\frac{\partial w}{\partial r}\right) + \frac{1}{2(1+\nu)}\left(\frac{\partial^2 u}{\partial r \partial z} + \frac{1}{r}\frac{\partial u}{\partial z}\right) = 0 \end{gathered} \tag{2.3}$$

(iv) Compatibility equation in terms of strain:

$$r\frac{\partial \varepsilon_\theta}{\partial r} + \varepsilon_\theta - \varepsilon_r = 0 \tag{2.4}$$

(v) Hooke's Law for anisotropy with the principal directions of anisotropy coinciding with the r, z, and θ directions:

$$\varepsilon_z = \frac{1}{E_z}\sigma_z - \frac{\nu_{zr}}{E_z}\sigma_r - \frac{\nu_{z\theta}}{E_z}\sigma_\theta$$

$$\varepsilon_r = -\frac{\nu_{zr}}{E_z}\sigma_z + \frac{1}{E_r}\sigma_r - \frac{\nu_{r\theta}}{E_r}\sigma_\theta$$

$$\varepsilon_\theta = -\frac{\nu_{z\theta}}{E_z}\sigma_z - \frac{\nu_{r\theta}}{E_r}\sigma_r + \frac{1}{E_\theta}\sigma_\theta \qquad (2.5)$$

$$\gamma_{zr} = \frac{2(1+\nu_{zr})}{E_z}\tau_{zr} = \frac{1}{G_{zr}}\tau_{zr}$$

Boundary conditions for the specific problems considered are given later.

The general solutions for displacements of points of an elastic body in the axisymmetric problem have the form:

$$u = 4(\nu - 1)\beta_\rho - \frac{\partial}{\partial\rho}(\rho\beta_\rho + z\beta_z + \beta_o)$$

$$\qquad (2.6)$$

$$w = 4(\nu - 1)\beta_z - \frac{\partial}{\partial z}(\rho\beta_\rho + z\beta_z + \beta_o)$$

where β_o, β_z and $\beta_\rho e^{i\phi}$ are harmonic functions, one of which may be set to zero without loss of generality, and ϕ is harmonic also.

Finding suitable harmonic functions which satisfy all boundary conditions of a particular problem is very difficult apart from some trivial cases, and therefore finding exact solutions is very difficult.

Because of the difficulty in obtaining exact solutions and of the inflexibility of resolving the equations for each set of

boundary conditions to be considered, a finite element method was chosen to obtain solutions to the problems to be investigated.

The exact solutions for the open ended cylinder under internal pressure are fairly easily worked out, and this is done in Appendix II.

2.2 FINITE ELEMENT FORMULATION

The problem of stress distribution in bodies of revolution is essentially two-dimensional. By symmetry, the two components of displacements in any plane section of the body define completely the state of strain and, therefore, the state of stress.

For the 8 degree of freedom quadrilateral element, with nodes $i = 1, \ldots, 4$ number in the anti-clockwise sense, a local coordinate system (ξ,η) was chosen (see Figure 1).

The general internal displacements $\tilde{u}$ and $\tilde{v}$ are related to the nodal displacements $\underline{u}$ and $\underline{v}$ by:

$$\{\tilde{u}\} = \{\phi\}_u^T \{\underline{u}\}$$

$$\{\tilde{v}\} = \{\phi\}_u^T \{\underline{v}\}$$

where { } designates a vector.

Therefore:

$$\left\{\begin{matrix}\tilde{u}\\ \tilde{v}\end{matrix}\right\} = \begin{bmatrix}\{\phi\}_u^T & \{0\}^T \\ \{0\}^T & \{\phi\}_u^T\end{bmatrix} \left\{\begin{matrix}\underline{u}\\ \underline{v}\end{matrix}\right\} = [N_u]\left\{\begin{matrix}\underline{u}\\ \underline{v}\end{matrix}\right\} \qquad (2.7)$$

where $[N_u]$ is the matrix of displacement coefficients.

The general internal positions $\tilde{r}$ and $\tilde{z}$ are related to the nodal positions $\underline{r}$ and $\underline{z}$ by:

$$\{\tilde{r}\} = \{\phi\}_G^T \{\underline{r}\}$$

$$\{\tilde{z}\} = \{\phi\}_G^T \{\underline{z}\}$$

or $$\left\{\begin{matrix}\tilde{r}\\ \tilde{z}\end{matrix}\right\} = \begin{bmatrix} \{\phi\}_G^T & \{0\}^T \\ \{0\}^T & \{\phi\}_G^T \end{bmatrix} \left\{\begin{matrix}\underline{r}\\ \underline{z}\end{matrix}\right\} = [N_G] \left\{\begin{matrix}\underline{u}\\ \underline{v}\end{matrix}\right\} \qquad (2.8)$$

where $[N_G]$ is the matrix of geometric coefficients. For an isoparametric element such as this:

$$\{\phi\}_u = \{\phi\}_G = \{\phi\}$$

$$\text{or} \qquad [N_u] = [N_G] = [N] \;. \qquad (2.9)$$

For this element it can be shown that

$$\phi_i = 1/4(1 + \xi_o)(1 + \eta_o) \quad i = 1, .., 4 \qquad (2.10)$$

where $\xi_o = \xi\, \xi_i$

$\eta_o = \eta\, \eta_i$

and ξ_i and η_i are values of ξ and η at node i.

The strain vector defined below lists all non-zero strain components possible in an axi-symmetric deformation and defines them in terms of the displacements of a point.

$$\{\tilde{\varepsilon}\} = \left\{\begin{matrix}\varepsilon_z\\ \varepsilon_r\\ \varepsilon_\theta\\ \gamma_{rz}\end{matrix}\right\} = \begin{bmatrix} \partial\tilde{v}/\partial z \\ \partial\tilde{u}/\partial r \\ \tilde{u}/\tilde{r} \\ \partial\tilde{u}/\partial z + \partial\tilde{v}/\partial r \end{bmatrix} = \begin{bmatrix} 00010 \\ 10000 \\ 00001 \\ 01100 \end{bmatrix} \left\{\begin{matrix}\partial\tilde{u}/\partial r\\ \partial\tilde{u}/\partial z\\ \partial\tilde{v}/\partial r\\ \partial\tilde{v}/\partial z\\ \tilde{u}/\tilde{r}\end{matrix}\right\} \qquad (2.11)$$

now:

$$\begin{Bmatrix} \partial\tilde{u}/\partial\xi \\ \partial\tilde{u}/\partial\eta \end{Bmatrix} = \begin{bmatrix} \{\partial\tilde{r}/\partial\xi\} & \{\partial\tilde{z}/\partial\xi\} \\ \{\partial\tilde{r}/\partial\eta\} & \{\partial\tilde{z}/\partial\eta\} \end{bmatrix} \begin{Bmatrix} \partial\tilde{u}/\partial r \\ \partial\tilde{u}/\partial z \end{Bmatrix}$$

$$= [J]\begin{Bmatrix} \tilde{u},_r \\ \tilde{u},_z \end{Bmatrix} \qquad (2.12)$$

where [J] is the Jacobian and the comma indicates differentiation,

and $$\begin{Bmatrix} \tilde{u},_r \\ \tilde{u},_z \end{Bmatrix} = [J]^{-1} \begin{Bmatrix} \tilde{u},_\xi \\ \tilde{u},_\eta \end{Bmatrix} \qquad (2.13)$$

Similarly

$$\begin{Bmatrix} \tilde{v},_r \\ \tilde{v},_z \end{Bmatrix} = [J]^{-1} \begin{Bmatrix} \tilde{v},_\xi \\ \tilde{v},_\eta \end{Bmatrix} . \qquad (2.14)$$

where $$[J]^{-1} = \frac{1}{\mathrm{DET}[J]} \begin{bmatrix} \partial\tilde{z}/\partial\eta & -\partial\tilde{z}/\partial\xi \\ -\partial\tilde{r}/\partial\eta & \partial\tilde{r}/\partial\xi \end{bmatrix}$$

$$= \frac{1}{\mathrm{DET}[J]} \begin{bmatrix} \{\phi,_\eta\}^T \{\underline{z}\} & -\{\phi,_\xi\}^T \{\underline{z}\} \\ -\{\phi,_\eta\}^T \{\underline{r}\} & \{\phi,_\xi\}^T \{\underline{r}\} \end{bmatrix} = \frac{1}{\mathrm{DET}[J]} [J_{C.T.}] \qquad (2.15)$$

and: $$\mathrm{DET}[J] = \{\underline{r}\}^T[\{\phi,_\xi\}\{\phi,_\eta\}^T - \{\phi,_\eta\}\{\phi,_\xi\}^T]\{\underline{z}\} . \qquad (2.16)$$

Also: $$\begin{Bmatrix} \tilde{u},_\xi \\ \tilde{u},_\eta \\ \tilde{v},_\xi \\ \tilde{v},_\eta \\ \tilde{u}/\tilde{r} \end{Bmatrix} = \begin{bmatrix} \{\phi,_\xi\}^T & \{0\}^T \\ \{\phi,_\eta\}^T & \{0\}^T \\ \{0\}^T & \{\phi,_\xi\}^T \\ \{0\}^T & \{\phi,_\eta\}^T \\ \dfrac{\{\phi\}^T}{\{\phi\}^T\{\underline{r}\}} & \{0\}^T \end{bmatrix} \begin{Bmatrix} \underline{u} \\ \underline{v} \end{Bmatrix} . \qquad (2.17)$$

Note: $[J_{C.T.}]$ is the conjugate transpose of [J].

Therefore, substituting 2.13, 2.14, 2.16 and 2.17 into 2.11;

$$\{\tilde{\varepsilon}\} = \frac{1}{\mathrm{DET}[J]} \begin{bmatrix} 0 & 0 & 0 & 1 & 0 \\ 1 & 0 & 0 & 0 & 0 \\ 0 & 0 & 0 & 0 & 1 \\ 0 & 1 & 1 & 0 & 0 \end{bmatrix} \begin{bmatrix} [J_{C.T.}] & [0] & \{0\} \\ [0] & [J_{C.T.}] & \{0\} \\ \{0\}^T & \{0\}^T & \mathrm{DET}[J] \end{bmatrix}$$

$$\begin{bmatrix} \{\phi,_\xi\}^T & \{0\}^T \\ \{\phi,_\eta\}^T & \{0\}^T \\ \{0\}^T & \{\phi,_\xi\}^T \\ \{0\}^T & \{\phi,_\eta\}^T \\ \dfrac{\{\phi\}^T}{\{\phi\}^T\{\underline{r}\}} & \{0\}^T \end{bmatrix} \left\{\frac{\underline{u}}{\underline{v}}\right\} \qquad (2.18)$$

Multiplying this out:

$$\{\tilde{\varepsilon}\} = \frac{1}{\mathrm{DET}[J]} \begin{bmatrix} \{0\}^T & -\{\underline{r}\}^T[L] \\ \{\underline{z}\}^T[L] & \{0\}^T \\ \mathrm{DET}[J]\{\phi\}^T/\{\phi\}^T\{\underline{r}\} & \{0\}^T \\ -\{\underline{r}\}^T[L] & \{\underline{z}\}^T[L] \end{bmatrix} \left\{\frac{\underline{u}}{\underline{v}}\right\} \qquad (2.19)$$

where $[L] = [\{\phi,_\eta\}\{\phi,_\xi\}^T - \{\phi,_\xi\}\{\phi,_\eta\}^T]$.

$$\therefore \; \{\tilde{\varepsilon}\} = [B]\left\{\frac{\underline{u}}{\underline{v}}\right\}$$

where [B] is the element strain-displacement matrix. From the generalized Hooke's Law:

$$\begin{aligned} \varepsilon_q &= S_{qp}\sigma_p \quad (q,p = 1,\ 2,\ \ldots\ 6) \\ &\text{where } S_{qp} = 1/E_q \qquad (q = p) \\ &\qquad\qquad = -\nu_{pq}/E_p = -\nu_{qp}/E_q \quad (q \neq p) \end{aligned} \qquad (2.20)$$

Expanding 2.20 and noting that for cylindrical coordinates:

$$[\varepsilon_1,\varepsilon_2,\varepsilon_3,\varepsilon_4,\varepsilon_5,\varepsilon_6] = [\varepsilon_z,\varepsilon_r,\varepsilon_\theta,\gamma_{zr},\gamma_{z\theta},\gamma_{r\theta}]$$

and $[\sigma_1,\sigma_2,\sigma_3,\sigma_4,\sigma_5,\sigma_6] = [\sigma_z,\sigma_r,\sigma_\theta,\tau_{zr},\tau_{z\theta},\tau_{r\theta}]$

and also noting that for axial symmetry:

$$\gamma_{z\theta} = \gamma_{r\theta} = \tau_{z\theta} = \tau_{r\theta} = 0 \tag{2.22}$$

The expanded form of Hooke's Law is then:

$$\begin{aligned} \varepsilon_z &= (1/E_z)\sigma_z - (\nu_{zr}/E_z)\sigma_r - (\nu_{z\theta}/E_z)\sigma_\theta \\ \varepsilon_r &= -(\nu_{zr}/E_z)\sigma_z + (1/E_r)\sigma_r - (\nu_{r\theta}/E_r)\sigma_\theta \\ \varepsilon_\theta &= -(\nu_{z\theta}/E_z)\sigma_z - (\nu_{r\theta}/E_r)\sigma_r + (1/E_\theta)\sigma_\theta \\ \gamma_{zr} &= 2(1+\nu_{zr})\tau_{zr}/E_z = (1/G)\tau_{zr} \end{aligned} \tag{2.23}$$

where $G = G_{zr} = E_z/2(1 + \nu_{zr})$

or

$$\{\tilde{\varepsilon}\} = \begin{Bmatrix} \varepsilon_z \\ \varepsilon_r \\ \varepsilon_\theta \\ \gamma_{zr} \end{Bmatrix} = \begin{bmatrix} 1/E_z & -\nu_{zr}/E_z & -\nu_{z\theta}/E_z & 0 \\ -\nu_{zr}/E_z & 1/E_r & -\nu_{r\theta}/E_r & 0 \\ -\nu_{z\theta}/E_z & -\nu_{r\theta}/E_r & 1/E_\theta & 0 \\ 0 & 0 & 0 & 1/G \end{bmatrix} \begin{Bmatrix} \sigma_z \\ \sigma_r \\ \sigma_\theta \\ \tau_{rz} \end{Bmatrix} = [C]^{-1}\{\tilde{\sigma}\} . \tag{2.24}$$

Therefore $\{\tilde{\sigma}\} = [C]\{\tilde{\varepsilon}\}$ (2.25)

where [C], the constitutive matrix, can be found by inverting $[C]^{-1}$ to be:

$$[C] = \frac{1}{H}\begin{bmatrix} E_z\{1-\nu_{r\theta}^2(\frac{E_\theta}{E_r})\} & \nu_{rz}(E_r)+\nu_{r\theta}\nu_{z\theta}(E_\theta) & E_\theta(\nu_{zr}\nu_{r\theta}+\nu_{z\theta}) & 0 \\ & E_r\{1-\nu_{z\theta}^2(\frac{E_\theta}{E_r})\} & E_\theta\{\nu_{r\theta}+\nu_{zr}\nu_{z\theta}(\frac{E_r}{E_z})\} & 0 \\ \text{SYMMETRIC} & & E_\theta\{1-\nu_{zr}^2(\frac{E_r}{E_z})\} & 0 \\ & & & E_rE_\theta E_zG^2\text{DET}[C]^{-1} \end{bmatrix} \tag{2.26}$$

In equation (2.26), $H = \{1-\nu_{r\theta}^2(E_\theta/E_r) - \nu_{zr}^2(E_r/E_z) - \nu_{z\theta}^2(E_\theta/E_z)$

$$-2\nu_{zr}\nu_{z\theta}\nu_{r\theta}(E_\theta/E_z)\} \; .$$

For an isotropic material:

$$E_r = E_\theta = E_z = E$$

and $\nu_{r\theta} = \nu_{zr} = \nu_{z\theta} = \nu$

and $$[C]_{iso} = \frac{E}{H_{iso}}\begin{bmatrix} 1-\nu^2 & \nu(1+\nu) & \nu(1+\nu) & 0 \\ & 1-\nu^2 & \nu(1+\nu) & 0 \\ \text{SYMMETRIC} & & 1-\nu^2 & 0 \\ & & & E^2G^2\text{DET}[C]^{-1} \end{bmatrix} \tag{2.27}$$

where $H_{iso} = 1 - 3\nu^2 - 2\nu^3$.

The elemental stiffness matrix, noting that the volume integral must be taken over the whole ring of material, is:

$$[K]^e = 2\pi \iint [B]^T[C][B] \; r\,dr\,dz \tag{2.28}$$

which may be written as

$$[K]^e = 2\pi\iint [B]^T[C][B]r \, DET[J]d\xi d\eta \tag{2.29}$$

as $\quad drdz = DET[J]d\xi d\eta$.

As [B] and [J] depend on the coordinates, the Gaussian Quadrature for numerical integration

$$\int_{-1}^{1}\int_{-1}^{1} f(\xi,\eta)d\xi d\eta = \sum_{i=1}^{n}\sum_{j=1}^{n} H_i H_j f(\xi_i,\eta_i) \tag{2.30}$$

was used where for this case $n = 2$, $H_i = H_j = 1$ and ξ_i and η_i take values $\pm 1/\sqrt{3}$. For n sampling points a polynomial of degree $2n - 1$ can be constructed and exactly integrated [3], therefore in this case the integration is approximate.

The structural stiffness matrix [K] is obtained by the direct stiffness assembly of the elemental stiffness matrices ;

$$\text{i.e.:} \quad [K_{ij}] = \Sigma[K_{ij}]^e \tag{2.31}$$

where the contribution of each element to [K] must be evaluated individually (see reference [3].)

Nodal displacements $\{\frac{\underline{u}}{\underline{v}}\}$ are found by Gaussian elimination from

$$\{R\} = [K]\{\frac{\underline{u}}{\underline{v}}\} \tag{2.32}$$

after the modifying of [K] and {R} for displacement boundary conditions.

After the nodal displacements are found, stresses are computed for each element in turn from:

$$\{\sigma\} = [C][B]\{\frac{\underline{u}}{\underline{v}}\} \ . \tag{2.33}$$

CHAPTER III

TEST CASE

In order to show that the program developed in Chapter II gives reasonable results, and also to estimate the accuracy and convergence of the results, solutions were obtained by modeling open ended cylinders of various heights and internal to external radii ratios subjected to internal pressure and made of steel and bovine cortical bone. The properties of the isotropic steel cylinders used were E = 30,000 K.S.I. and $\nu = .3$. The properties of the bovine cortical bone are given in the discussion of assumptions in Chapter IV.

These particular problems were chosen as test cases because exact solutions to them are available for the isotropic [6], as well as anisotropic behaviour (developed in the appendix).

The finite element results for the principal stresses at the midplanes of these cylinders are plotted in nondimensional form in figures 2 to 19. These were all obtained using a 300 element grid (see Figure 1).

3.1 TEST CASE RESULTS

Figures 2, 3, and 4 are graphs of σ_r/p vs r/b for isotropic steel cylinders of H/a = .8, 4, and 16 respectively, each having plots for cylinders of a/b = .25, .5, .67, and .91. The solid lines plotted are exact open end cylinder solutions corresponding to the finite element solutions at nodal points along the cylinder midplanes. The agreement between the exact and finite element solutions can be seen qualitatively to be good, the average error in radial stress:

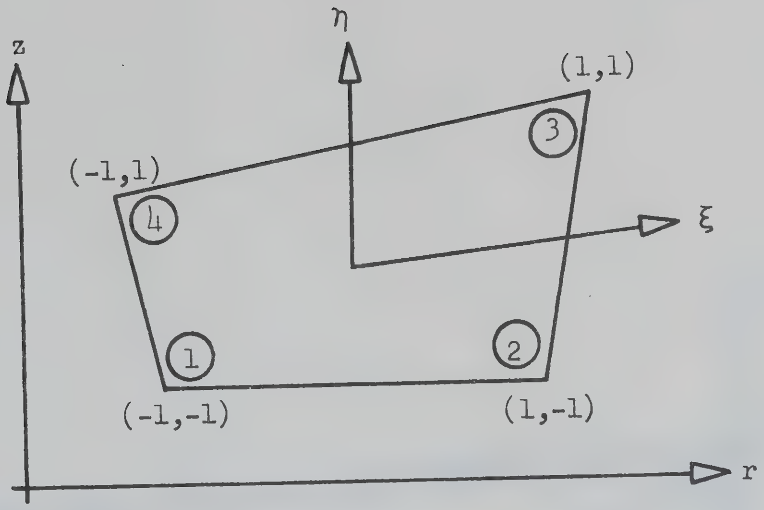

Figure 1.a Eight Degree of Freedom Quadrilateral Element Crosssection.

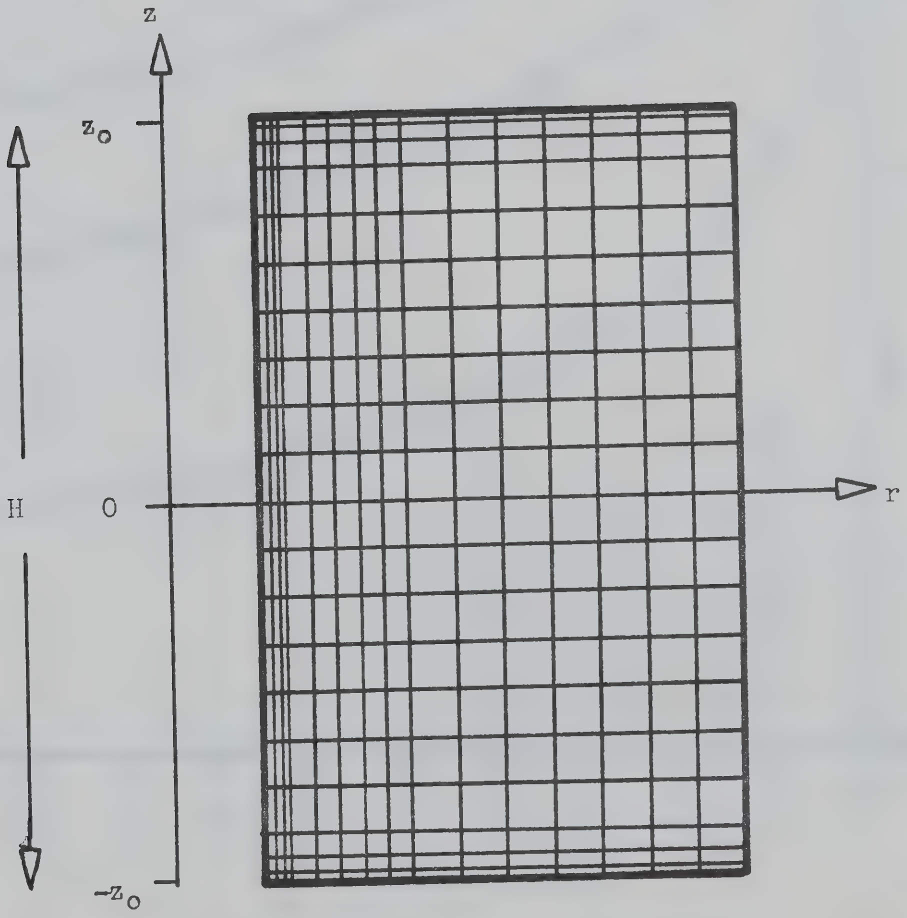

Figure 1.b Three Hundred Element Grid.

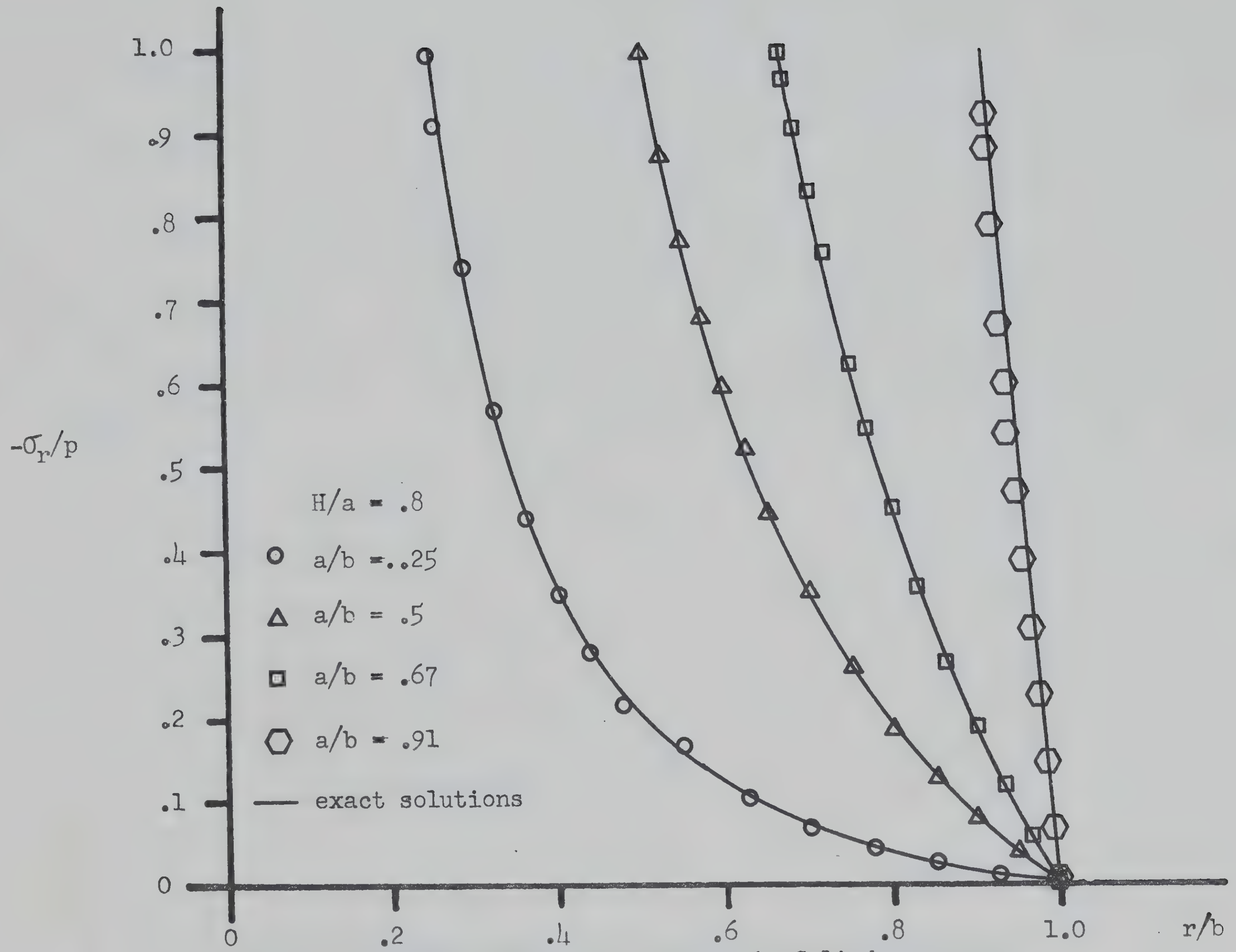

Figure 2. Midplane Radial Stress for Isotropic Cylinders.

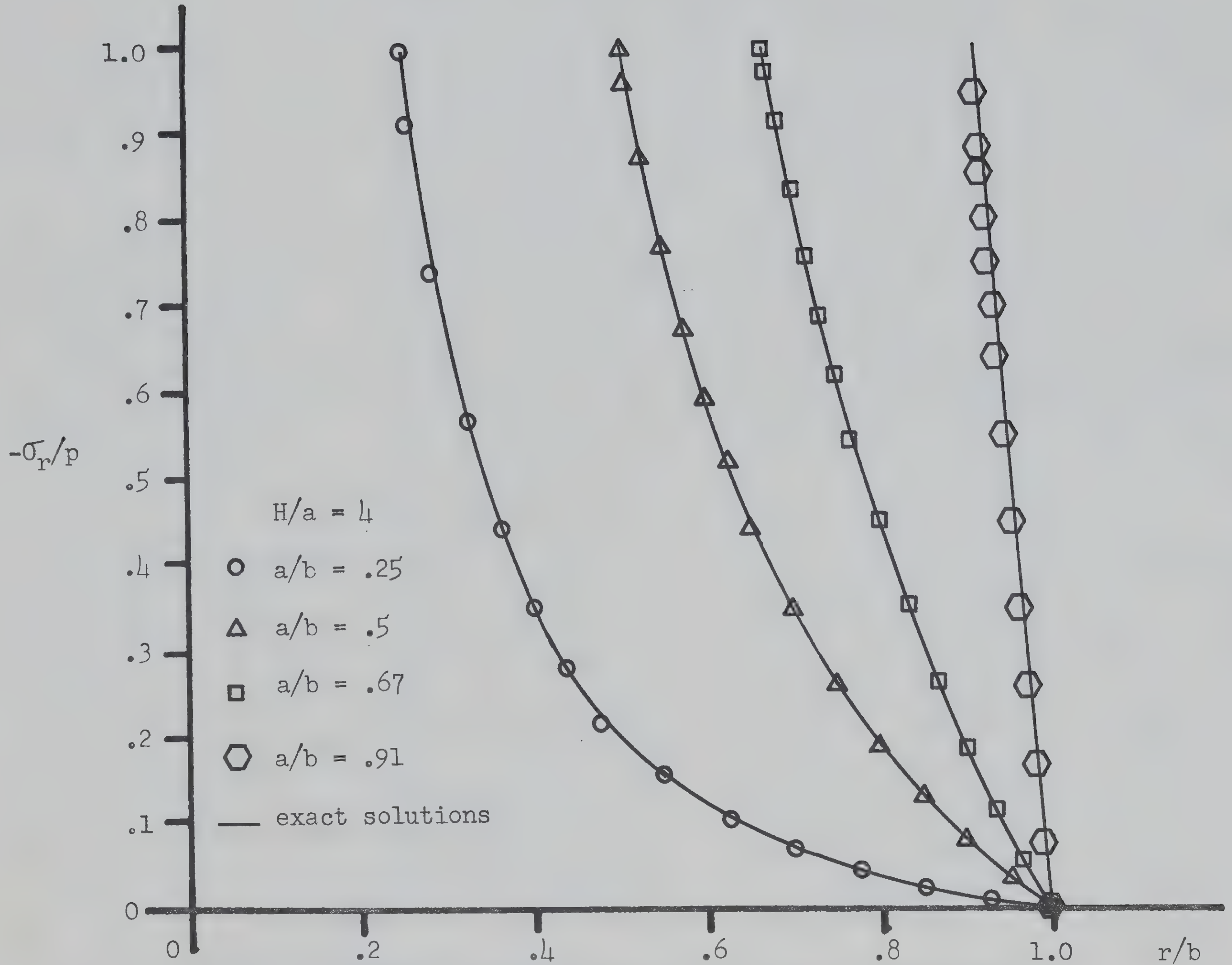

Figure 3. Midplane Radial Stress for Isotropic Cylinders.

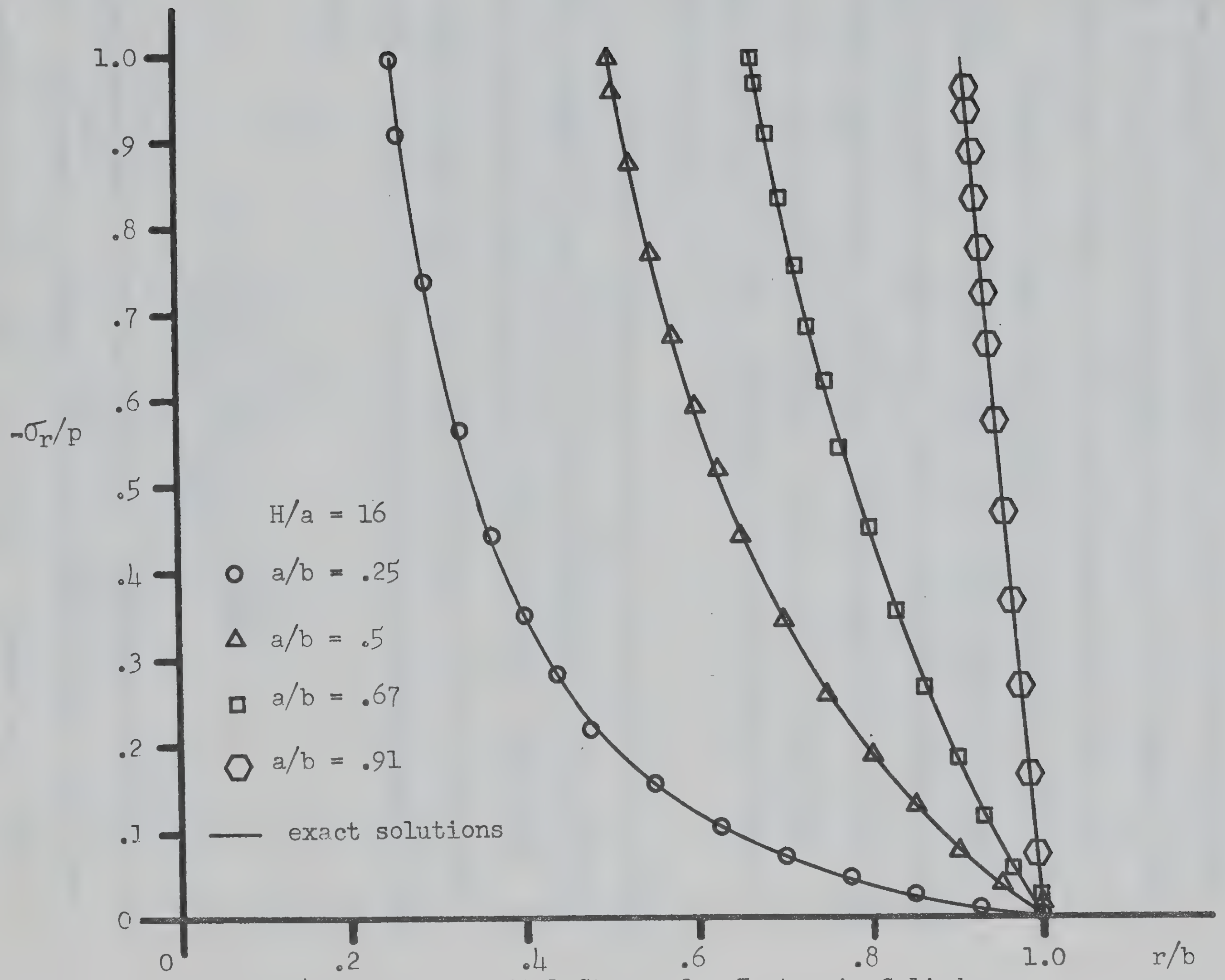

Figure 4. Midplane Radial Stress for Isotropic Cylinders.

$$e_r = \frac{|\sigma_{r_{FE}} - \sigma_{r_o}|}{\sigma_{r_o}\Big|_{r=a} - \sigma_{r_o}\Big|_{r=b}} \times 100\%$$

at the nodal points being approximately .5% for cylinders with a/b from .25 to .67. The average error for a/b = .91 is higher: 7.88%, 3.21% and 1.93% for H/a = .8, 4, and 16 respectively (see Table 1).

Figures 5, 6, and 7 are similar to 2, 3, and 4, with the cylinder material being bone. Here the average error is slightly larger than that in figures 2, 3, and 4, being approximately .6% for cylinders with a/b from .25 to .67. The average error for a/b = .91 is 2.52%, 1.04%, and 1.32% for H/a = .8, 4, and 16 respectively, higher than that for other a/b ratios, as was the error in these cases for steel.

Figures 8, 9, and 10 are graphs of σ_θ/p vs r/b for isotropic steel cylinders of H/a = .8, 4, and 16 respectively, the solid line plots again being exact open end cylinder solutions. Again the agreement between the finite element solutions and exact open end cylinder solutions can be seen to be good, the average error in hoop stress:

$$e_\theta = \frac{\sigma_{\theta_{FE}} - \sigma_{\theta_o}}{\sigma_{\theta_o}\Big|_{r=a} - \sigma_{\theta_o}\Big|_{r=b}} \times 100\%$$

being approximately 1.0% (see Table 2). Exceptions to this are for a/b = .91, where e_θ = 38.62%, 1.3% and 12.95% for H/a = .8, 4, and 16 respectively and for a/b = .67 and H/a = .8 where e_θ = 4.35%.

Table 1. Average Error in Midplane Radial Stress

MATERIAL	a/b	H/a		
		.8	4.	16.
Steel	.25	0.61%	0.59%	0.58%
Steel	.5	0.51%	0.50%	0.46%
Steel	.67	0.54%	0.46%	0.45%
Steel	.91	7.88%	3.21%	1.93%
Bone	.25	0.79%	0.71%	0.65%
Bone	.5	0.55%	0.41%	0.55%
Bone	.67	0.56%	0.61%	0.49%
Bone	.91	2.52%	1.04%	1.32%

Table 2. Average Error in Midplane Hoop Stress

MATERIAL	a/b	H/a		
		.8	4.	16.
Steel	.25	1.03%	0.91%	0.90%
Steel	.5	1.88%	1.28%	0.55%
Steel	.67	4.35%	0.59%	0.51%
Steel	.91	38.62%	1.30%	12.95%
Bone	.25	1.23%	1.03%	0.92%
Bone	.5	1.01%	1.21%	0.49%
Bone	.67	2.31%	2.93%	0.48%
Bone	.91	33.57%	1.79%	6.61%

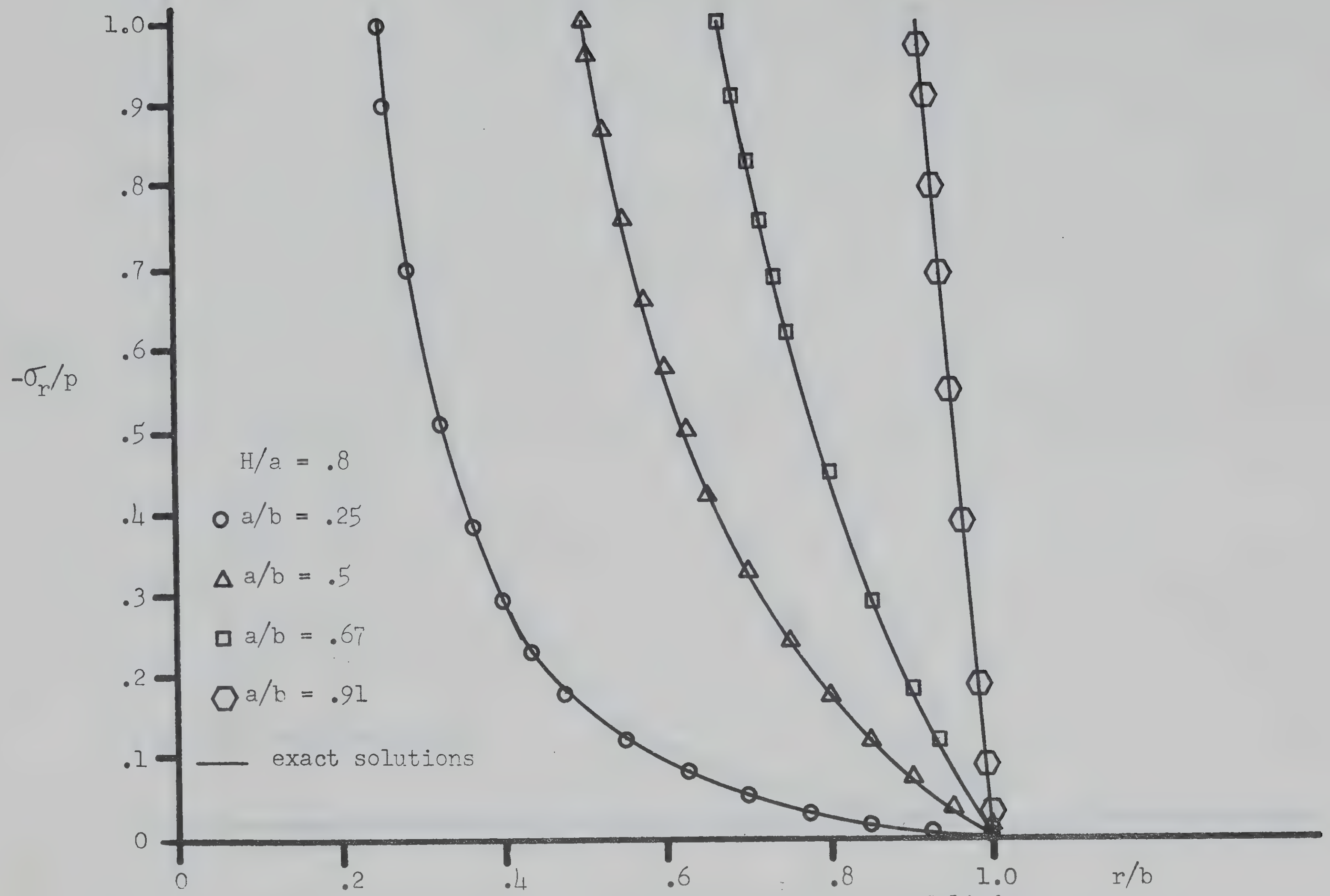

Figure 5. Midplane Radial Stress for Anisotropic Cylinders.

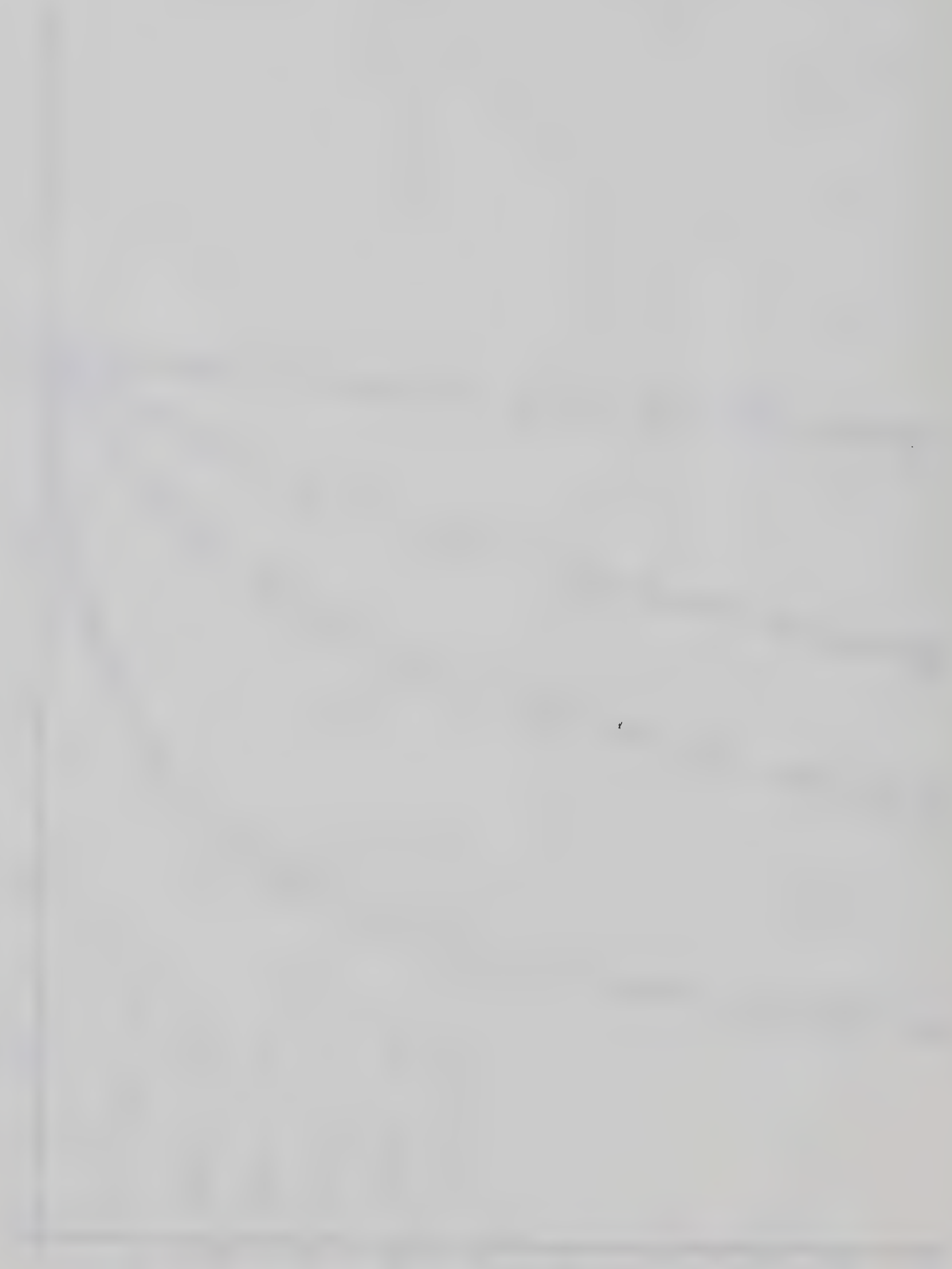

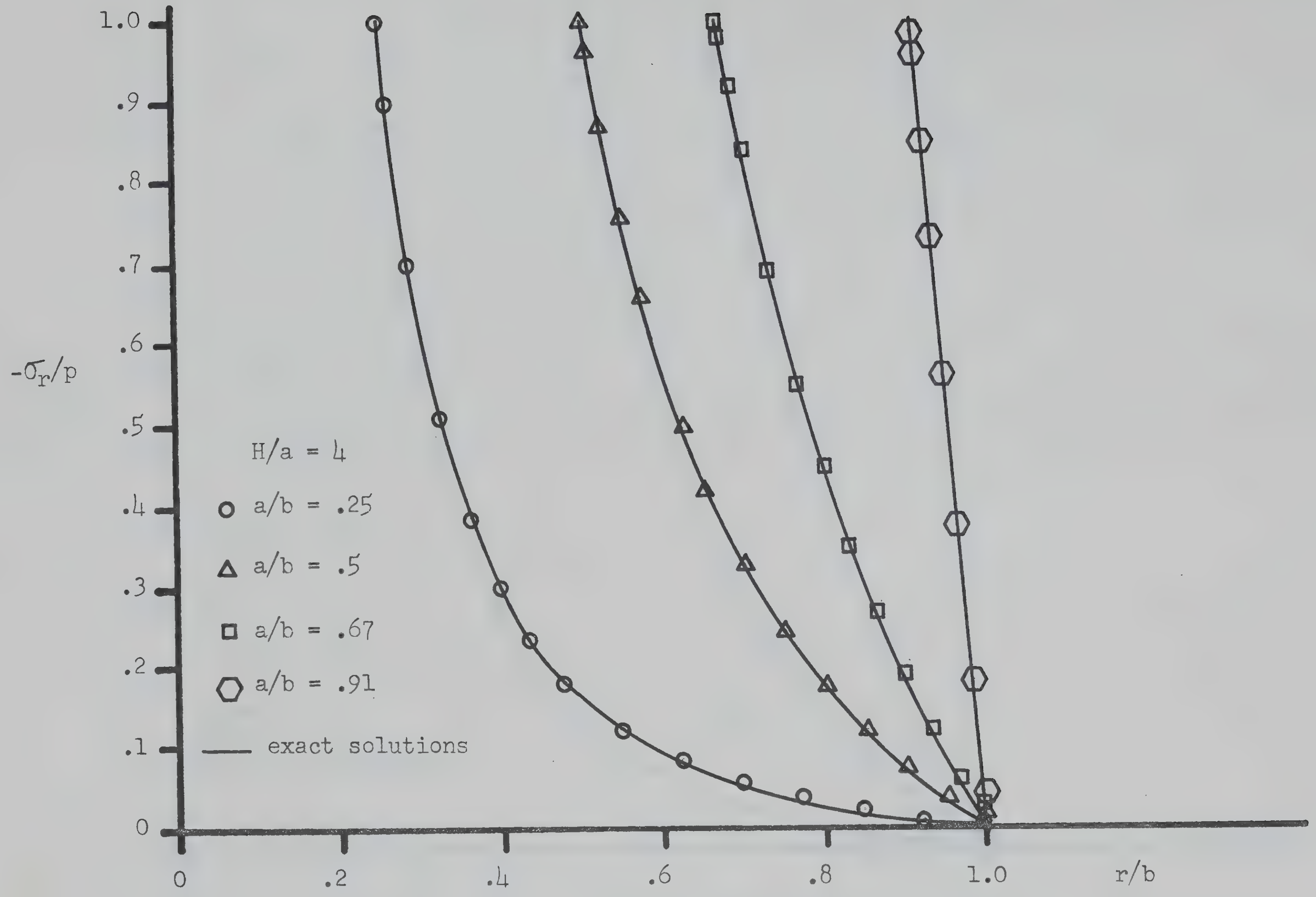

Figure 6. Midplane Radial Stress for Anisotropic Cylinders.

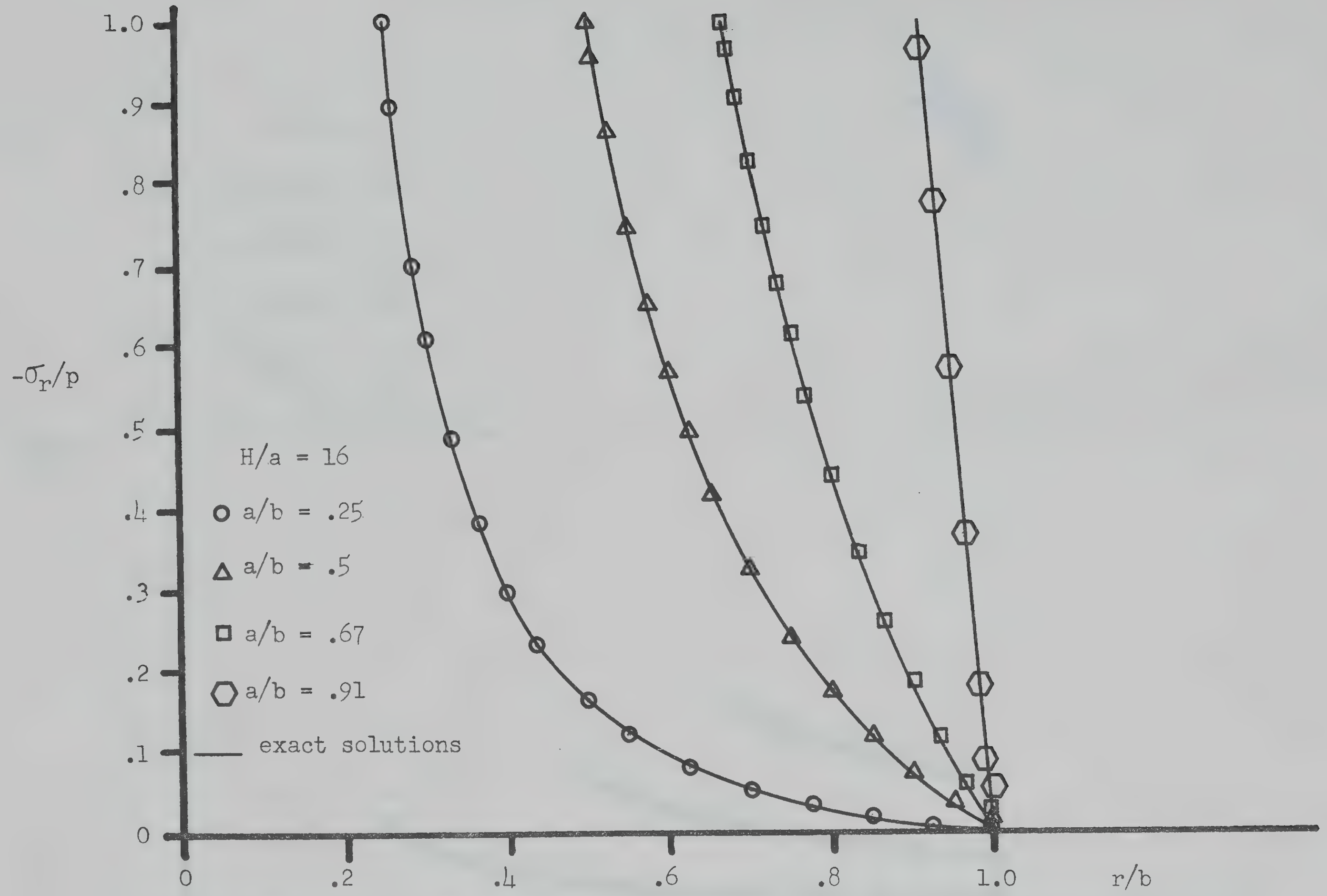

Figure 7. Midplane Radial Stress for Anisotropic Cylinders.

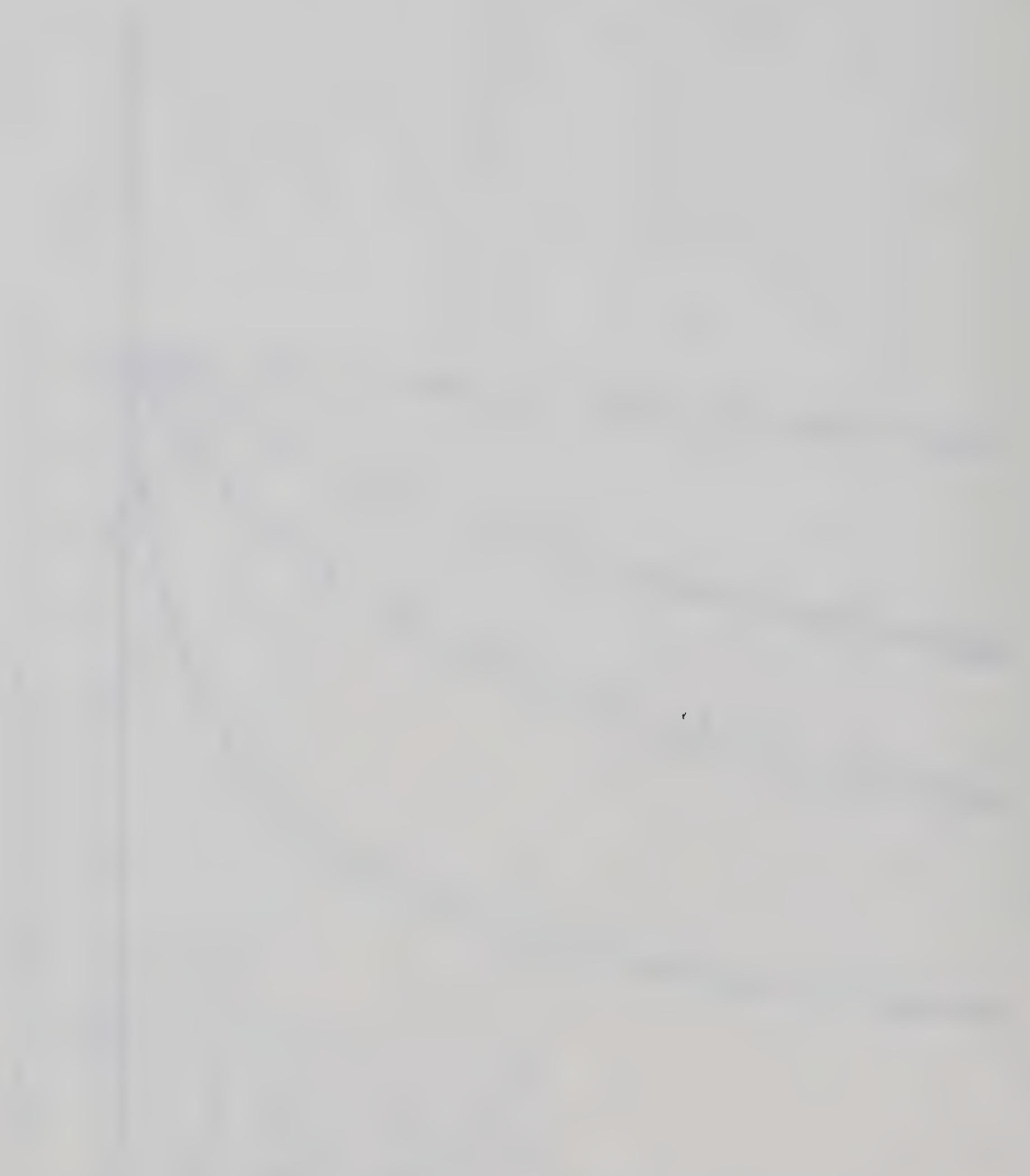

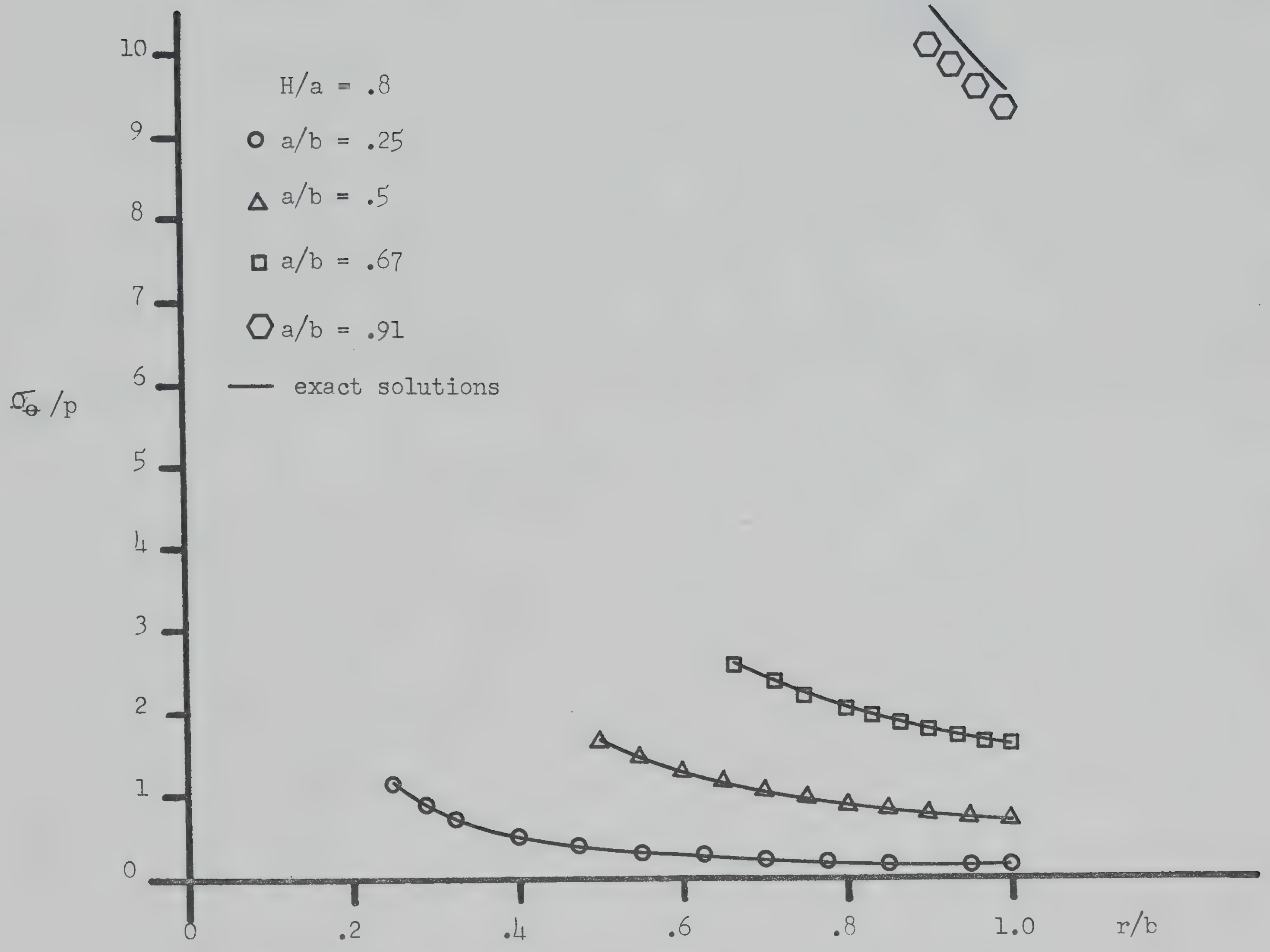

Figure 8. Midplane Hoop Stress for Isotropic Cylinders.

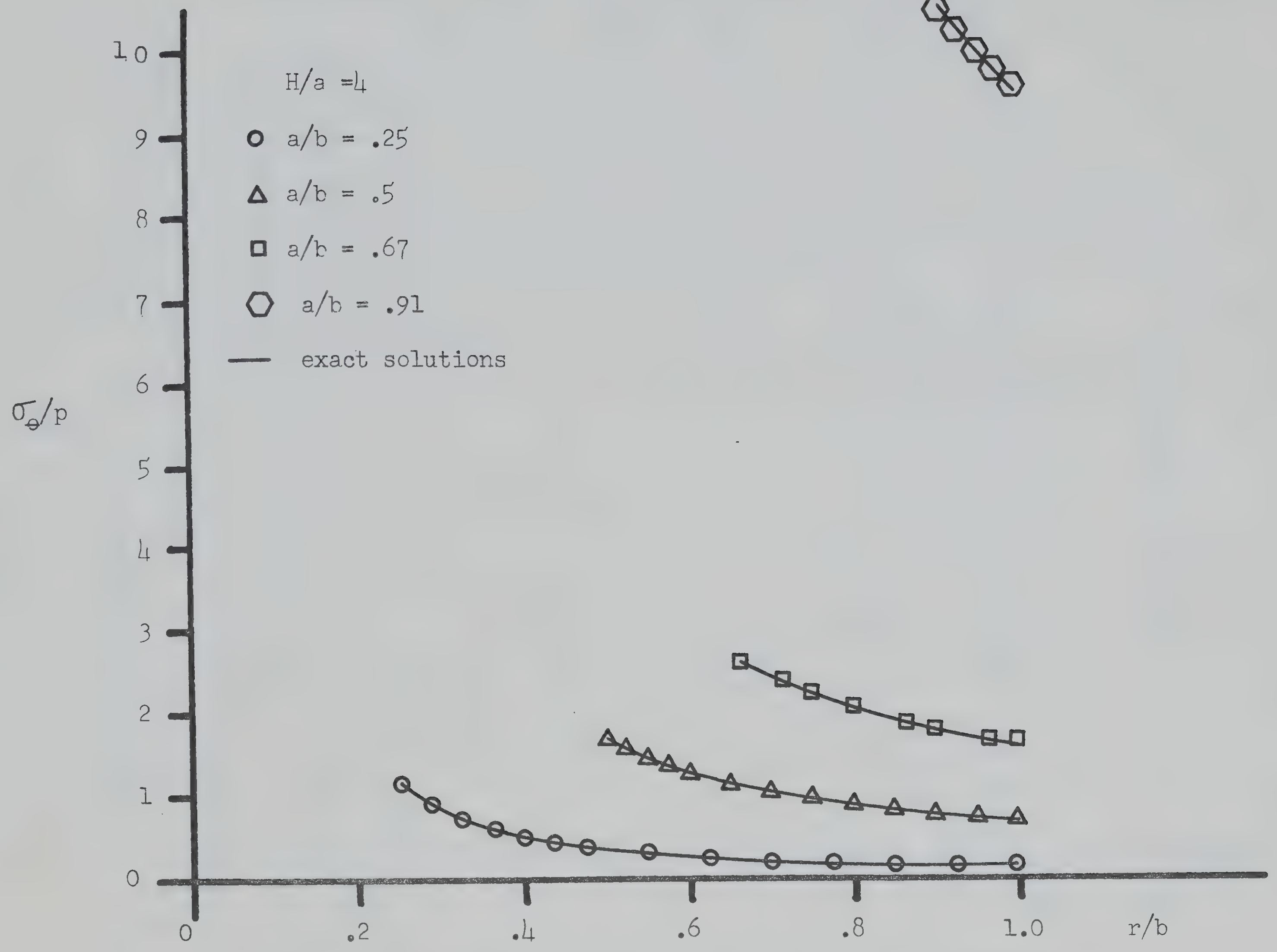

Figure 9. Midplane Hoop Stress for Isotropic Cylinders.

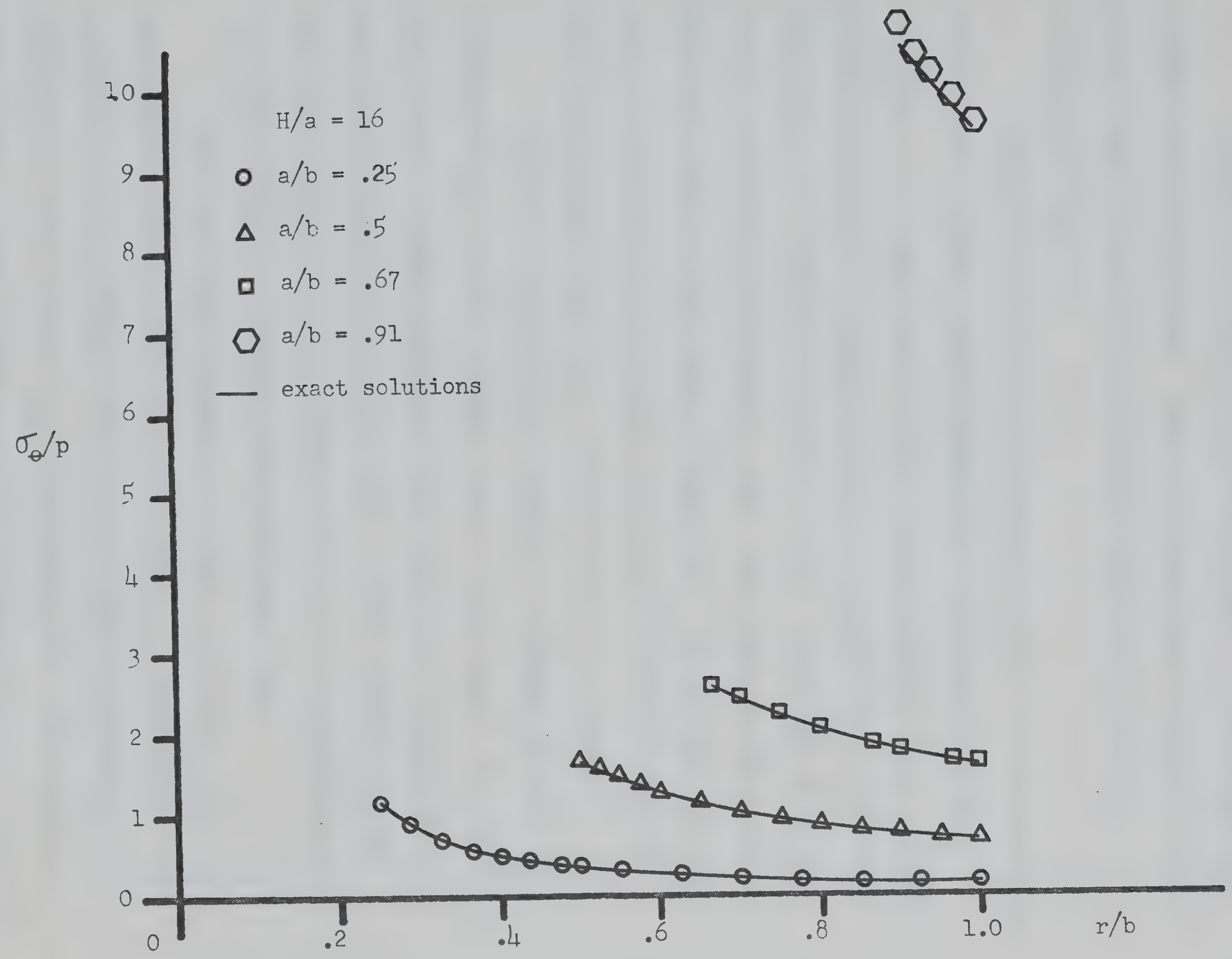

Figure 10. Midplane Hoop Stress for Isotropic Cylinders.

The reasons for these large errors are given in the following section.

Figures 11, 12, and 13 are similar to 8, 9, and 10 with the cylinder material being bone. Again the magnitude of errors for bone are very close to those for the corresponding cases with steel cylinders (see Table 2).

Figures 14, 15, and 16 are graphs of σ_z/p vs r/b for the same sets of steel cylinder geometry mentioned in reference to figures 2, 3, and 4. For open ended cylinders theory predicts that σ_z should be zero everywhere for loading by internal pressure only, therefore these graphs also indicate the error in σ_z/p. The errors in axial stress can be seen to be generally small when compared with p, and are largest close to the inner cylinder radii. As was the case with errors in radial and hoop stresses, the errors in axial stress are larger for cylinders with $a/b = .91$ than for other cylinders.

Figures 17, 18, and 19 are similar to figures 14, 15, and 16 respectively, with the cylinder material being bone. The errors in axial stress in these cases are of the same order of magnitude as those for corresponding cases for steel cylinders except near the inner radii where the errors, although still small are significantly larger than those in the corresponding isotropic cases.

For torsionless axisymmetry the shear stresses $\tau_{r\theta}$ and $\tau_{z\theta}$ are necessarily zero, and for the test cases τ_{rz} should also be zero everywhere in the cylinders [6]. In all cases the errors in nondimensional shear stresses τ_{rz}/p predicted by the finite element program were very small (several orders of magnitude smaller than the corresponding errors in σ_z/p) and were therefore not plotted.

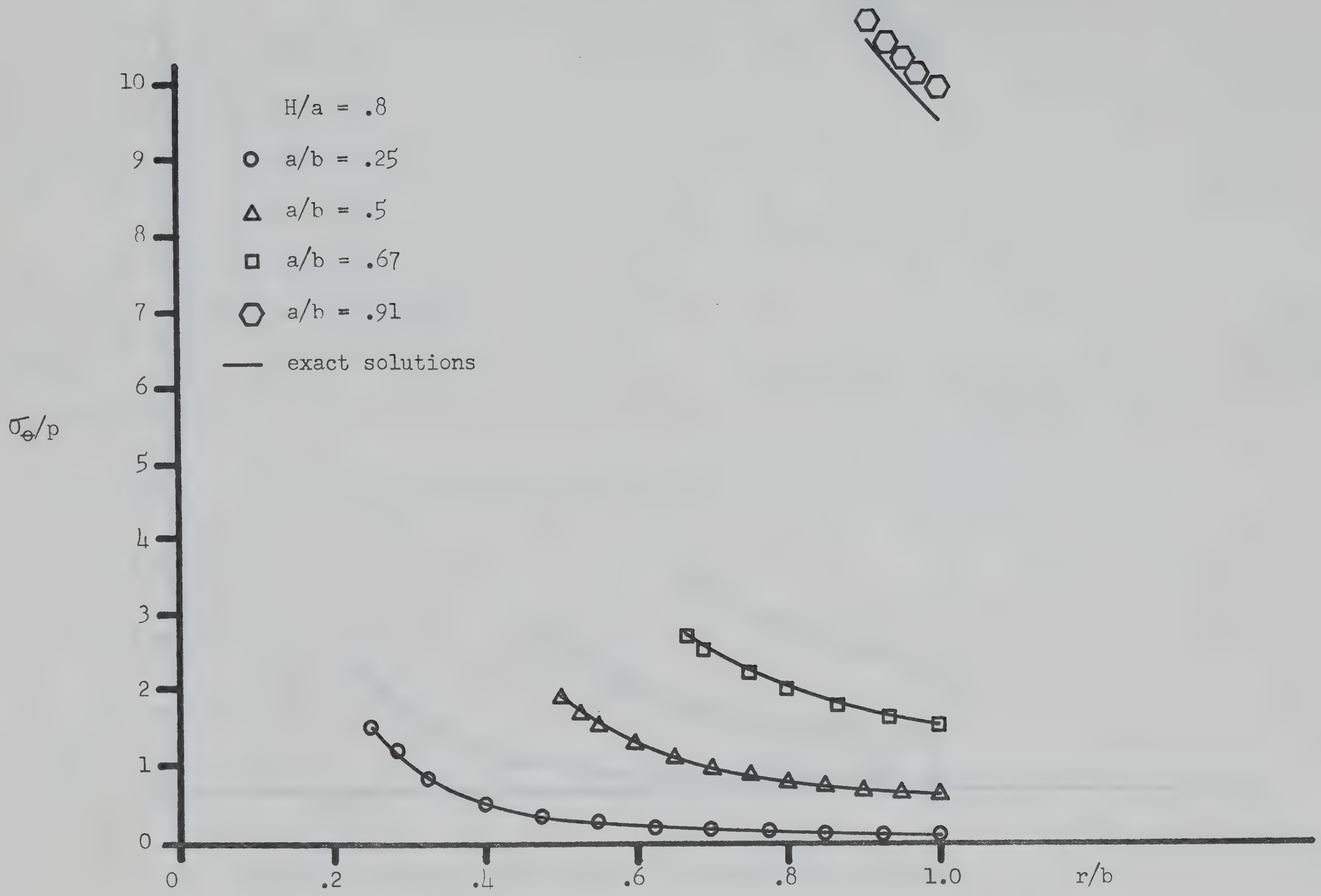

Figure 11. Midplane Hoop Stress for Anisotropic Cylinders.

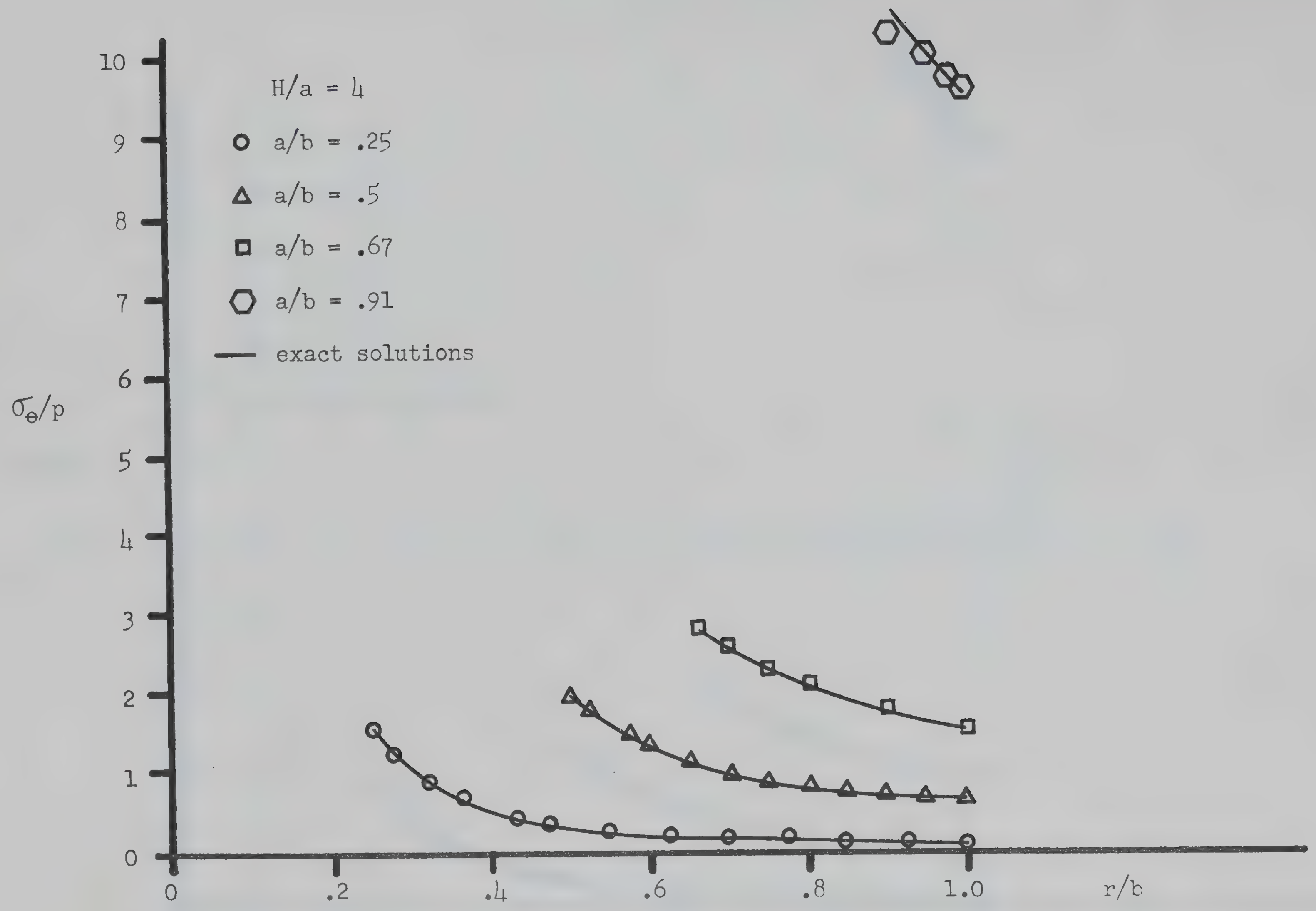

Figure 12. Midline Hoop Stress for Anisotropic Cylinders.

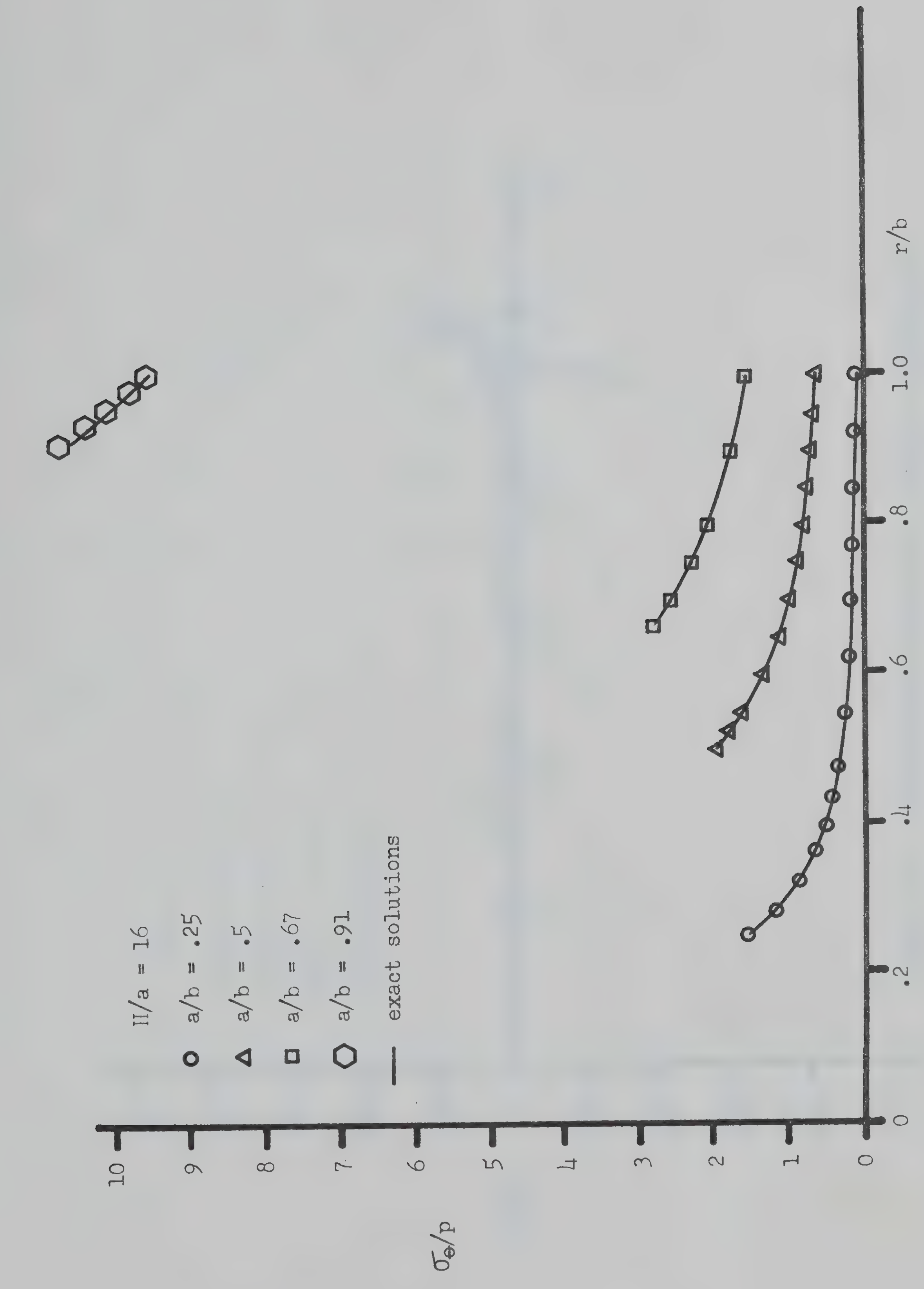

Figure 13. Midplane Hoop Stress for Anisotropic Cylinders.

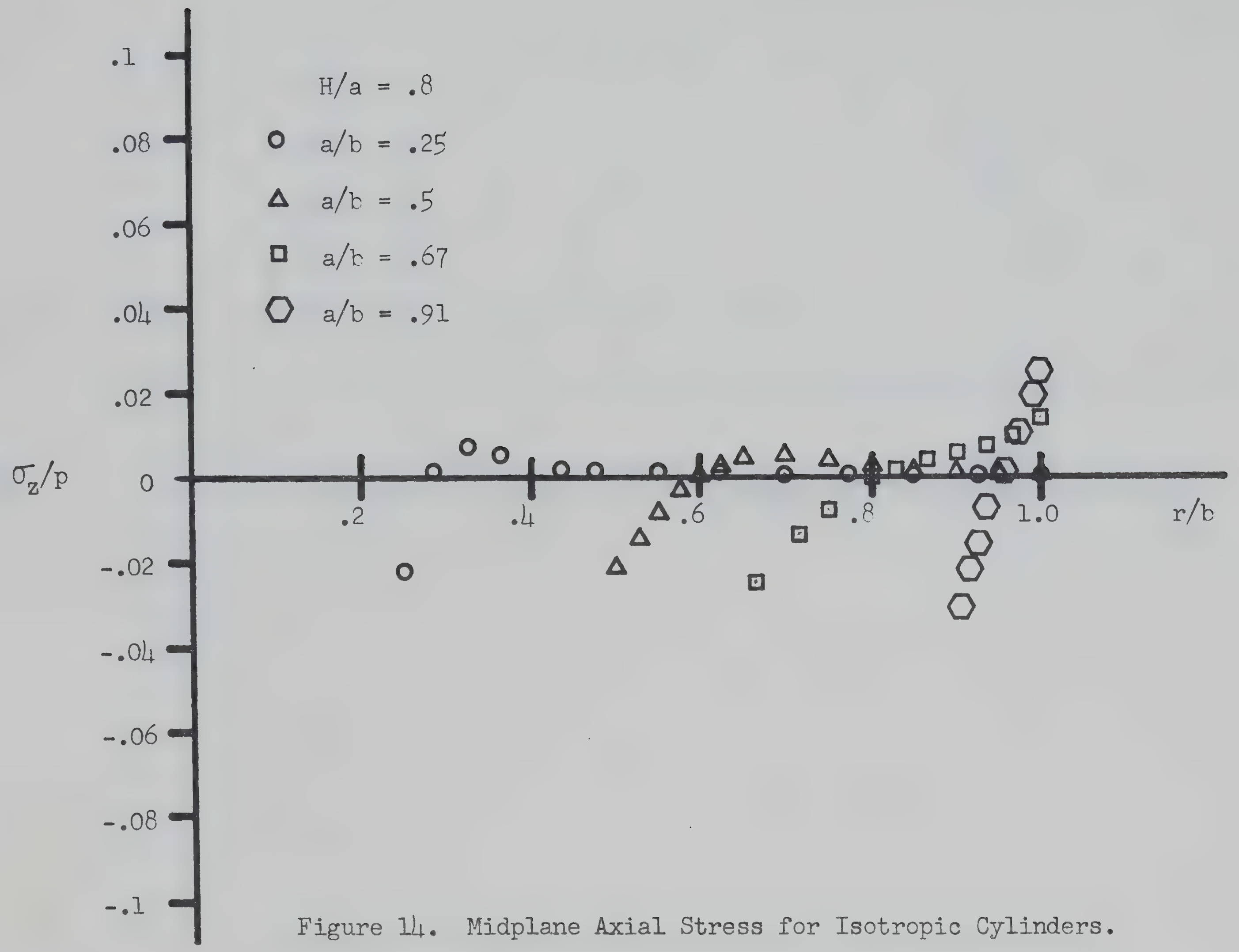

Figure 14. Midplane Axial Stress for Isotropic Cylinders.

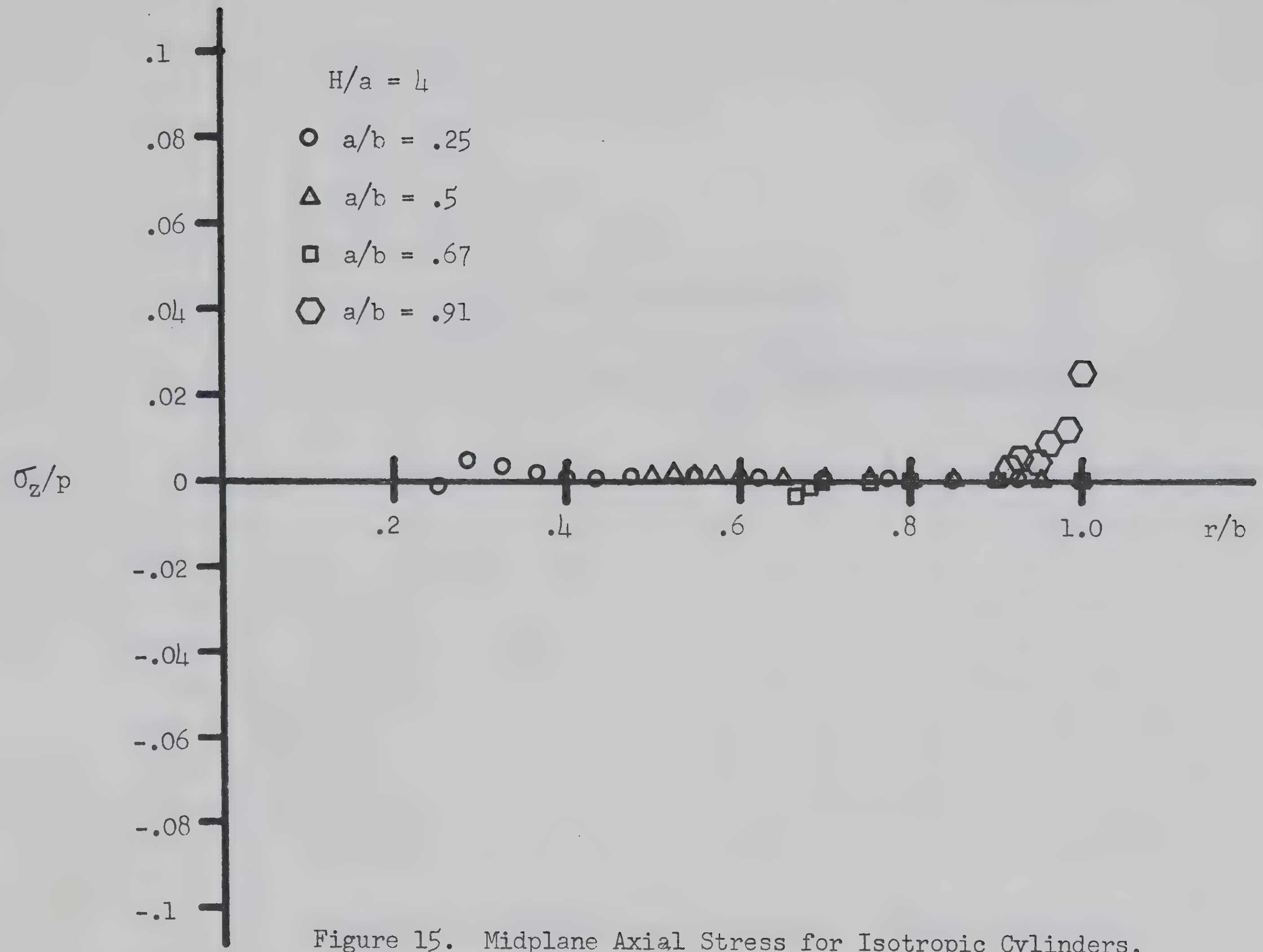

Figure 15. Midplane Axial Stress for Isotropic Cylinders.

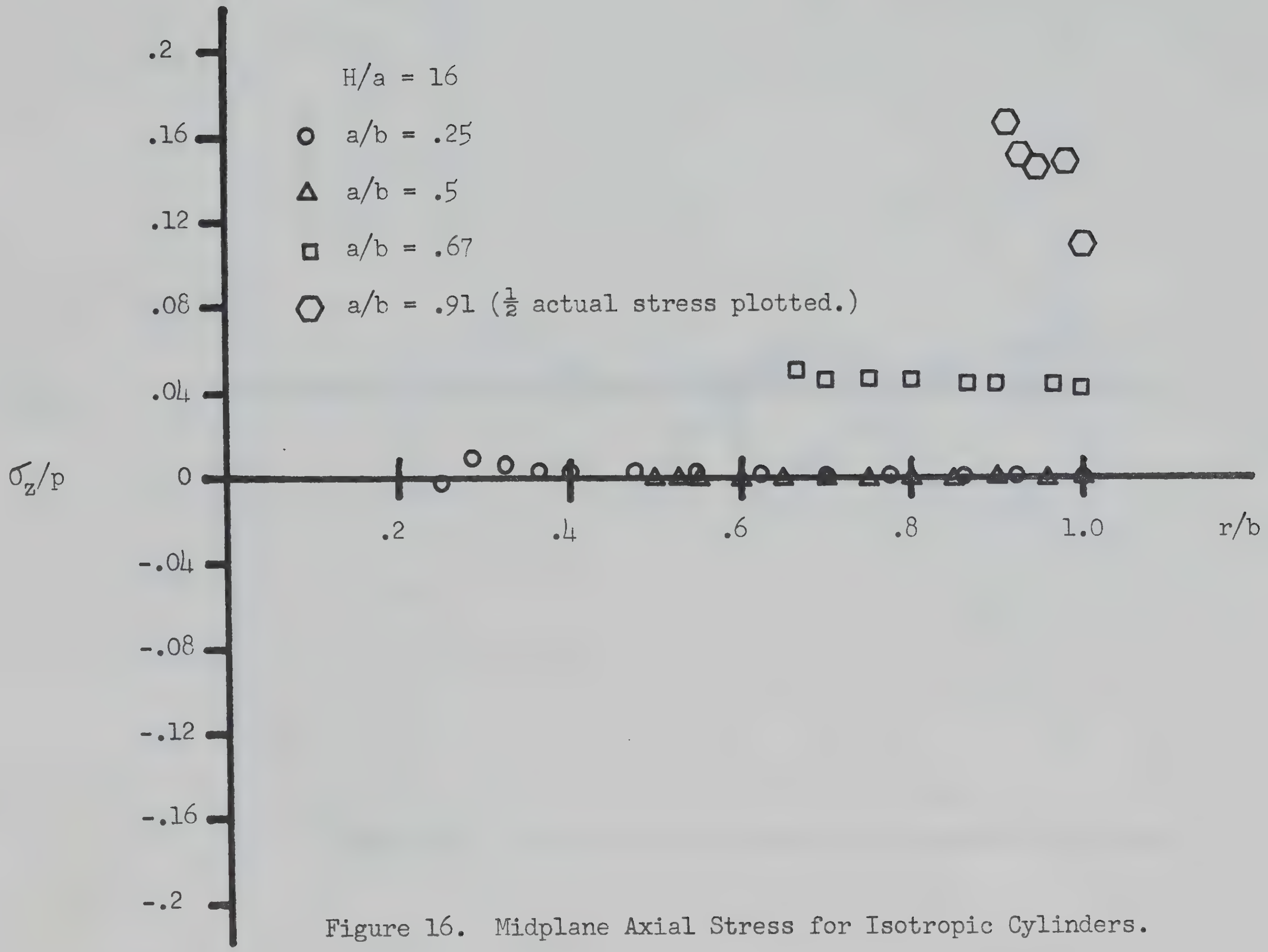

Figure 16. Midplane Axial Stress for Isotropic Cylinders.

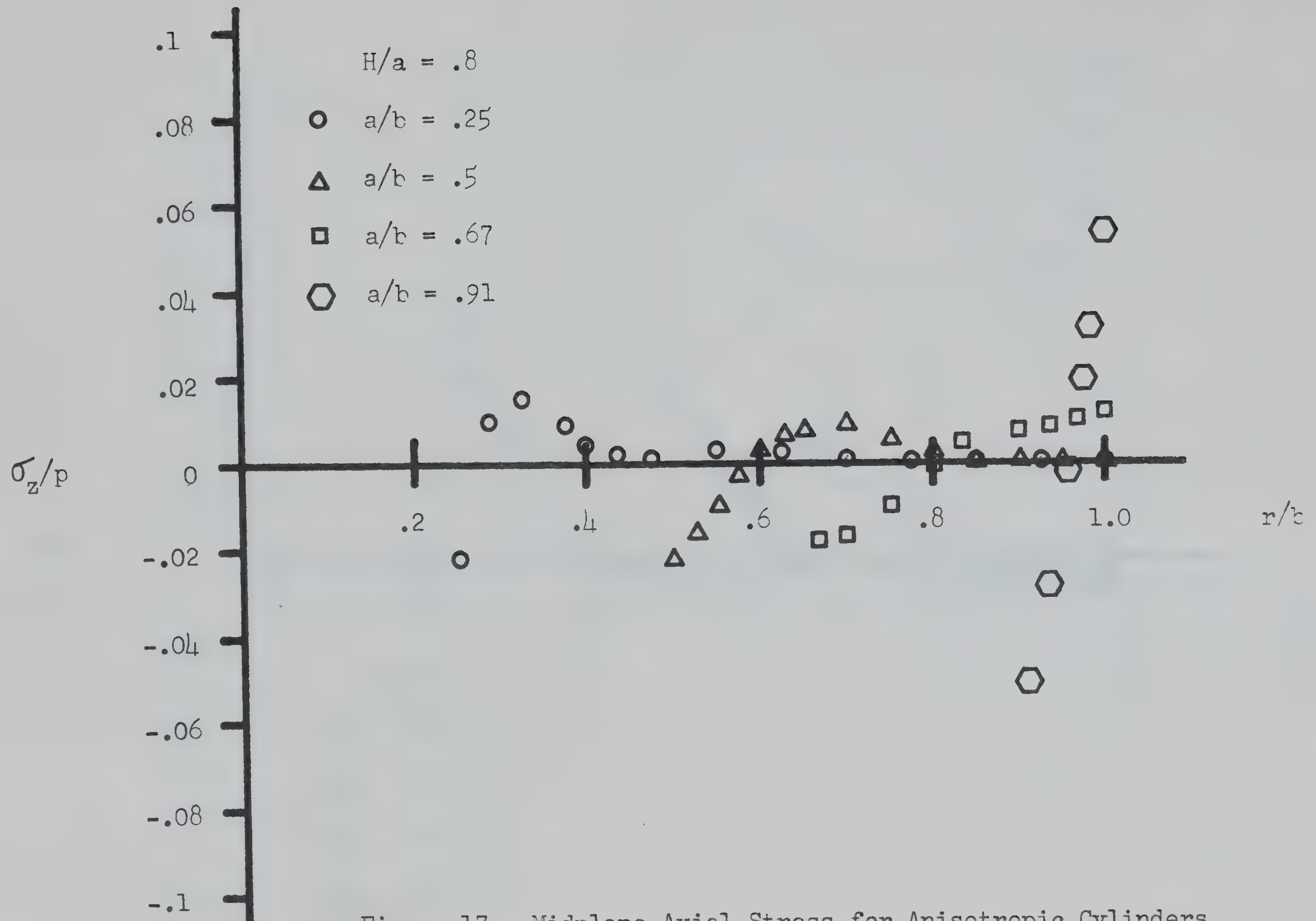

Figure 17. Midplane Axial Stress for Anisotropic Cylinders.

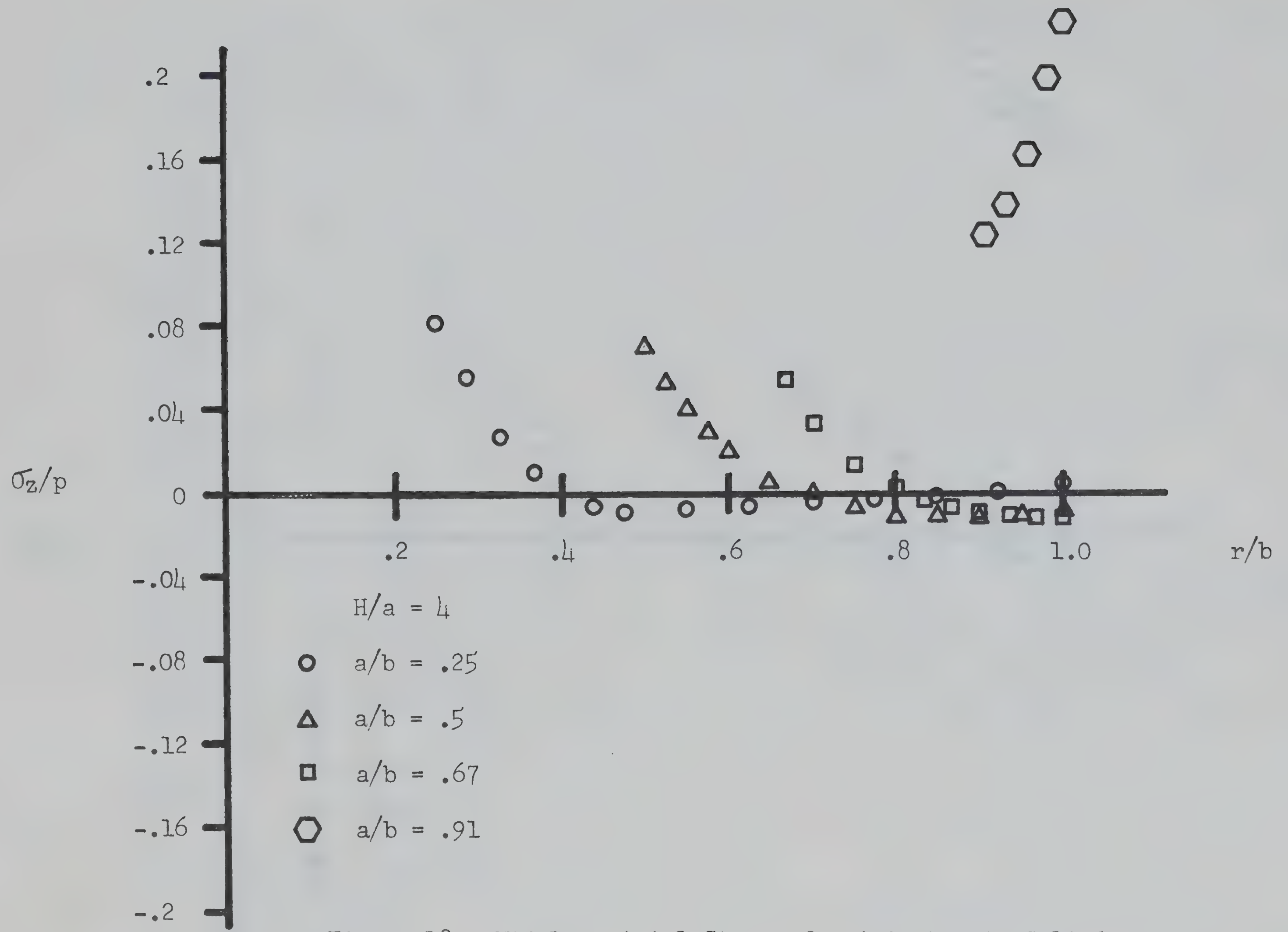

Figure 18. Midplane Axial Stress for Anisotropic Cylinders.

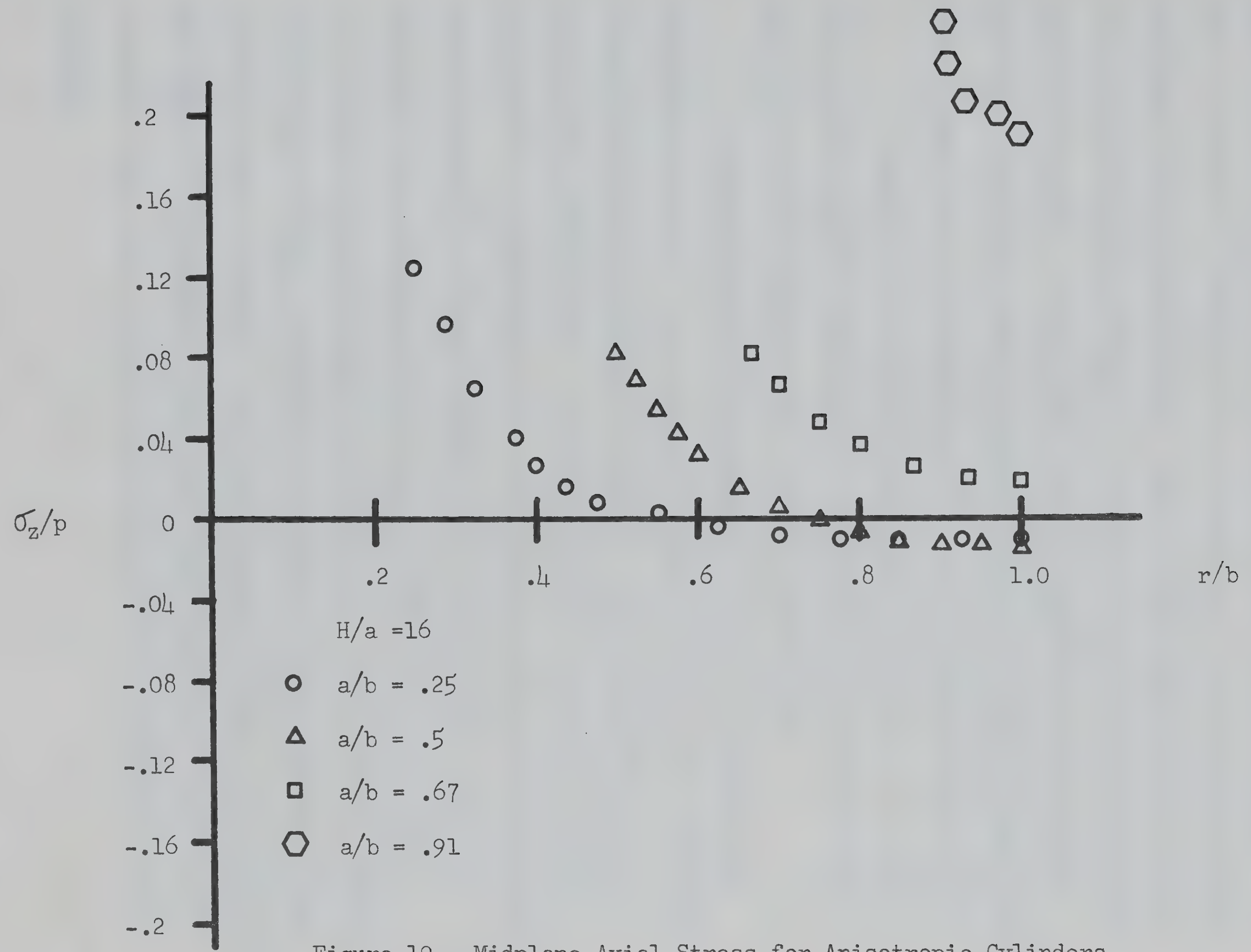

Figure 19. Midplane Axial Stress for Anisotropic Cylinders.

Figures 20, 21, and 22 are graphs of $-\sigma_r/p$ vs z/z_0, σ_θ/p vs z/z_0 and σ_z/p vs z/z_0 respectively for a steel cylinder of $H/a = 4$ and $a/b = .5$ at $r/b = .5$, .75 and 1.0; i.e. the inside, middle, and outer radii of the cylinder. These results were obtained using the 300 element grid of Figure 1. The solid lines are again open end cylinder solutions. These plots indicate that there are increased errors in the finite element results at the ends of the cylinders, and give a rough idea of the magnitudes of this increase for this grid.

Figures 23, 24, and 25 are similar to 20, 21, and 22 with the cylinder material being bone. These also show the presence and magnitude of the increased errors at the cylinder ends.

Figures 26 and 27 are graphs of the log of the absolute percentage error in $-\sigma_r/p$ and σ_θ/p (compared to the exact solutions) versus the log of the number of elements in the radial direction through the cylinder wall. A cylinder of $H/a = 4$ and $a/b = 5$ was used for this illustration of the convergence of these stresses to the correct answer [5]. Values of these errors were plotted for both isotropic and anisotropic (bovine bone) cylinders at $r = a$ and $r = (b-a)/4$ at the mid-height of the cylinders. The errors in these stresses can be seen, in general, to decrease with an increase in the number of radial elements. This approximately follows a relationship of the form $e = A/n^x$ where n = number of radial elements. A and x are constants which vary with position and mechanical properties of the cylinder.

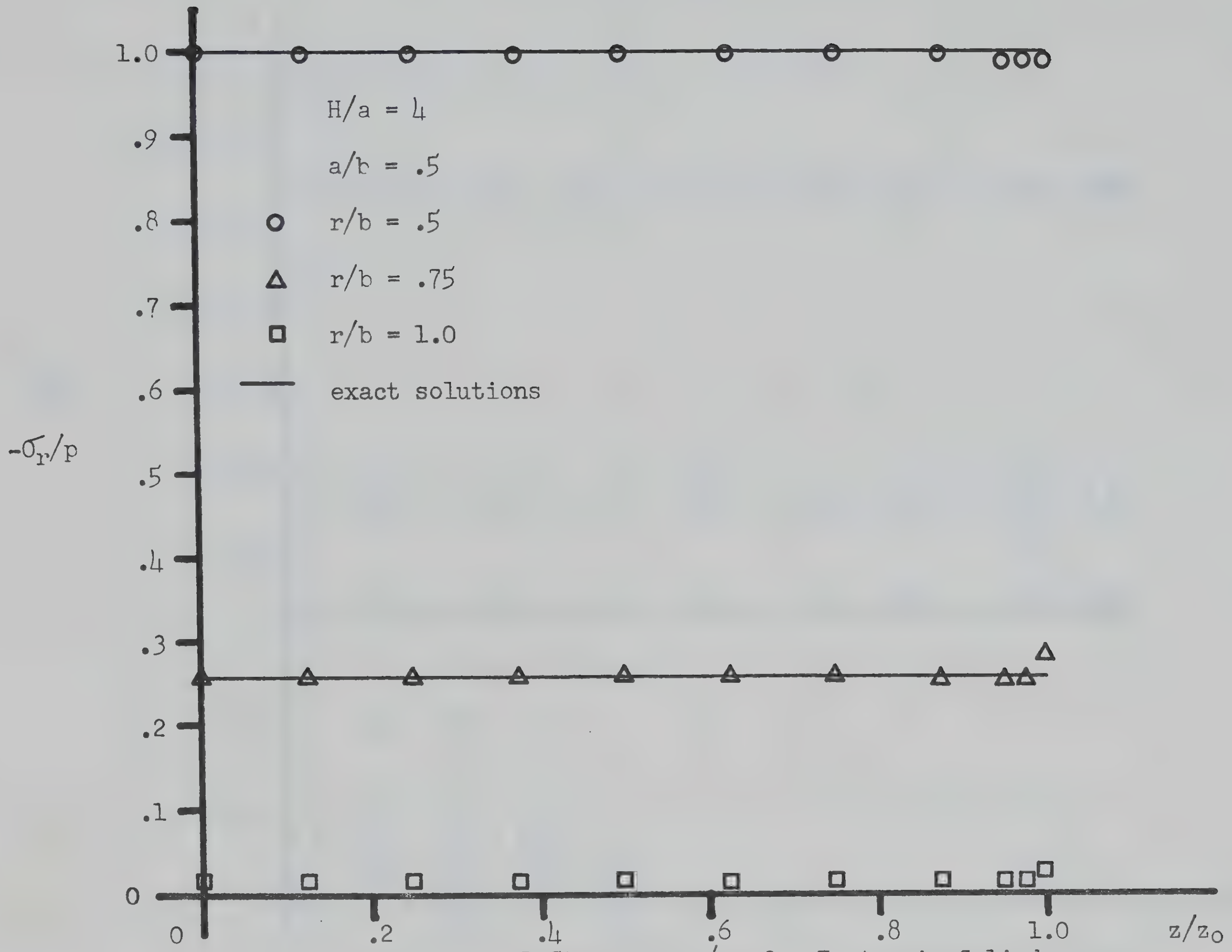

Figure 20. Radial Stress vs z/z_o for Isotropic Cylinders.

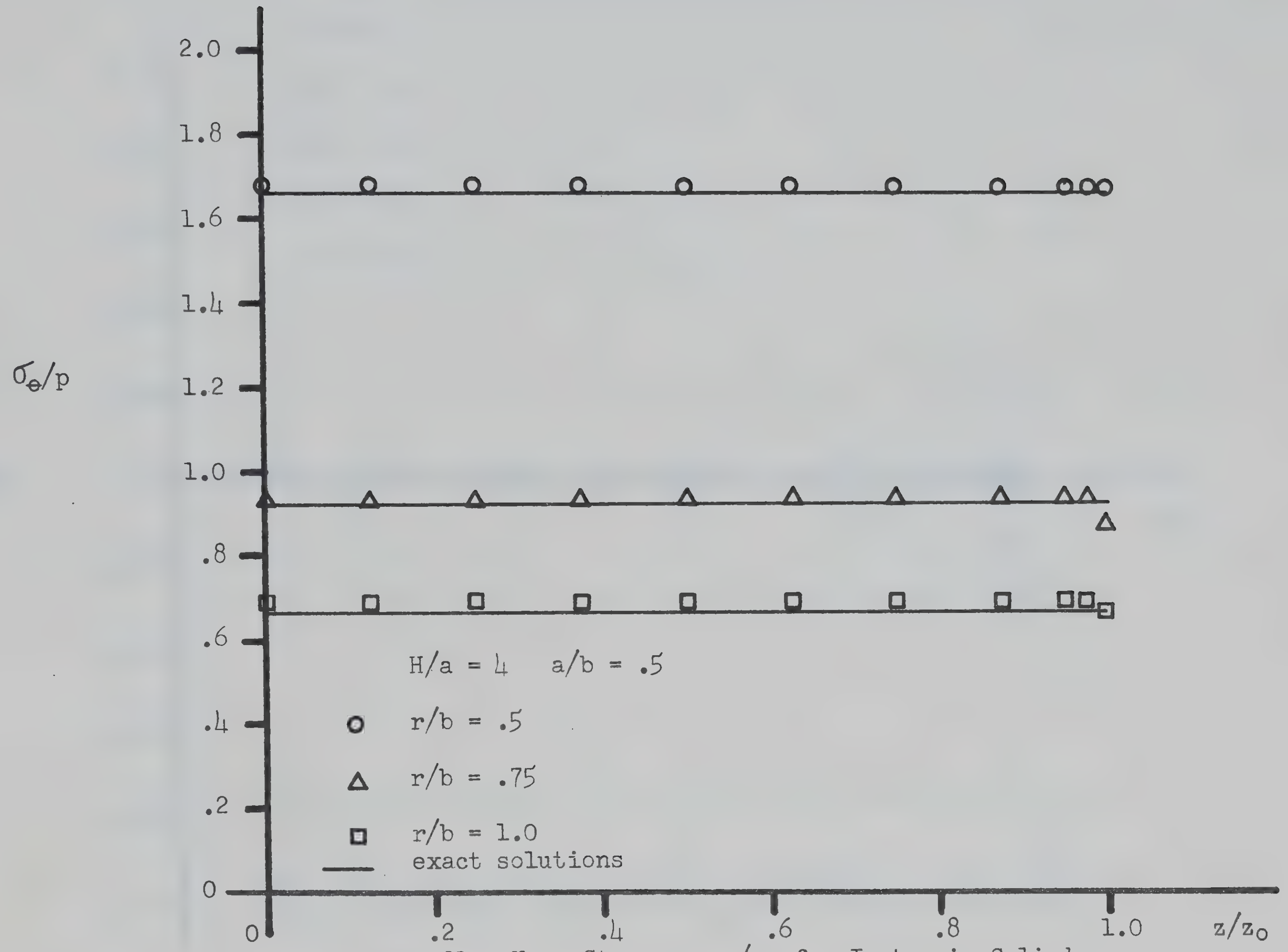

Figure 21. Hoop Stress vs z/z_o for Isotropic Cylinders.

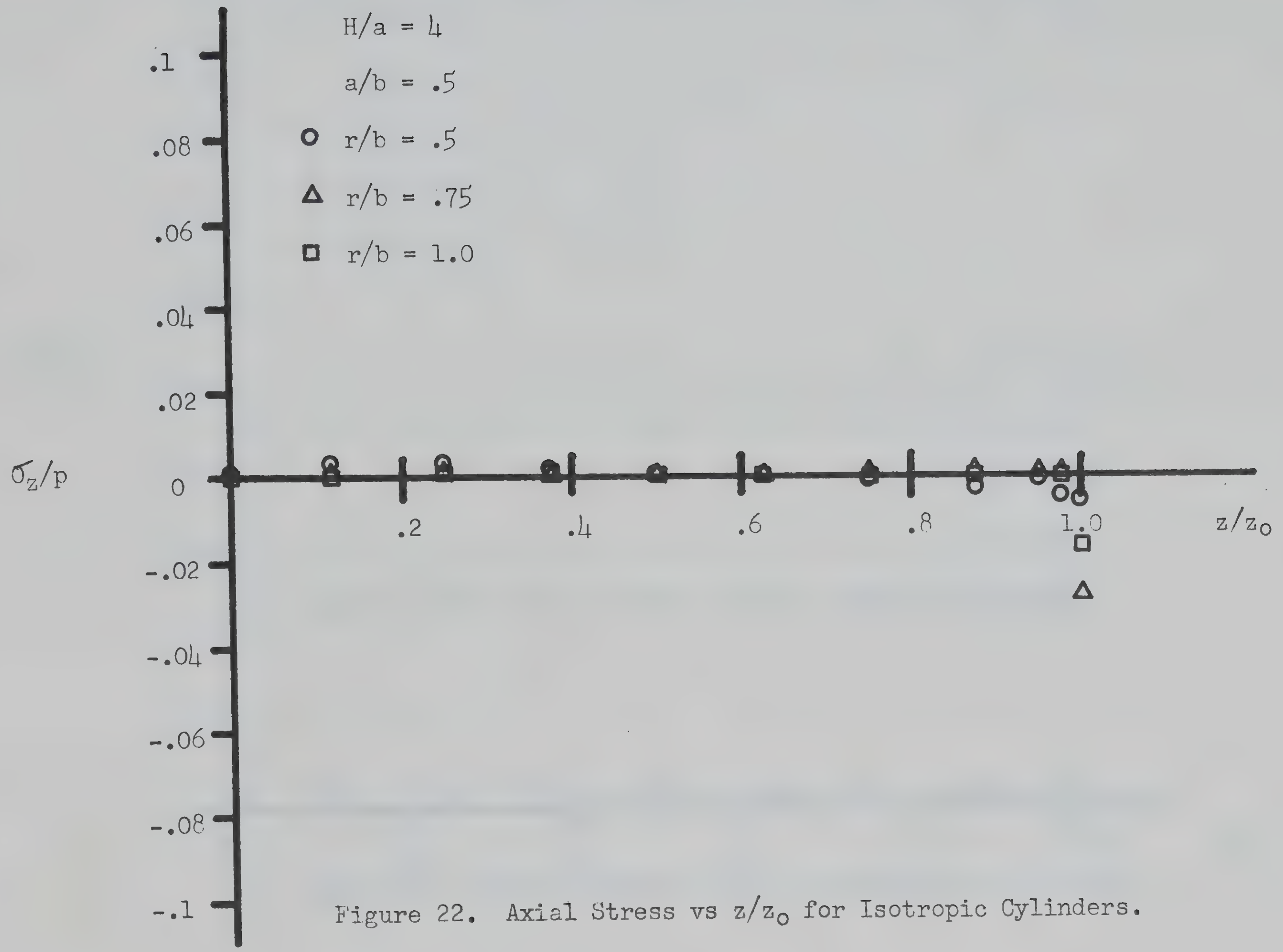

Figure 22. Axial Stress vs z/z_o for Isotropic Cylinders.

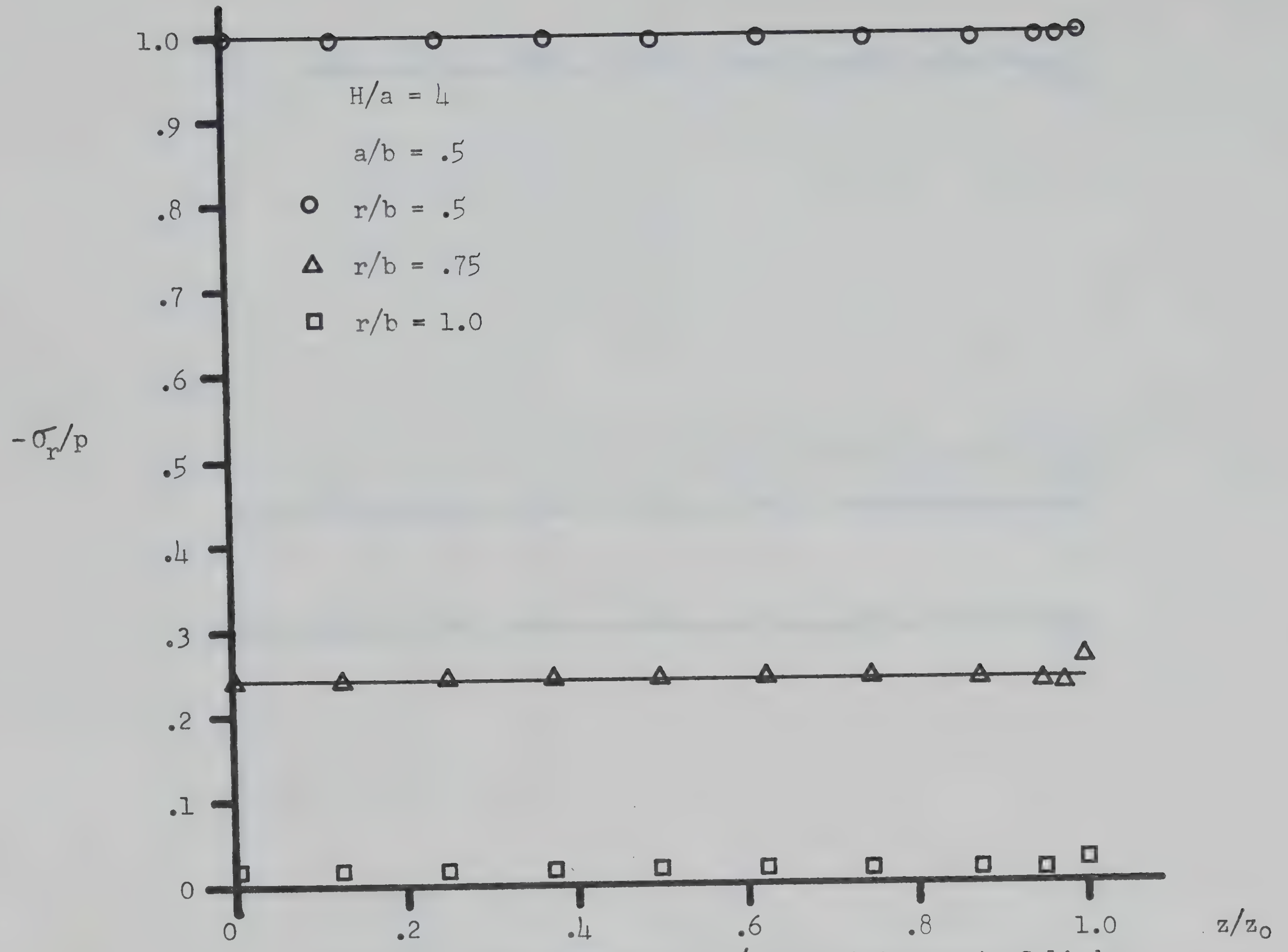

Figure 23. Radial Stress vs z/z_o for Anisotropic Cylinders.

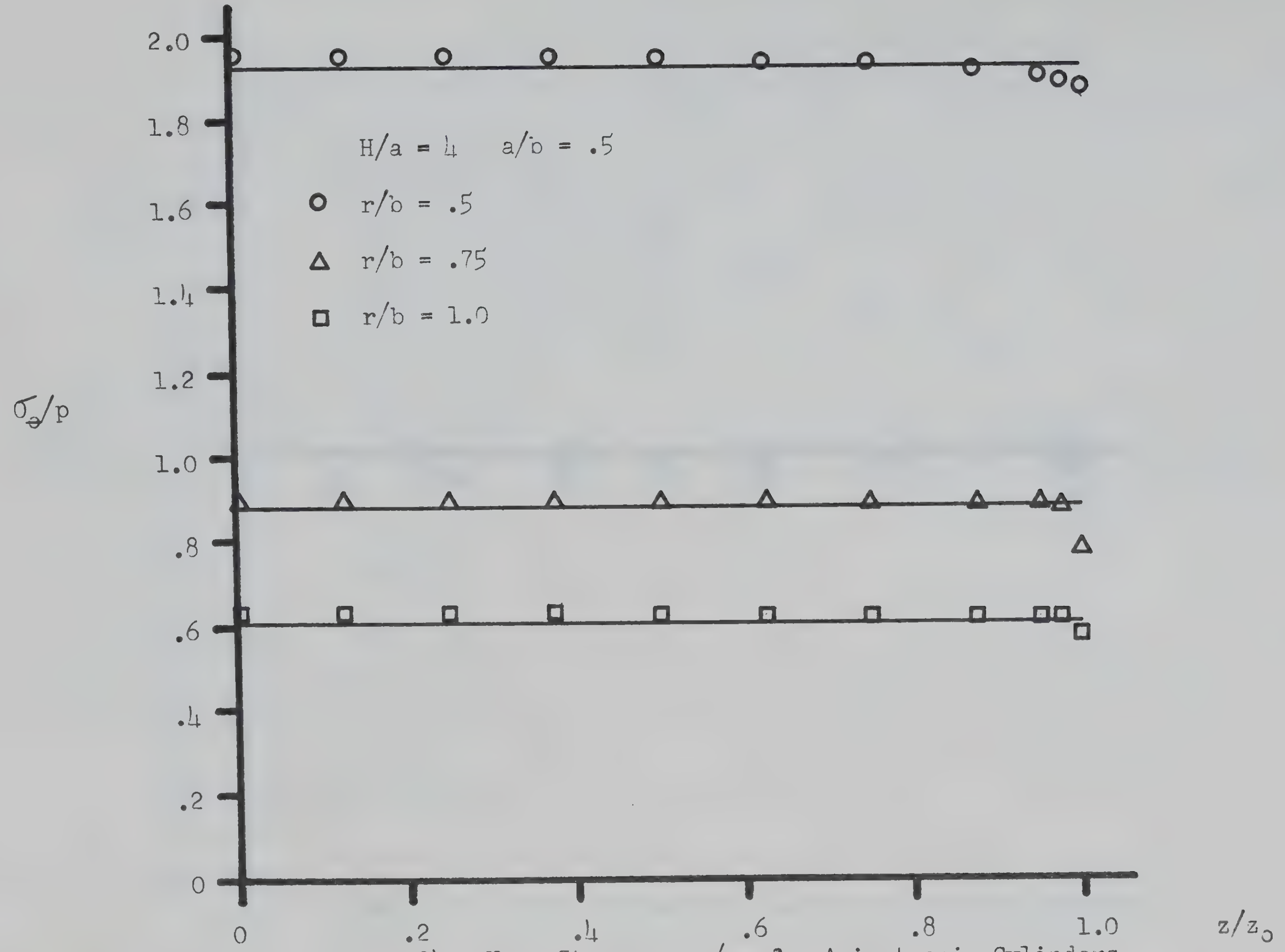

Figure 24. Hoop Stress vs z/z_o for Anisotropic Cylinders.

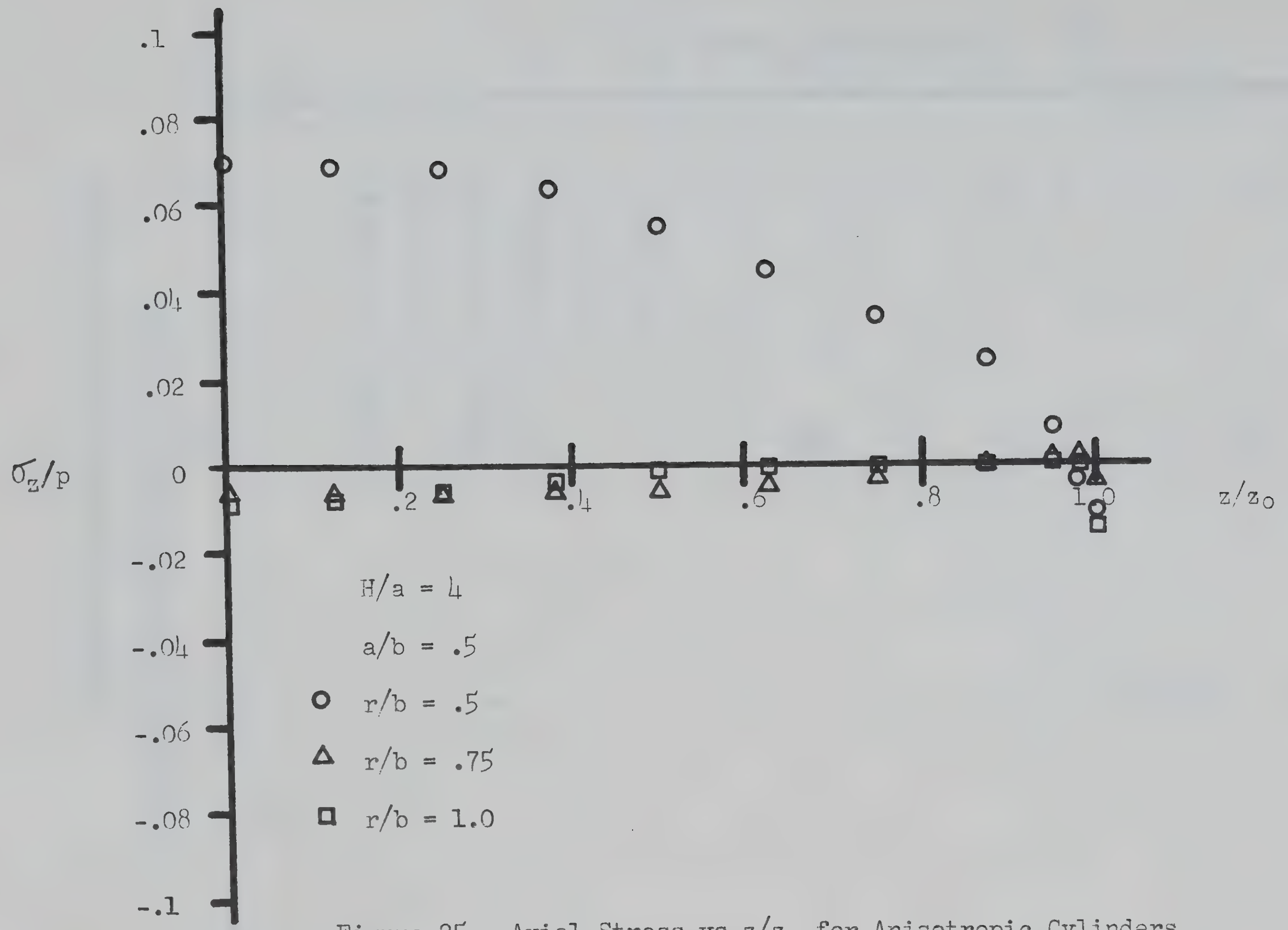

Figure 25. Axial Stress vs z/z_o for Anisotropic Cylinders.

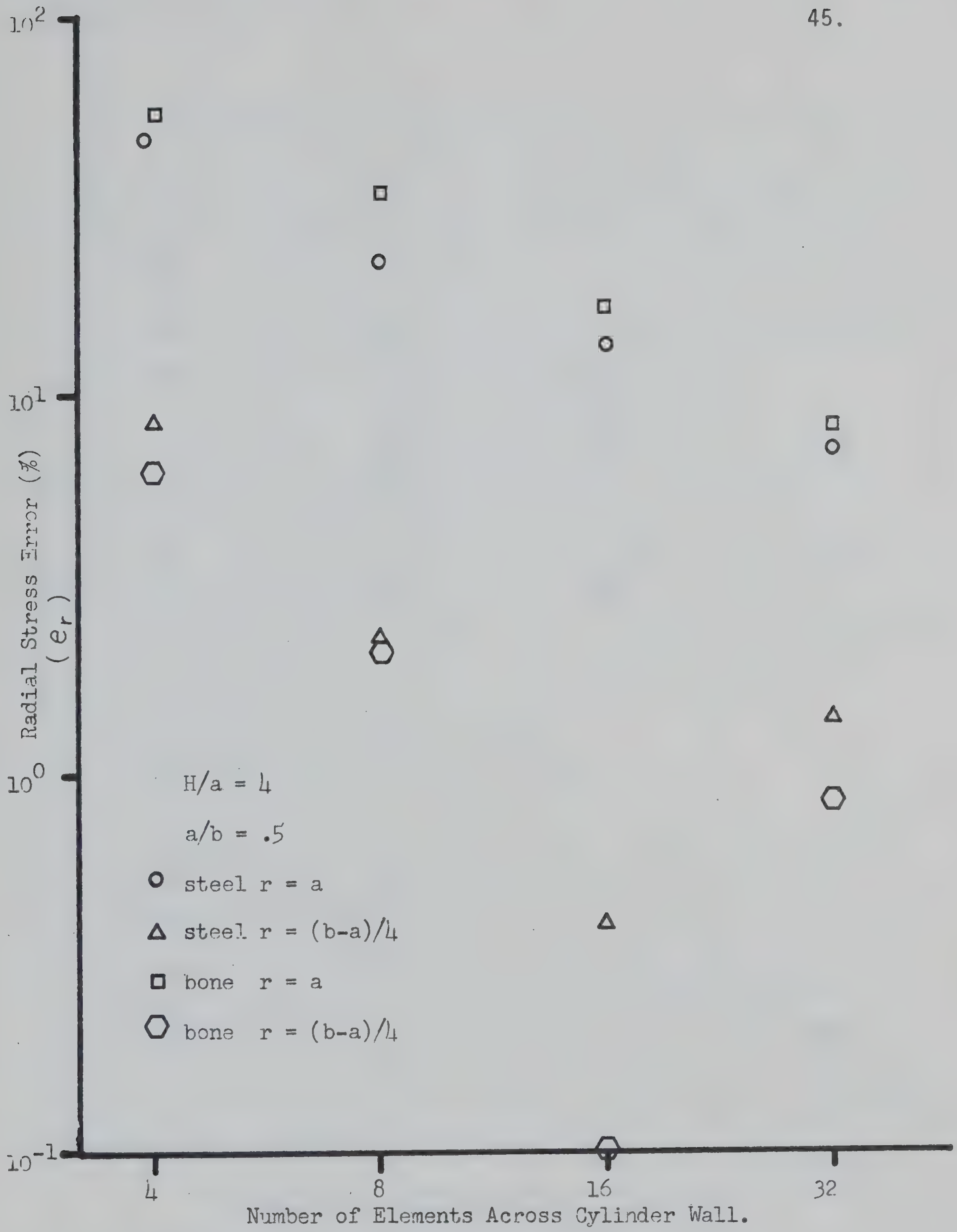

Figure 26. Radial Stress Convergence.

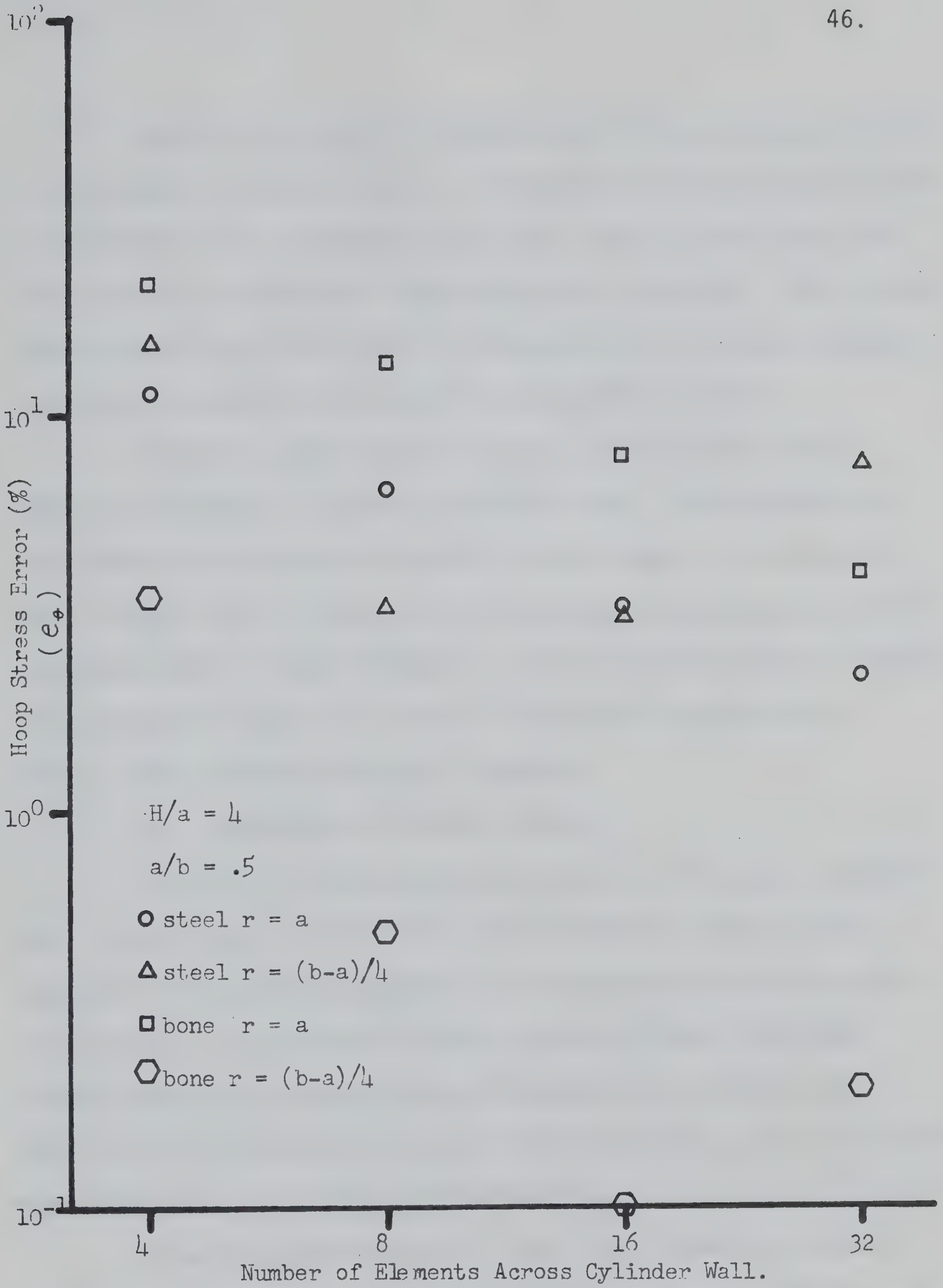

Figure 27. Hoop Stress Convergence.

Figure 28 is a plot of absolute error in σ_z/p versus the log of the number of radial elements. Absolute error was used here instead of percentage error because the true axial stress in this test case should be zero, which makes a percentage error undefined. This figure indicates that the axial stress is converging to the correct solution in a similar manner as the radial and tangential stresses.

Cylinders under internal pressure, modeled with varying numbers of elements in the axial direction only, indicated that for this loading the accuracy of results did not depend on the number of axial elements; (i.e. there was no convergence of any stresses for an increased number of axial elements). This was expected because ideally stresses should change very little in the axial direction (at a certain radius) under this type of loading.

3.2 DISCUSSION OF TEST CASE RESULTS

In general it would be expected that for the test cases used here, the accuracy of the results would increase as the a/b ratio approached unity. This is because as a/b approaches unity the radial and tangential stresses more closely resemble straight lines when plotted against the radius; the axial stresses are constant, and therefore the linear strain finite element used here can more accurately model the strain and stress distribution [3].

It can be seen from Tables 1 and 2 and Figures 8, 9, and 10 that this is true to a certain extent. The error decreases for a while in all cases as a/b increases, but then increases. This is mainly due

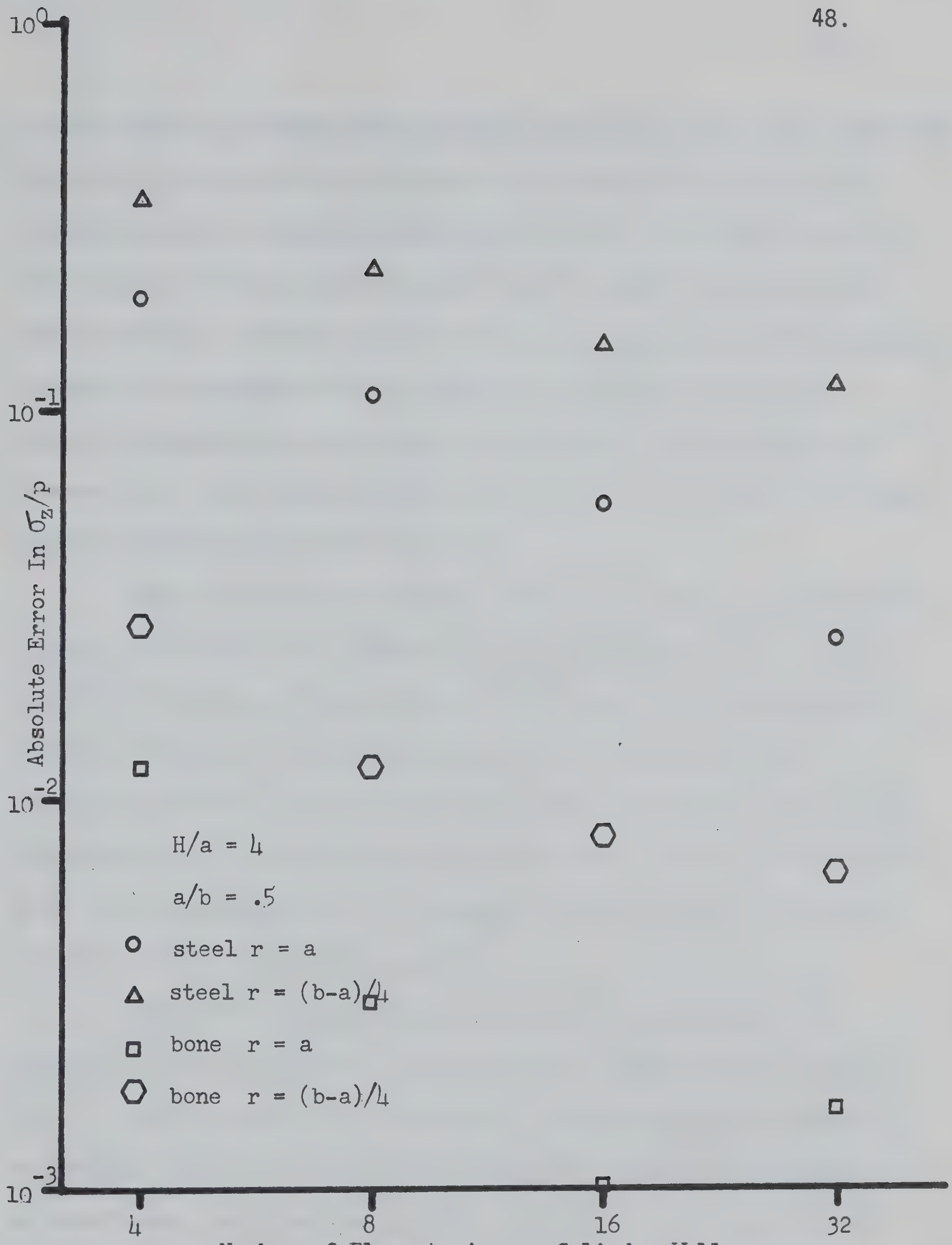

Figure 28. Axial Stress Convergence.

to the number of elements used becoming too large, (i.e: for a completely linear strain or stress distribution one element should give very accurate results) increasing the numerical errors incurred. For the case of a/b = .91 much more accurate results could be obtained using fewer elements. The 300 element grid was used throughout the test cases (except for convergence tests) because the problems discussed in Chapter IV were solved using this grid or grids similar to the 300 element grid. For these problems a/b was equal to .5, which is in the region of good accuracy for this grid.

Some of this error increase could also be due to the increased "aspect ratio"[15] of the elements as a/b approaches unity. This is numerical error due to the lengths of the sides of an element being greatly different. As this must also account for most of the variation of error with cylinder height seen in the tables and figures mentioned above, it can be seen that the errors caused by it can become quite large, especially as a/b approaches unity, and particularly for the hoop stress. (See tables 1 and 2).

Larger than average errors were found to occur near the boundaries of the cylinders, and in particular near the inner radius. This is probably partly due to the fact that loadings which should be distributed evenly over the inner surface are assumed concentrated on external nodes, and also that stresses and strains are changing most rapidly near the inner radius [3]. These errors were lessened by using more elements near the inner radius and at the cylinder ends.

The errors found for the anisotropic (bone) cylinders were generally slightly larger than the corresponding errors for isotropic cylinders at low a/b ratios and lower at high a/b ratios, however for the a/b ratio of the bovine bone model used in the problems of Chapter IV for this grid, the magnitudes of the average errors in stress are about the same.

It should be noted that the'average errors' used here are defined as

$$e_{avg} = \sum_{i=1}^{n} e_i/n$$

where n is the number of nodal points along the mid-height of the cylinder and e_i is the absolute percentage error in stress at that node for radial and tangential stress and the absolute error for axial stress. This gives a weighted average as there are more nodal points near the inner radius. As the largest errors occur here, this 'weighted average' is larger than true average would be.

In Figures 26, 27, and 28, the errors in stress were seen to decrease as n increased, then increase as n further increased at $r = (b-a)/2$. The increase in error here was probably due to increased numerical error, ie: too many elements for optimum accuracy. At this radius the radial and tangential stresses change at a slower rate than near the inner radius, therefore fewer elements are required here to give the same accuracy as near the inner radius.

The errors in the finite element results could in some cases be lessened by further subdivision of the elements. The limit of the

effectiveness of this subdivision is the point where roundoff errors become the same order of magnitude as the errors caused by the finite element size. After this point, greater accuracy can be achieved by using double precision and then possibly still further reduction of element size. Generally, for most applications sufficient accuracy can be obtained with single precision and a relatively coarse grid size.

It should be noted that the large errors in hoop stress (e_θ) are in most cases due to the definition of this error. By comparing the absolute error to the range of σ_θ across the cylinder wall, errors very small in comparison with the actual value of σ_θ result in large errors as the range is much smaller than the value of σ_θ.

CHAPTER IV

RESULTS AND DISCUSSION OF THE FINITE ELEMENT ANALYSIS FOR BONE UNDER VARIOUS LOADING CONDITIONS

4.1 ASSUMPTIONS

In the problems analysed the following assumptions were made:

1. The bone material is homogeneous.
2. The portion of the bovine femur used is axisymmetric.
3. The material has constant elastic physical properties.
4. The material has similar physical properties in tension and compression.
5. Rods and prosthetic devices are rigid.
6. Strains are small compared to unity.

The assumption of homogeneity of bone is incorrect in that bone is not homogeneous in the microscopic sense. Bone is composed mainly of light, dark, and intermediate osteons which are made up of collagen fibers, interfibrillar calcified substance, and pores (Haversian systems and Volkmann's canals). [12] and [10]. The modulus of elasticity and mechanical properties of bone are dependent upon collagen fiber orientation and distribution, and on the composition and distribution of minerals in the interfibrillar calcified substance. Fortunately, however, these components are small enough that for engineering purposes, in most cases, a segment of bone when viewed macroscopically is virtually homogeneous in terms of its mechanical properties. In the macroscopic sense, although as just stated, a segment of bone may be considered homogeneous, different parts or

orientations in a bone, different bones in a particular animal (or human), and similar bones (and areas in bones) in different animals of the same species may differ substantially in mechanical properties and physical makeup, and the same part of the same bone may change with time. When considering one portion (say the middle third) of a long bone (cortical bone), however, the assumption of homogeneity in the macroscopic sense is fairly well justified in most cases [11].

The assumption of axisymmetry of a portion (middle third) of a typical long bone is obviously an inaccurate one, however, the assumption of any "typical" cross-section would be inaccurate, as the true cross-section of a particular bone will vary from place to place in that bone, and the cross-section of similar bones in different animals will vary also. Usually before the insertion of a prosthesis, the intramedullary canal (interior of the bone) is reamed out to a near perfect cylindrical bore, but the outside of the bone is untouched. This makes the assumption of axisymmetry (particularly near the interior of the bone) a little better. Despite the errors necessarily induced by this assumption it was felt that useful information could still be obtained from an axisymmetric bone model, in that results for the model would be of the same order of magnitude as those for a real bone particularly near the more axisymmetric interior of the bone.

Constant elastic physical properties (Young's moduli and Poisson's ratios) were assumed for the bone models. As bone is viscoelastic, this is not absolutely true, the physical properties

actually being dependent on both strain, strain rate and previous stress-strain history [7],[13], however in general the assumption is acceptable as the stress-strain curve for bone is nearly linear up to failure [17]. The assumption of perfect elasticity itself is not quite correct, but in the range of stresses with which the test problems deal, it is probably close. The elastic constants used for the test problems were E_r = 670 ksi, E_θ = 1500 ksi, E_z = 2500 ksi, $\nu_{r\theta} = \nu_{zr} = \nu_{z\theta} = .3$. These were taken from references [7] and [8], the moduli of elasticity being estimates for low loading rates of bovine bone from reference [7] and Poisson's ratio was taken from reference [8] ($\nu_{r\theta}$). ν_{zr} and $\nu_{z\theta}$ were assumed to be the same as $\nu_{r\theta}$ as no published data could be found giving their values.

The assumption of similar physical properties of bone in tension and compression is probably fairly good. Comparison of moduli of elasticity in tension [11] with those in compression [7] for longitudinal cortical bone samples indicates that this assumption is good for this particular property. The values of E_z in tension and compression are the same within the limits which could be expected due to the differences in different bones. It was assumed that this was true for the other properties as well, as no data could be found to make further comparisons.

The assumption of rigid rods, wedges and prosthetic devices is justified in view of the fact that the modulus of elasticity for steel (of which most prosthetics are composed) is more than an order of magnitude greater than that of the largest modulus of elasticity for bone (E_z).

Infinitesimal strains were assumed for the finite element model, and therefore significant errors would arise if strains were allowed to become too large (greater than .005"/in). If results are converted from the non-dimensional form presented here it should be ascertained that the strains for a particular case are not beyond the limit mentioned above.

4.2 RESULTS AND DISCUSSION

To illustrate the usefulness of the finite element method in general and of this program in particular to the analysis of anisotropic axisymmetric bodies, specifically idealized long bones, two test problems were analysed:

(1) Idealized long bones strained by the insertion of interference fit rods with and without shearing traction applied.

(2) An idealized long bone under axial loading with flat and hemispherically shaped prosthetic caps.

The first problem, that of interference fits of rods into bones has significance in orthopedic intramedullary nailing techniques. Here a rod is inserted in the reamed intramedullary canal of a long bone (usually broken) to increase its rigidity during healing. At the present 'state of the art' the canal is reamed to a slightly larger diameter than the rod to be inserted and the rod is inserted from one of the bone ends and glued in place. It is possible, that in certain cases the use of an interference fit rod of shorter length and inserted into the bone halves through the break area could

achieve greater rigidity and cause less trauma to the rest of the bone (in particular to the bone's blood supply). This problem may also have significance in the insertion of some prosthetic devices (e.g. knee joints etc.) into bone, where a rod is pushed into the intramedullary canal to help secure the prosthesis. Here some interference fit may help stabilize the prosthesis and avoid localized contact areas between the prosthesis and the bone. [14]

Figure 29 shows the shape of an idealized long bone of $a/b = .5$ before and after the insertion of a rod with an interference fit of $I/a = .005$, where I is the difference between the rod radius and the inner bone radius.

The boundary conditions for this problem are; $u/a = .005$ from $z/z_0 = 1/3$ to 1 on the inner radius, where u is the radial displacement; $v/a = 0$ at $z/z_0 = -1$, where v is the axial displacement. All other boundaries are free.

The outline of the top half of the bone before insertion of the rod is drawn in heavy lines, while the outline of the bone after insertion of the rod is drawn in light lines. The non-dimensional displacements are exaggerated by a factor of 10^2 (i.e. an actual displacement of .01/a would be displaced by 1 inch on the drawing in both the r and z directions).

This figure shows the radial displacement of the outer radius of the cylinder as nearly constant near the top of the cyliner, and approaching zero below the lowest part of the rod in a gentle "S" shaped curve. The radial displacement of the inner radius of the bone

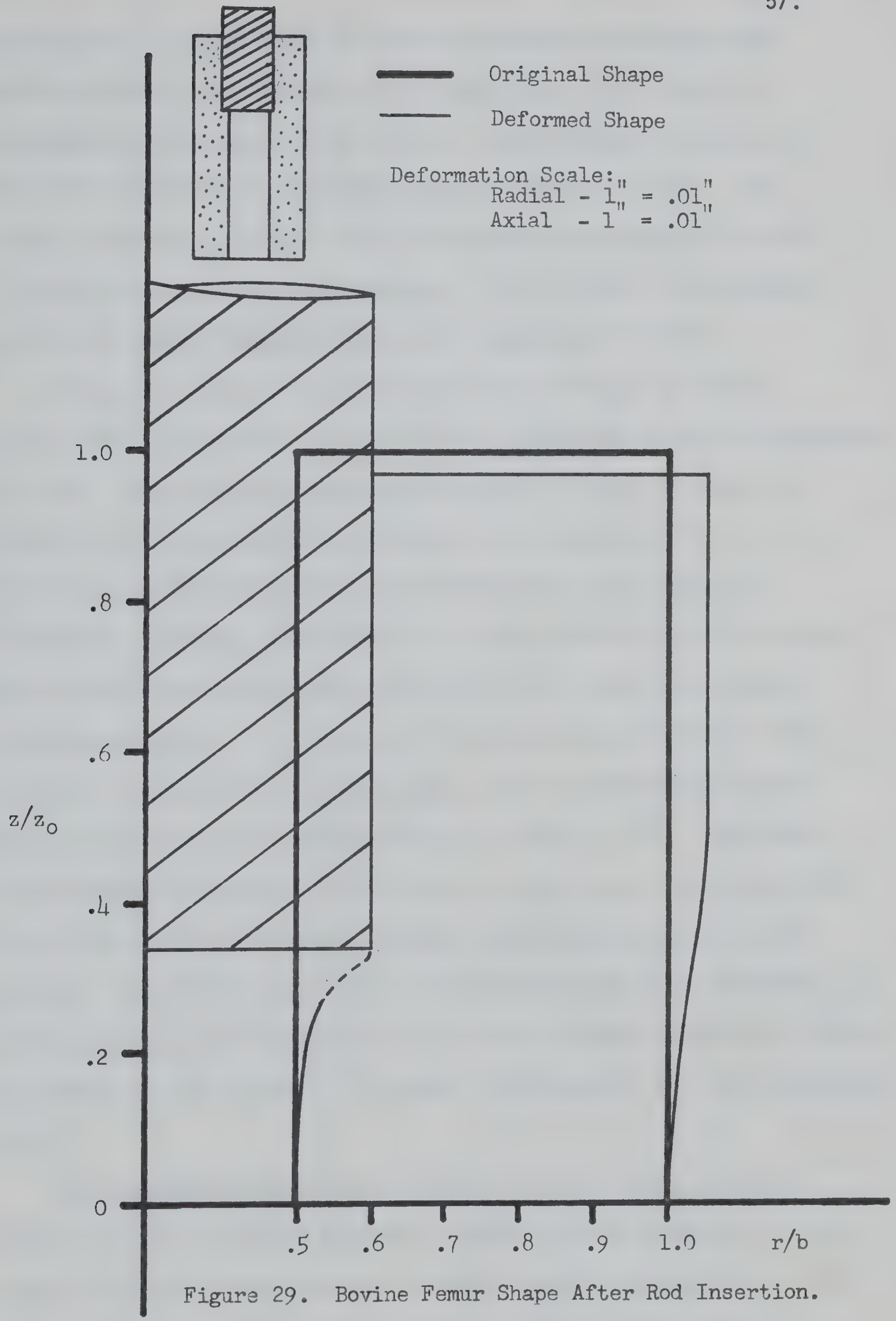

Figure 29. Bovine Femur Shape After Rod Insertion.

corresponds to the outside of the rod to where the rod ends and approaches zero below the rod in a sharp curve. This curve is indicated as a dashed line as the grid used here was too coarse to show the "S" nature of the curve near the edge of the rod. The actual curve must be an "S" curve to prevent a discontinuity in the first derivative of the displacement. The cylinder is also shown to shorten in height somewhat due to the insertion of the rod.

Figure 30 shows the shape of the bone of figure 29 before (dark lines) and during (light lines) the insertion of the interference fit rod. The boundary conditions here were the same as those for figure 29 with the exception that at $r = a$, from $z/z_o = 1/3$ to 1 a shearing traction was applied. The magnitude of the shear was determined assuming a coefficient of sliding friction of .25 between the rod and bone, and a normal force due to σ_r found from internal displacement alone. Only this one iteration was taken as the coefficient of friction is assumed anyway. The non-dimensional radial displacements are again exaggerated by a factor of 10^2. The radial displacements are similar in this case to those shown by Figure 29 but due to the shearing traction the axial displacements here are much greater. The inside upper edge of the cylinder has been 'rounded' due to the shearing traction and the top of the cylinder slopes down towards the centre of the cylinder. The axial displacements are only exaggerated by 10^1.

The non-dimensional radial and hoop stresses (σ_θ/σ_o) for the bone of Figure 29 without shearing traction (solid lines) and for the bone of Figure 30 with shearing tractions applied (dashed lines) are plotted in Figure 31 versus r/b where σ_o is the radial stress at

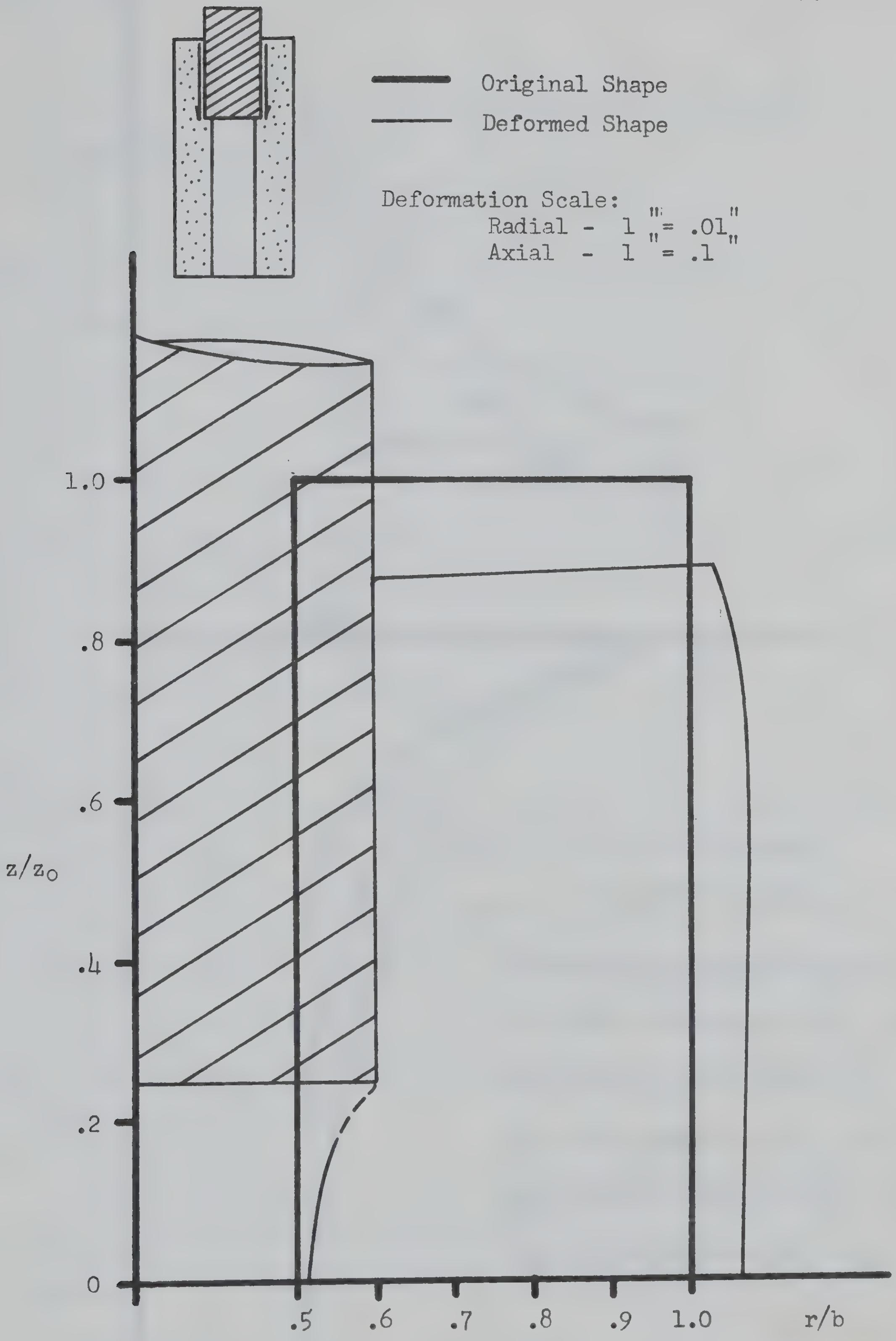

Figure 30. Bovine Femur Shape During Rod Insertion.

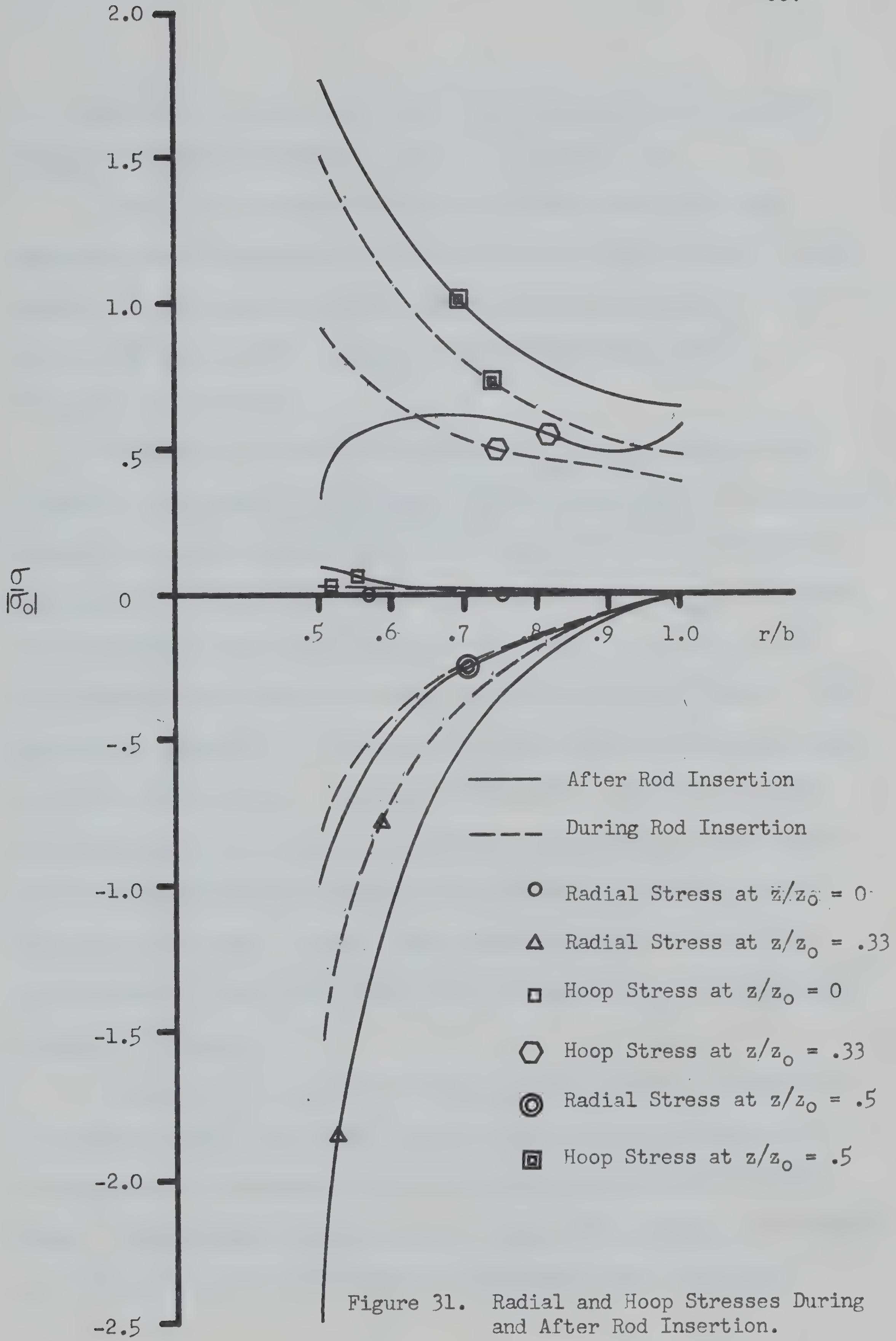

Figure 31. Radial and Hoop Stresses During and After Rod Insertion.

$r = a$ and $z/z_0 = .5$ for $I/a = .005$ and no shearing traction applied. These are plotted for values of $z/z_0 = 0, .33$, and .5.

Figure 32 consists of plots of non-dimensional axial and shearing stress versus r/b for the problems mentioned above. In this case τ_0 is the shearing traction applied at $r = a$ and $z/z_0 = .5$ for $I/a = .005$ and $\mu = .25$. These are also plotted for values of $z/z_0 = 0$, .33, and .5.

Figure 33 is a series of plots of $\sigma_{\theta max}/\sigma_{\theta ult}$ versus I/a for idealized long bones of various a/b ratios, where $\sigma_{\theta ult}$ is the ultimate tensile strength of bovine bone in the hoop direction. No shearing traction is applied here. The maximum hoop stress ($\sigma_{\theta max}$) was found in each case to occur near the tip of the rod, i.e. at $z/z_0 = 1/3$. The maximum hoop stress was plotted because it was felt that for this particular problem it is an important (and perhaps the most important) criterion for failure. To predict adequately the failure of bone a failure theory for anisotropic bodies probably taking into account elastic deformation due to hydrostatic pressure or tension, would have to be developed. These plots indicate that the maximum hoop stress varies linearly with the ratio of interference fit to internal radius of the bone.

Figure 34 is a series of plots similar to those in Figure 33 with the exception that here a shearing traction is applied to the inside radius of the bone as if the rod were being pushed into the bone. The magnitude of the shear was determined assuming a coefficient of sliding friction of .25 between the rod and bone. Again the

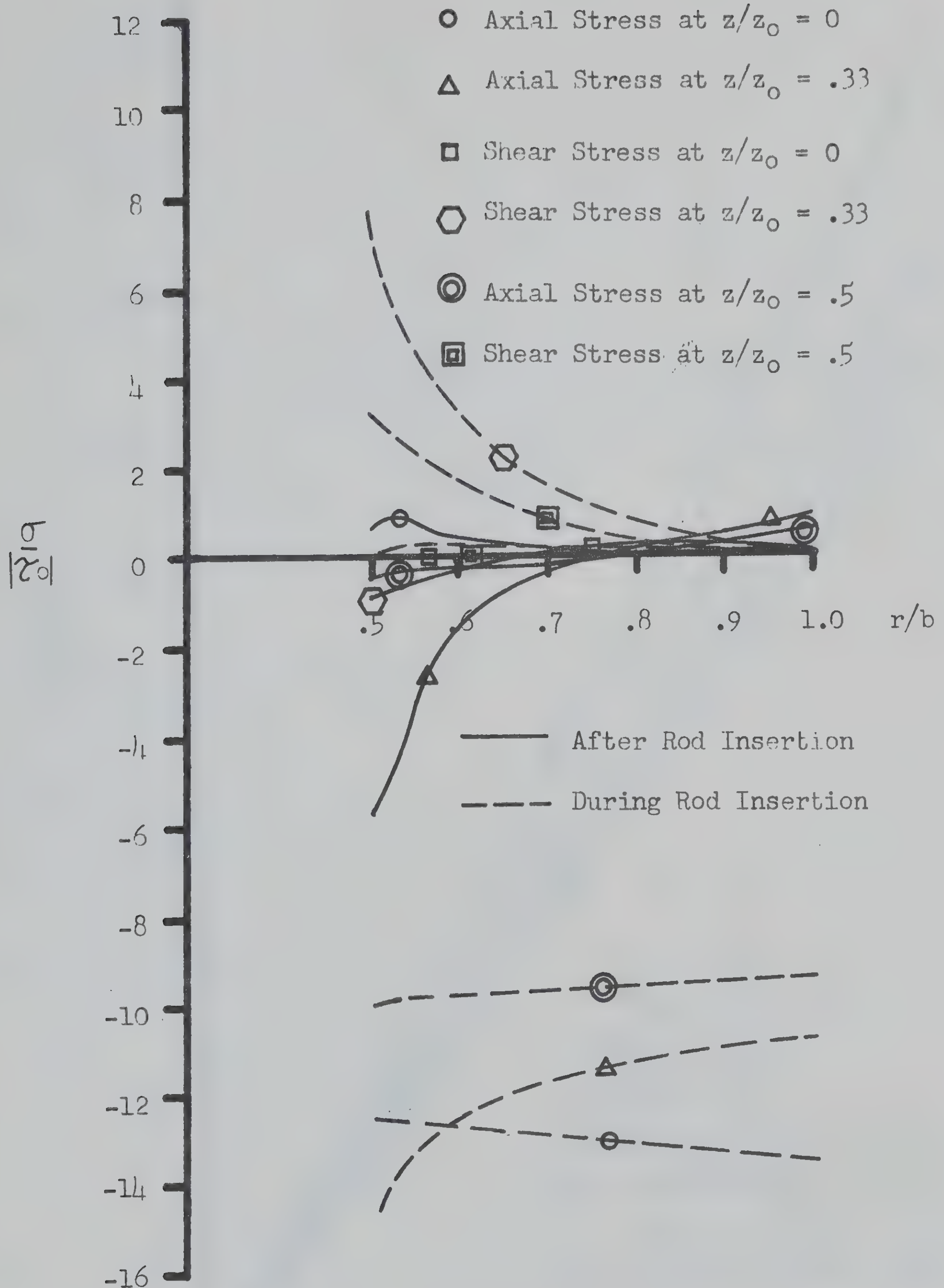

Figure 32. Axial and Shear Stresses During and After Rod Insertion.

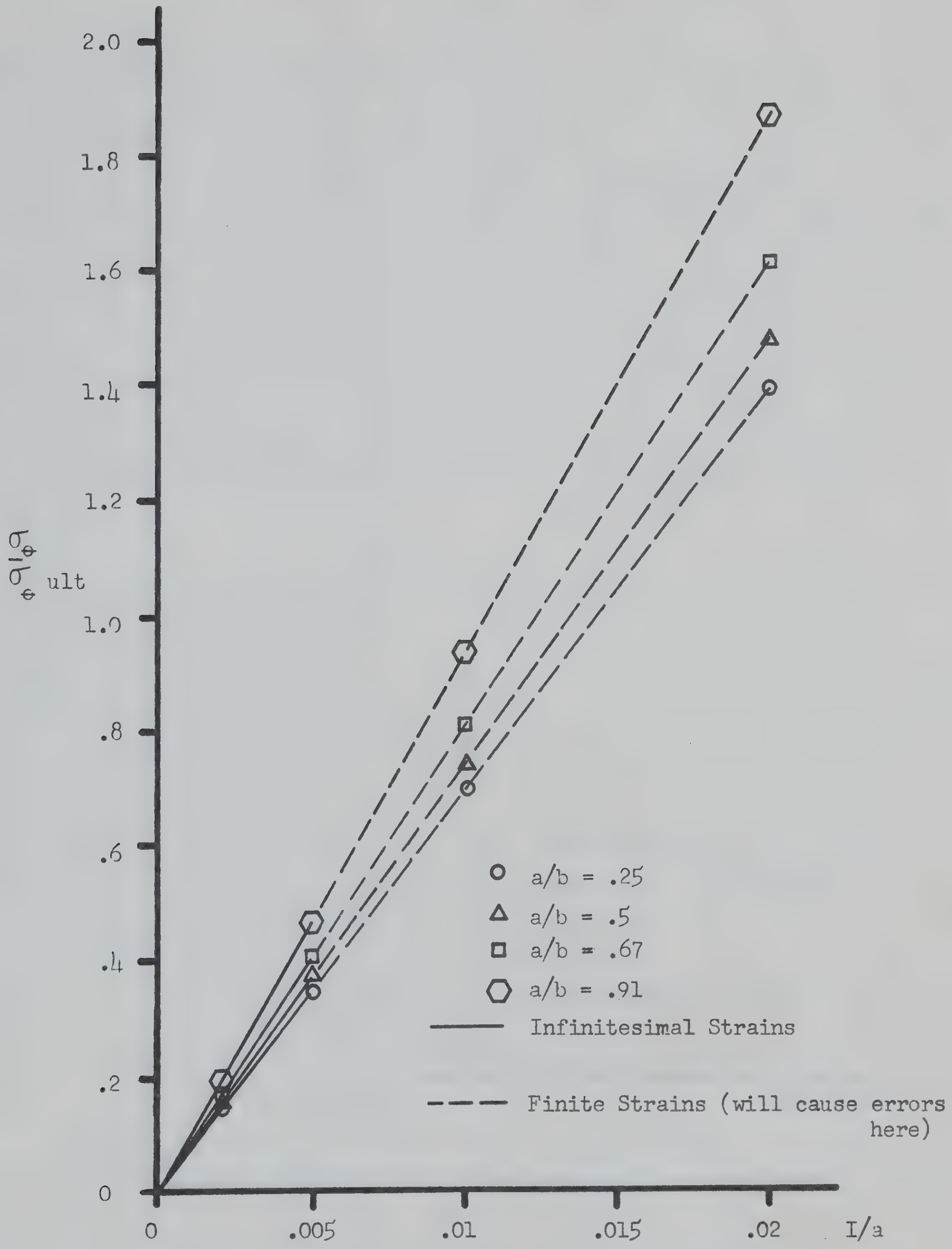

Figure 33. Hoop Stress vs Interference Fit After Rod Insertion.

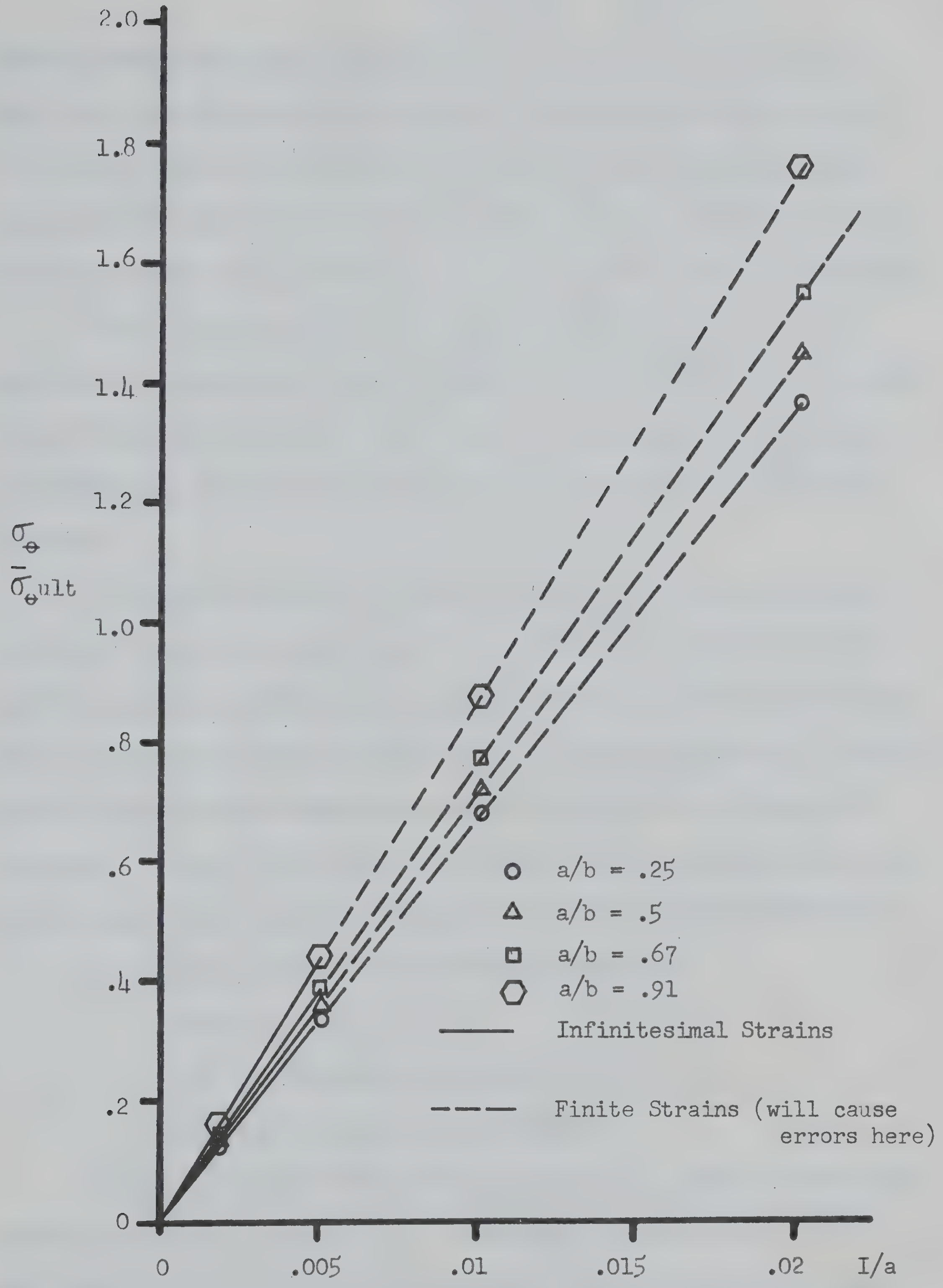

Figure 34. Hoop Stress vs Interference Fit During Rod Insertion.

maximum hoop stress was found to occur near the tip of the rod in each case and the maximum hoop stress varied linearly with the ratio of interference fit to internal bone radius. The magnitude of the maximum hoop stress under these conditions (shear applied) was found to be less than the magnitude for the corresponding case without shear.

Such plots as those which occur in Figures 33 and 34 could possibly be drawn up for various bones, sizes of bones, similar bones in different age groups etc. and could be beneficial in orthopedics; providing easy to use, quickly accessible estimates of maximum bone stresses.

The second problem is that of a bovine bone with a prosthetic rigid cap fixed on one end (as if it were glued). An axial force is applied causing an axial stress at the interface of the bone and cap. This is similar to the situation found at the bone prosthesis interface of an artificial knee joint when weight is placed on the leg as in standing. In the first case a flat rigid cap was analysed and in the second case a cap hemispherical across the bone wall was analysed.*

The boundary conditions for these cases are:

at $z/z_o = 0$, $\sigma_z = p_z$
at the bone-cap interface $u = v = 0$
all other boundaries are free.

Figure 35 contains plots of σ_r/p_z and σ_θ/p_z versus r/b at the bone-cap interface and at $z/z_o = .9$ for the flat cap (solid lines) and the hemispherical cap (dashed lines). Both the radial and hoop stresses approached zero as z/z_o approached zero.

---

* The toroidal cap is hereafter called a hemispherical cap.

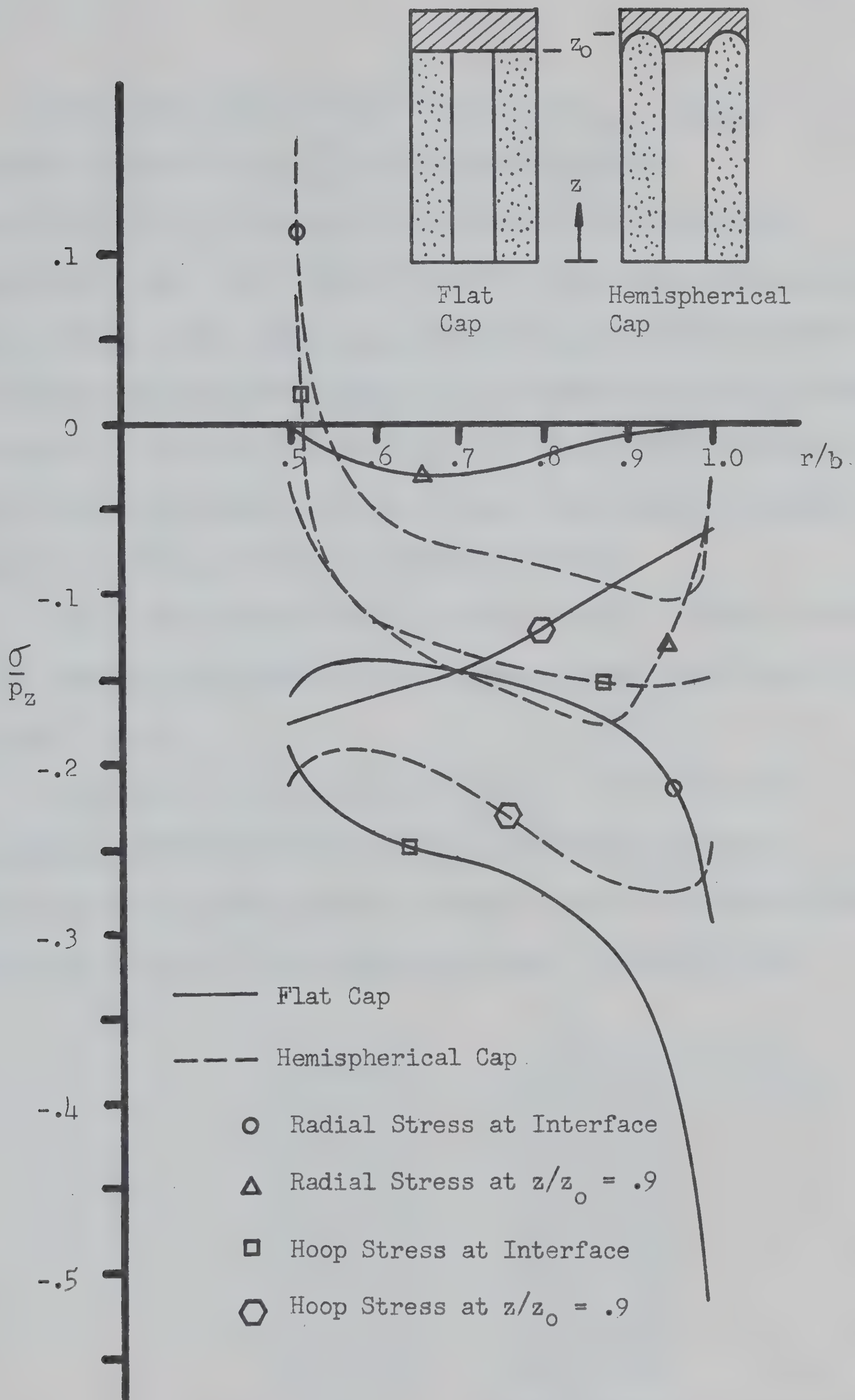

Figure 35. Radial and Hoop Stress for Capped Bone.

Figure 36 contains plots of σ_z/p_z and τ_{rz}/p_z versus r/b at the bone-cap interface, at $z/z_0 = .9$. Again the solid lines indicate the flat cap and the dashed lines indicate the hemispherical cap. This figure indicates that there are axial stress concentrations at the inner and outer radii of the bone for both caps, but that the average axial stress at the interface is less for the hemispherical cap than for the flat cap. This is due to some of the axial force being taken up in the form of shear stress along the interface in the case with the hemispherical cap.

Figure 35 indicates that the average radial and hoop stresses at the interface are smaller for the hemispherical cap as well as the axial stress.

Plots such as these could be helpful in the design of prostheses, pointing out areas of high stress and giving an indication of the best prosthetic shapes to use to eliminate stress concentrations or to lower average stresses in problem areas.

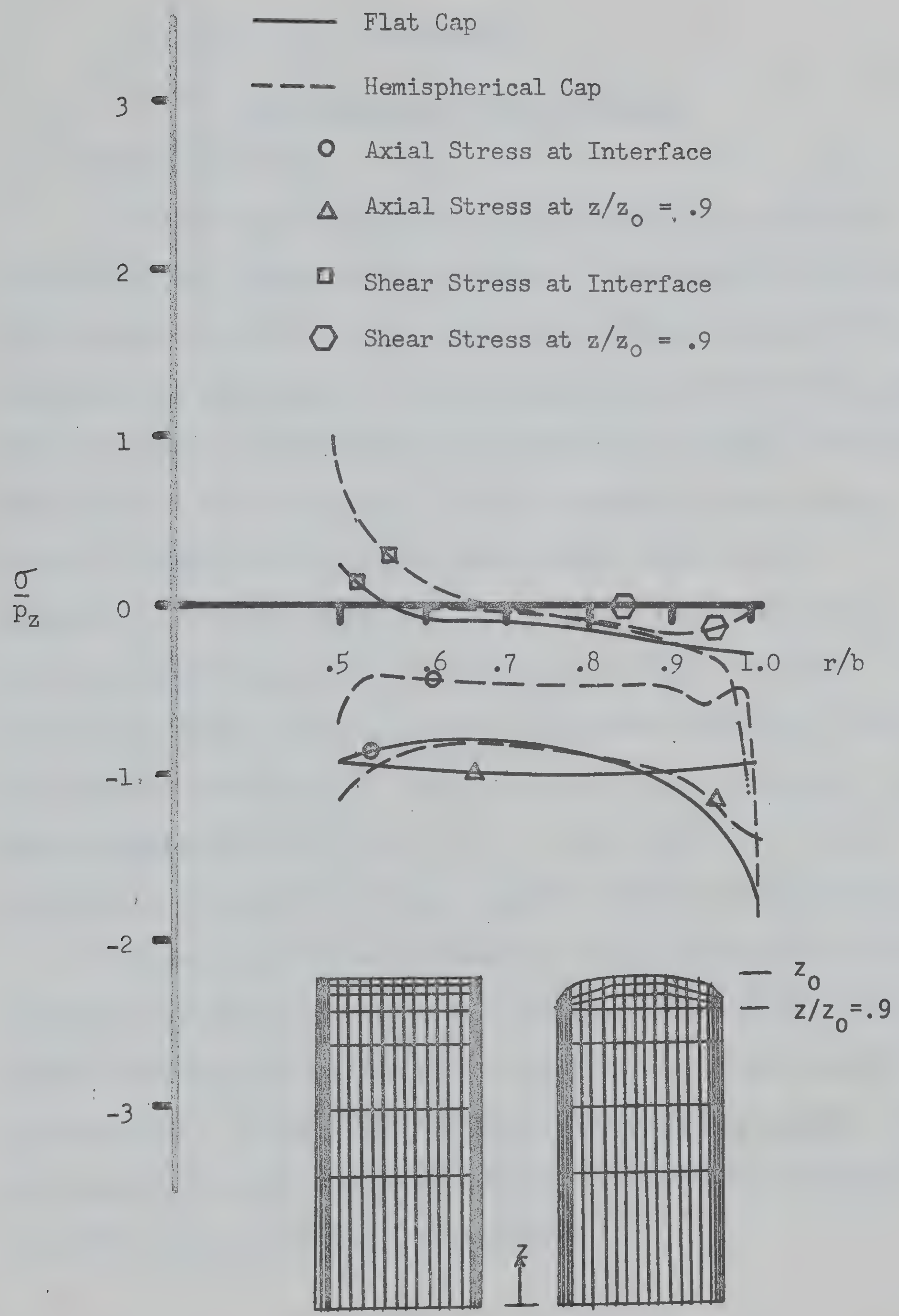

Flat
cap grid

Hemispherical
cap grid

Figure 36. Axial and Shear Stress for Capped Bone.

CHAPTER V

CONCLUSIONS AND FUTURE RESEARCH

5.1 Conclusions

A finite element program capable of modelling axisymmetric linearly elastic bodies under axisymmetric loadings was developed. This program was shown to give reasonably accurate results for both isotropic and anisotropic cylinders subjected to internal pressure. The program was applied to the solution of two problems, the results for which are given in Chapter IV. The accuracy of these results should in general be as good as the accuracy shown for the anisotropic cylinders under internal pressure as similar grids, cylinder geometry and elastic properties were used throughout. Larger errors than normal may be expected to occur at points where stresses are changing rapidly (e.g. at the tip of the rod in problem 1) and where singularities exist (e.g. at $r = a$ or b and $z/z_0 = 1$ for problem 2.) The results in these instances should be taken with caution.

The results obtained in Chapter IV show that within the limitations imposed by assumptions, this method could be useful as an aid for future prosthesis design and in the analysis of stresses and strains in long bones. As most real bones are not adequately modeled under the assumptions used here, more research is needed to eliminate the need for as many assumptions as possible.

5.2 Future Research

To model adequately the geometry of some parts of long bones and of many other bones, a three dimensional anisotropic element (e.g. a curvilinear hexahedron) should be developed. As well as adequate geometric representation, such an element would be able to model non-axisymmetric loading conditions and could to a certain extent account for regional differences in the material properties of bone. This is because each element may be given different properties.

More information on the material properties of different bones and positions in bones is needed. In particular, estimates of Young's moduli and Poisson's ratios for the radial, tangential and axial directions in long bones are required to predict accurately stresses and strains in these bones.

Present commonly used failure theories (Tresca and Von Mises) [18] do not take into account hydrostatic pressure which may produce distortion in anisotropic materials. A failure theory for anisotropic materials should be developed to aid in the design of prosthesis which will not cause bone failure.

BIBLIOGRAPHY

1. Evans, F.G., Stress and Strain in Bones, 1957, Ryerson Press, Toronto.

2. Kraus, H., Farfan,H.,and Jones,T.,"Stress Analysis of Human Invertebral Discs", Proceedings of the 25th Annual Conference on Engineering in Medicine and Biology, 1972, Vol. 14, pp. 242.

3. Zienkiewicz, O.C., The Finite Element Method in Engineering Science, 1971, McGraw-Hill, London.

4. Hearman, R., Applied Anisotropic Elasticity, 1961,Oxford University Press, London.

5. Tong, P., and Pian,T.,"The Convergence of Finite Element Method in Solving Linear Elastic Problems", International Journal of Solids and Structures, Vol. 3, 1967, pp. 865-879.

6. Wang, C., Applied Elasticity, 1953, McGraw-Hill, London.

7. Bird, F., Becker, H., Healer, J., and Messer, M., "Experimental Determination of the Mechanical Properties of Bone", Journal of Aerospace Medicine, 1968, pp. 44-48., Vol.39

8. McElhaney, J.H., "Dynamic Response of Bone and Muscle Tissue", Journal of Applied Physiology, 1966, pp. 1231-1236.,Vol. 21

9. Dempster, W.T., and Coleman,R.,"Tensile Strength of Bone Along and Across the Grain", Journal of Applied Physiology, 1961, pp. 355-360.,Vol. 16.

10. Evans, F.G., and Vincentelli, R., "Relation of Collagen Fiber Orientation to Some Mechanical Properties of Human Cortical Bone", Journal of Biomechanics, Vol. 2, 1969, pp. 63-71.

11. Evans, F.G., and Lebow, M., "Regional Differences in Some of the Physical Properties of the Human Femur", Journal of Applied Physiology, Vol. 3, 1951, pp. 563-572.

12. Amtmann, E., "The Distribution of Breaking Strength in the Human Femur Shaft", Journal of Biomechanics, Vol. 1, 1968, pp. 271-277.

13. Lugassy, A.A., Ph.D. Thesis, University of Pennsylvania, 1968.

14. Fung, Y.C., Perrone, N., and Anliker, M., Biomechanics, Its Foundations and Objectives, 1972, Prentice Hall, New Jersey.

15. Desai, C.S., and Abel, J., Introduction to the Finite Element Method, 1972, Van Nostrand Reinhold, New York.

16. Washizu, K., Variational Methods in Elasticity and Plasticity, 1968, Pergamon Press.

17. Klenerman, S.A.V., Swanson, S., and Freeman, M., "A Method for the Clinical Estimation of the Strength of a Bone", Proceedings of the Royal Society of Medicine, Vol. 60, 1967, pp. 10-14.

18. Hill, R., The Mathematical Theory of Plasticity, 1950, Oxford University Press, London.

19. Murray, D., CST-F E VERS1, "Simple Two Dimensional Finite Element Program". U. of Alta., Civil Eng. Department.

20. Akin, J.E., Fenton, D., and Stoddart, W., The Finite Element Method, A Bibliography of its Theory and Applications, 1972, University of Tennessee.

21. Luré, A.I., Three Dimensional Problems of the Theory of Elasticity, 1964, Interscience Publishers, New York.

22. Charnley, J., The Closed Treatment of Common Fractures, 1950, E. and S. Livingstone Ltd., Edinburgh.

APPENDIX I

BASICS OF FINITE ELEMENT DISPLACEMENT METHOD [3]

Conventional engineering structures can be visualized as an assemblage of structural elements interconnected at a discrete number of nodal points. If the force-displacement relationships for the individual elements are known, it is possible to derive the properties and study the behaviour of the assembled structure.

In an elastic continuum there are an infinite number of interconnection points and here lies the biggest difficulty in obtaining a numerical solution (e.g. for stresses or strain) for the continuum. The concept of finite elements attempts to overcome this difficulty by assuming the real continuum to be divided into elements interconnected at only a finite number of nodal points at which some fictitious forces, representative of the distributed stresses actually acting on the element boundaries, are supposed to be introduced. This idealization reduces the problem to that of a conventional structural type which may be treated numerically.

Using the displacement approach, this may be done in the following manner:

a) The continuum is separated by imaginary lines on surfaces into a number of 'finite elements'.

b) The elements are assumed to be connected at a discrete number of nodal points situated on their boundaries. The displacements of these nodal points, $\{\delta\}$, are the basic unknown parameters of the problem.

c) A function (or functions), $\{\phi\}_u$, is chosen to define uniquely the state of displacement within each 'finite element' in terms of its nodal displacements.

e.g. for the case $\{\delta\} = \left\{\begin{matrix}\underline{u}\\ \underline{v}\end{matrix}\right\}$

$\{\tilde{u}\} = \{\phi\}_u^T\,\{\underline{u}\}$ and

$\{\tilde{v}\} = \{\phi\}_u^T\,\{\underline{v}\}$

where $\{\tilde{u}\}$ and $\{\tilde{v}\}$ are general internal displacements and $\{\underline{u}\}$ and $\{\underline{v}\}$ are nodal displacements.

This function must impose compatible deformations on the structure, i.e. always satisfying geometry and boundary conditions.

Note: For an isoparametric element $\{\phi\}_u = \{\phi\}_G = \{\phi\}$ where $\{\phi\}_G$ is a function or functions giving the relation between coordinate locations in the deformed element. e.g: $\{\tilde{r}\} = \{\phi\}_G^T\{\underline{r}\}$

$\{\tilde{z}\} \quad \{\phi\}_G^T\{\underline{z}\}$

where $\{\tilde{r}\}$ and $\{\tilde{z}\}$ are the coordinate locations in the deformed element. In the above equations $\{\underline{r}\}$ and $\{\underline{z}\}$ are the nodal coordinates of the deformed element.

d) The displacement functions now define uniquely the state of strain within an element in terms of the nodal displacements

$$\{\tilde{\varepsilon}\} = [B]\{\delta\} \tag{A1.1}$$

These strains together

with any initial strains and the elastic properties of the material will define the state of stress throughout the element and hence also on its boundaries.

e) A system of forces concentrated at the nodes and equilibrating the boundary stresses and any distributed loads is determined, resulting in a stiffness relationship for the structure.

To make the nodal forces statically equivalent to the actual boundary stresses and distributed loads, the simplest procedure is to impose an arbitrary nodal displacement and to equate the external and internal work done by the various forces and stresses during that displacement. This is the principle of virtual work.

Let such a virtual displacement be $d\{\delta\}^e$ at the nodes. This results in displacements and strains within the element equal to

$$d\{f\} = [N]d\{\underline{\delta}\}^e \tag{A1.2}$$

and

$$d\{\tilde{\varepsilon}\} = [B]d\{\underline{\delta}\}^e \tag{A1.3}$$

respectively as:

$$\{\underline{f}\} = [N]\{\delta\}^e = [N_i, N_j, N_m \ldots] \begin{pmatrix} \delta_i \\ \delta_j \\ \delta_m \\ \vdots \end{pmatrix}^e \tag{A1.4}$$

= vector of displacements at any point within the element.

and

$$\{\tilde{\varepsilon}\} = \begin{pmatrix} \varepsilon_i \\ \varepsilon_j \\ \varepsilon_m \\ \vdots \end{pmatrix} = [B]\{\delta\}^e = \text{vector of nodal strains.} \tag{A1.5}$$

where $$[N] = \begin{bmatrix}\phi & 0\\ 0 & \phi\end{bmatrix} \qquad \text{(A1.6)}$$

and superscript e designates elemental properties.

The work done by the nodal forces is equal to the sum of the products of the individual force components and corresponding displacements,

i.e. $$(d\{\delta\}^e)^T \cdot \{F\}^e \qquad \text{(A1.7)}$$

where $$\{F\}^e = \begin{pmatrix} F_i \\ F_j \\ \vdots \end{pmatrix}$$

are nodal forces statically equivalent to the boundary stresses and distributed loads on the element. Similarly the internal work per unit volume done by the stresses and distributed forces is:

$$d\{\tilde{\varepsilon}\}^T\{\sigma\} - d\{\delta\}^T\{p\} \qquad \text{(A1.8)}$$

where $\{\sigma\}$ is the stress vector = $[C]\{\tilde{\varepsilon}\}$ (no initial strains or stresses)

$\{p\}$ is the vector of distributed loads acting on a unit volume of material within the element with directions corresponding to those of $\{\delta\}$ at that point,

or $$(d\{\delta\}^e)^T([B]^T\{\sigma\} - [N]^T\{p\}) \qquad \text{(A1.9)}$$

Equating the external work with the internal work obtained by integrating over the volume of the element:

$$(d\{\delta\}^e)^T\{F\}^e = (d\{\delta\}^e)^T\left(\int[B]^T\{\sigma\}d(VOL) - \int[N]^T\{p\}d(VOL)\right) \qquad \text{(A1.10)}$$

As this relation is valid for any value of the virtual displacement, the equality of the multipliers must exist.

$$\therefore \quad \{F\}^e = \left(\int[B]^T[C][B]d(VOL)\right)\{\delta\}^e - \int[N]^T\{p\}d(VOL) \qquad \text{(A1.11)}$$

This relation can be recognized as one typical of characteristics of any structural element in the form:

$$\{F\}^e = [K]^e\{\delta\} + \{F\}_p^e \tag{A1.12}$$

Comparing the two:

$$[K]^e = \int [B]^T[C][B]d(VOL) = \text{the element stiffness matrix} \tag{A1.13}$$

and nodal forces due to distributed loads are

$$\{F\}_p^e = -\int [N]^T\{\rho\}d(VOL) \,. \tag{A1.14}$$

In general, external concentrated forces may exist at the nodes and the matrix

$$\{R\} = \begin{pmatrix} R_1 \\ R_2 \\ \vdots \\ R_n \end{pmatrix}$$

will be added to the consideration of equilibrium at the nodes.

If at the boundary, displacements are specified, no special problem arises, however, if the boundary is subject to a distributed loading, say {g} per unit area, a loading term on the nodes of the element which has a boundary face will have to be added. By the virtual work consideration, this will simply result in

$$\{F\}_b^e = -\int [N]^T\{g\}d(\text{area}) \tag{A1.15}$$

An integration of this type is seldom explicitly carried out. Often by 'physical intuition' the analyst will consider the boundary loading to be represented simply by concentrated loads acting on the boundary nodes and calculate these by direct static procedures.

Once the nodal displacements have been determined by solution of the overall 'structural' type equations, the stresses at any point in the element can be found from:

$$\{\sigma\} = [C][B]^e\{\delta\}^e \tag{A1.16}$$

This development for an element may be applied directly to the whole continuum, that is let:

$$\{f\} = [\bar{N}]\{\delta\} \tag{A1.17}$$

in which $\{\delta\}$ list all the nodal points and $\bar{N}_i = N_i^e$ when the point concerned is within a particular element e and i is a point associated with that element. If point i does not occur within the element, $\bar{N}_i = 0$. Matrix [B] will follow a similar definition and the virtual work principle will be now applied to the whole structure. Interelement forces no longer need be considered and external virtual work during any virtual displacement of all nodes $d\{\delta\}$ becomes

$$d\{\delta\}^T\{R\} \tag{A1.18}$$

while the internal virtual work is

$$\int_V d\{\tilde{\varepsilon}\}^T\{\sigma\}d(\mathrm{VOL}) - \int_V d\{f\}^T\{p\}d(\mathrm{VOL}) - \int d\{f\}^T\{g\}d\ (\mathrm{area}) \tag{A1.19}$$

where the integrals are now taken over the whole region.

On substitution of

$$d\{f\} = [\bar{N}]d\{\delta\} \text{ and } d\{\tilde{\varepsilon}\} = [\bar{B}]d\{\delta\}$$

together with $\{\sigma\} = [C]\{\delta\}$

we have immediately on equating internal and external virtual work

$$[K]\{\delta\} + \{F\}_p + \{F\}_b - \{R\} = 0 \tag{A1.20}$$

and typical terms of the stiffness matrix become

$$[K_{ij}] = \int [\bar{B}]_i [C][\bar{B}_j] d(\text{VOL}) \tag{A1.21}$$

with the integral being taken over the whole region.

Considering, however, the relationship between $[\bar{B}]_i$ and $[B]_i$ it is obvious that

$$[K_{ij}] = \Sigma [K_{ij}]^e \tag{A1.22}$$

The same can be shown to be true of the various force components.

The principle of virtual displacements ensures satisfaction of equilibrium conditions within the limits prescribed by the assumed displacement pattern. If the number of parameters of $\{\delta\}$ which describes the displacement increases without limit then ever closer approximation of all equilibrium conditions can be ensured.

The virtual work principle can be restated in a different form. Equating (18) and (19):

$$\int d\{\tilde{\varepsilon}\}^T \{\sigma\} d(\text{VOL}) - [d\{\delta\}^T R + \int d\{f\}^T \{p\} d(\text{VOL}) + \int d\{f\}^T \{g\} d(\text{area})] = 0 . \tag{A1.23}$$

The first term of (23) is the variation of strain energy of the structure while the second is the variation of the potential energy of the external loads.

Equation (23) means that for equilibrium to be ensured the total potential energy must be stationary for variations of admissible displacements. The finite element equations developed previously are the statements of this variation with respect to displacements constrained to a finite number of parameters $\{\delta\}$.

It can be shown that in elastic situations the total potential energy is not only stationary but is a minimum [16]. Thus the finite element process seeks such a minimum within the constraint of an assumed displacement pattern.

APPENDIX II

ELASTIC OPEN ENDED CYLINDER SOLUTIONS

Considering cross-sections that are far enough away from the cylinder ends such that planes before cylinder distortion remain planes after distortion, stresses and strains are functions of the radial coordinate only. Therefore equation 2.4 becomes:

$$r \frac{d\varepsilon_\theta}{dr} + \varepsilon_\theta - \varepsilon_r = 0 \qquad \text{(A2.1)}$$

As the cylinder is open ended, $\sigma_z = 0$ everywhere. Therefore, from equations 2.5

$$\varepsilon_\theta = C_1\sigma_\theta + C_2\sigma_r \qquad \text{(A2.2)}$$

$$\varepsilon_r = C_2\sigma_\theta + C_3\sigma_r$$

where $C_1 = 1/E_\theta$, $C_2 = -\nu_{r\theta}/E_r$, $C_3 = 1/E_r$

and $$\frac{d\varepsilon_\theta}{dr} = C_1 \frac{d\sigma_\theta}{dr} + C_2 \frac{d\sigma_r}{dr} \ .$$

Substituting into equation (A2.1) gives:

$$r(C_1 \frac{d\sigma_\theta}{dr} + C_2 \frac{d\sigma_r}{dr}) + C_1\sigma_\theta + C_2\sigma_r - C_2\sigma_\theta - C_3\sigma_r = 0 \ . \qquad \text{(A2.3)}$$

Choosing

$$\sigma_r = \frac{1}{r}\frac{\partial\psi}{\partial r} = \frac{1}{r}y$$

$$\sigma_\theta = \frac{\partial^2\psi}{\partial r^2} = y' \qquad \text{(A2.4)}$$

$$\frac{d\sigma_r}{dr} = \frac{1}{r}y' - \frac{1}{r^2}y$$

$$\frac{d\sigma_\theta}{dr} = y''$$

the equilibrium equations (2.2) are satisfied identically.

Substituting (A2.4) into (A2.3) and collecting terms gives:

$$y'' + \frac{1}{r} y' - \frac{C_3}{C_1 r^2} y = 0 \ . \qquad \text{(A2.5)}$$

Let $\xi = \ln r$ (A2.6)

then $y' = \frac{1}{r}\frac{dy}{d\xi}$, $y'' = \frac{1}{r^2}(\frac{d^2y}{d\xi^2} - \frac{dy}{d\xi})$

Substituting into (A2.5), multiplying by r^2 and collecting terms gives:

$$\frac{d^2y}{d\xi^2} - \frac{C_3}{C_1} y = 0 \qquad \text{(A2.7)}$$

which is an ordinary differential equation with constant coefficients to which the solution is:

$$y = A_1 e^{\sqrt{C_4}\xi} + A_2 e^{-\sqrt{C_4}\xi} \qquad \text{(A2.8)}$$

where $C_4 = C_3/C_1$, and A_1 and A_2 are constants

or, using (A2.6)

$$y = A_1 \, r^{\sqrt{C_4}} + A_2 r^{-\sqrt{C_4}} \ . \qquad \text{(A2.9)}$$

For an open ended cylinder under internal pressure only the boundary conditions are:

$$\begin{aligned} &\text{at } r = a, \quad \sigma_r = \frac{1}{a} y(a) = -p \\ &\text{at } r = b, \quad \sigma_r = \frac{1}{b} y(b) = 0 \end{aligned} \qquad \text{(A2.10)}$$

where p is the internal pressure. Substituting these into (A2.9) gives:

$$-ap = A_1 a^{\sqrt{C_4}} + A_2 a^{-\sqrt{C_4}} \tag{A2.11}$$

$$0 = A_1 b^{\sqrt{C_4}} + A_2 b^{-\sqrt{C_4}} \quad . \tag{A2.12}$$

Multiplying (A2.12) by $a^{-\sqrt{C_4}}/b^{-\sqrt{C_4}}$ and subtracting this from (A2.11) yields:

$$A_1 = (-ap\ b^{-\sqrt{C_4}})/D \tag{A2.13}$$

where $D = a^{\sqrt{C_4}}\ b^{-\sqrt{C_4}} - b^{\sqrt{C_4}} a^{-\sqrt{C_4}}$.

Substituting (A2.13) into (A2.12) and solving for A_2 gives:

$$A_2 = (ap\ b^{\sqrt{C_4}})/D \ . \tag{A2.14}$$

Substituting (A2.13) and (A2.14) into (A2.9):

$$y = \frac{ap}{D}\left(b^{\sqrt{C_4}} r^{-\sqrt{C_4}} - b^{-\sqrt{C_4}} r^{\sqrt{C_4}}\right) . \tag{A2.15}$$

Therefore from (A2.14) and (A2.15)

$$\sigma_r = \frac{ap}{rD}\left(b^{\sqrt{C_4}} r^{-\sqrt{C_4}} - b^{-\sqrt{C_4}} r^{\sqrt{C_4}}\right) \tag{A2.16}$$

$$\sigma_\theta = \frac{-ap\sqrt{C_4}}{rD}\left(b^{\sqrt{C_4}} r^{-\sqrt{C_4}} + b^{-\sqrt{C_4}} r^{\sqrt{C_4}}\right) \quad . \tag{A2.17}$$

From equations (A2.2) $C_4 = E_\theta/E_r$.

For isotropy $C_4 = 1$ and (A2.16) and (A2.17) reduce to the Lamé equations:

$$\sigma_r = a^2 p \left(\frac{b^2/r^2 - 1}{a^2 - b^2}\right) \tag{A2.18}$$

$$\sigma_\theta = -a^2 p \left(\frac{b^2/r^2 + 1}{a^2 - b^2}\right) \quad . \tag{A2.19}$$

APPENDIX III

FINITE ELEMENT PROGRAM

This program performs a finite element analysis for linear, elastic axisymmetric problems using an eight degree of freedom isoparametric quadrilateral element. It outputs displacements, element stresses, element principal stresses, maximum principal stresses, nodal stresses, non-dimensional nodal stresses, and nodal corrections due to weight of element material. The flow chart, showing all subroutines, is presented in Figure 37.

3.1 Explanation of Subroutines

MAIN - Calls other subroutines in order.

READIN - Reads and prints input data. Generates intermediate nodes and elements. Calculates half-band width and number of equations.

ASTIF - Forms the element stress-strain matrix if one material only is used. Assembles the element stiffness matrices into STIF. Assembles the applied load vector.

ELSTIF - Forms the element stress strain matrix if more than one material is used. Forms the element stiffness matrix for each element in turn.

BETA - Forms the element strain-displacement matrix and element stress matrix for each element in turn.

MODIFY - Modifies the stiffness matrix and applied load vector for displacement boundary conditions.

BAND1 - Solves for and writes displacements using a Gaussian elimination technique for symmetric banded matrices.

STRESS - Computes nodal and elemental stresses, element principal stresses and directions and characteristic nodal stresses.

3.2 Definition of Variables

The major arrays and variables used in the code are defined below.

AP - applied load vector

DJ - determinate of the Jacobian

EBM - matrix [B]

ECM - constitutive matrix [C]

ER - Young's modulus in the radial direction

ESM - element stress matrix [C][B]

ESMRC - matrix $[C][B]2\pi r$

ESTIF - element stiffness matrix $[K]^e$

ET - Young's modulus in the tangential direction

EZ - Young's modulus in the axial direction

ISODIM - 1 for isotropic material, 2 for anisotropic material

KODE - index of displacement or load conditions

M - element number

MAT - material number

MBAND=MM - half-band width

NEQ = NN- number of equations

NCW - number of corners of an element where weight compensation is required.

NODE - nodal point number

NP - element node number

NUMAT - number of materials

NUMEL - number of elements

NUMNP - number of nodal points

PRRT - Poissons ratio $\nu_{r\theta}$

PRRZ - Poissons ratio ν_{rz}

PRTZ - Poissons ratio $\nu_{\theta z}$

R - radial coordinate of node

RAD - radial coordinate in an element

RCHAR - characteristic radius

RO - unit material weight

SIGRO - radial stress

SIGRZO - shearing stress τ_{rz}

SIGTO - tangential stress

SIGZO - axial stress

SRCHAR - characteristic radial stress

STCHAR - characteristic tangential stress

STIF - stiffness matrix [K]

SZCHAR - characteristic axial stress

TUCHAR - characteristic shearing stress

U - radial displacement or force

V - axial displacement or force

WP - nodal weight compensation term

WT - one quarter of the element weight

Z - axial coordinate of node

ZCHAR - characteristic radius

3.3 Guide for Data Input

(i) Input

a) Heading Card (1 card)(FORMAT 18A4)

b) Problem Card (1 card)(FORMAT 3I6)

NUMNP	NUMEL	NUMAT

c) Characteristics card (1 card)(FORMAT 6F12.4)

RCHAR	ZCHAR	SZCHAR	SRCHAR	STCHAR	TUCHAR

d) Material cards (1 for each material)(FORMAT 3F12.0, 4F6.0, I6)

ER	ET	EZ	PRRT	PRRZ	PRTZ	RO	ISODIM

e) Nodal point cards (FORMAT 2I6, 4F12.0)

NODE	KODE	R	Z	U	V

KODE 0 0 = R FORCE AND Z FORCE

1 1 = R DISPLACEMENT AND Z DISPLACEMENT

1 0 = R DISPLACEMENT AND Z FORCE

0 1 = R FORCE AND Z DISPLACEMENT

Nodal point cards must be in order.

If nodes are omitted, the program generates co-ordinates for intermediate nodal points and sets

KODE = 00, U = 0, V = 0 for these points.

f) Element Cards (FORMAT 6I6)

M	NP(1,M)	NP(2,M)	NP(3,M)	NP(4,M)	MAT(M)

Element cards must be in order. If elements are omitted, the program will generate intermediate elements given a starting and ending element if node numbers along corresponding sides increase steadily by one.

(ii) Progam Limitations

- Number of nodal points $\leq$ 400
- Number of elements $\leq$ 400
- Half-band width $\leq$ 80
- Number of materials $\leq$ 8
- Elements may not be used where their centroids lie on or outside their boundary.

3.4 Program Flow Chart

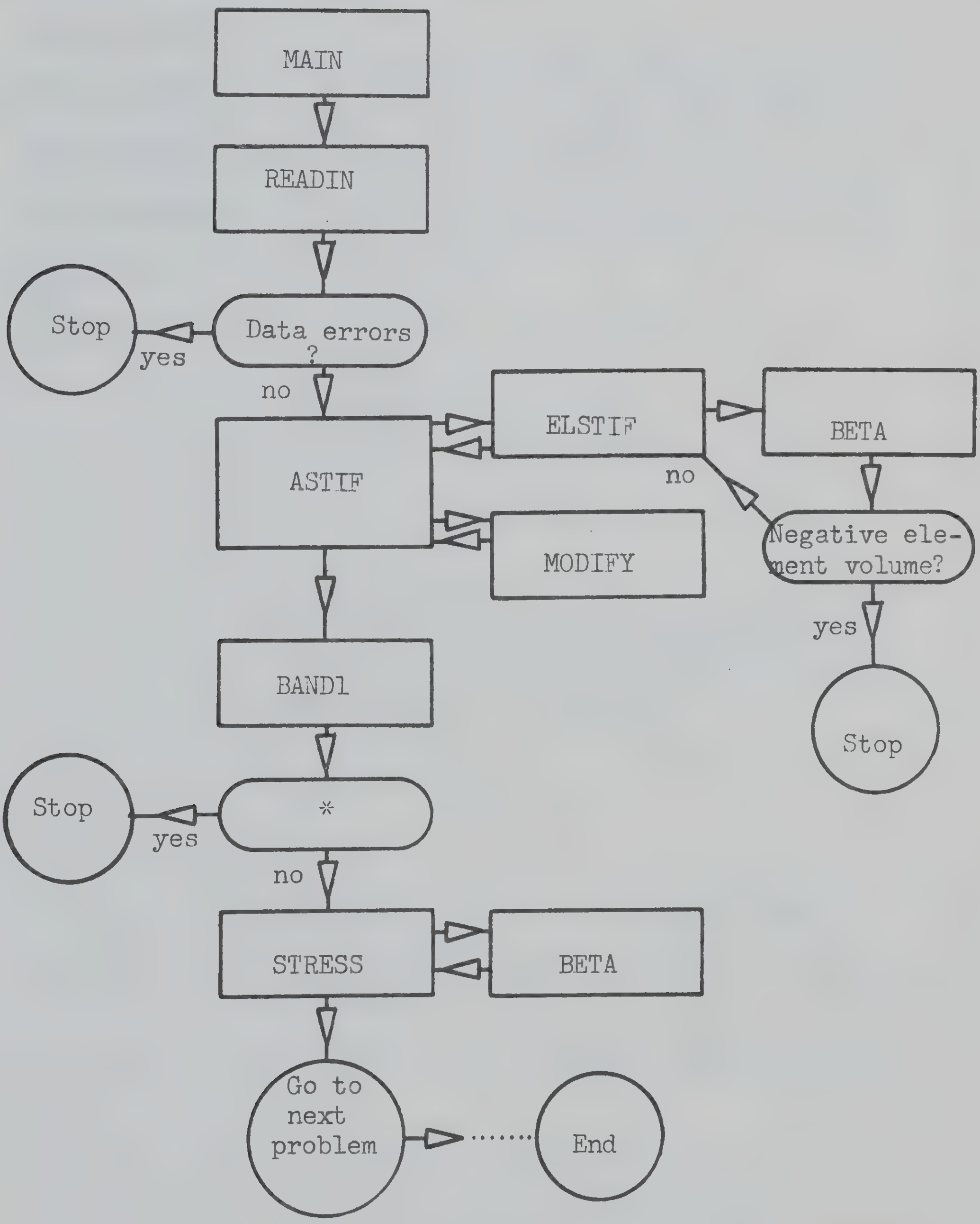

* Is there a zero or negative entry on the main diagonal of the triangularized matrix?

Figure 37. Program Flow Chart.

3.5 PROGRAM

```
      COMMON ER(8),ET(8),EZ(8),PRRT(8),PRRZ(8),PRTZ(8),
     1 Z(400),U(400),V(400),ISODIM(8),STIF(800,80)
      COMMON ECM(4,4),EBM(4,8),ESM(4,8),WT,NUMNP,NUMEL,
     1 NP(4,400),MAT(400),NEQ,MBAND,M,LM(8)
      COMMON RCHAR,ZCHAR,SZCHAR,SRCHAR,STCHAR,TUCHAR,
     1 RR(400),ZR(400),SIGZO(400),SIGRO(400),SIGTO(400)
      COMMON RO(8),R(400),AP(800),ESTIF(8,8),
     1NUMAT,KODE(400),SIGRZO(400)
C
1     CALL READIN
C
      CALL ASTIF
C
      CALL BAND1
C
      CALL STRESS
C
      GO TO 1
      END
```

```
      SUBROUTINE READIN
C
C  THIS SUBROUTINE READS AND PRINTS MATERIAL DATA,
C  NODAL DATA, ELEEMENT DATA. IT GENERATES
C  COORDINATES OF INTERMEDIATE NODAL POINTS AND
C  CALCULATES THE BAND WIDTH AND NUMBER OF
C  EQUATIONS
C
C
C
      COMMON ER(8),ET(8),EZ(8),PRRT(8),PRRZ(8),PRTZ(8),
     1 Z(400),U(400),V(400),ISODIM(8),STIF(800,80)
      COMMON ECM(4,4),EBM(4,8),ESM(4,8),WT,NUMNP,NUMEL,
     1 NP(4,400),MAT(400),NEQ,MBAND,M,LM(8)
      COMMON RCHAR,ZCHAR,SZCHAR,SRCHAR,STCHAR,TUCHAR,
     1 RR(400),ZR(400),SIGZO(400),SIGRO(400),SIGTO(400)
      COMMON RO(8),R(400),AP(800),ESTIF(8,8),
     1NUMAT,KODE(400),SIGRZO(400)
C
      DIMENSION HED(18)
C  READ PRELIMINARY INFORMATION
      READ(5,1000) HED,NUMNP,NUMEL,NUMAT
      WRITE(6,2000) HED,NUMNP,NUMEL,NUMAT
      READ(5,4000)RCHAR,ZCHAR,SZCHAR,SRCHAR,STCHAR,
     1TUCHAR
      WRITE(6,4010) RCHAR,ZCHAR,SZCHAR,SRCHAR,STCHAR,
     1TUCHAR
 4000 FORMAT (6F12.4)
 4010 FORMAT(//,'R CHARACTERISTIC =',F12.6/1H ,'Z CHAR
     1ACTERISTIC =',F12.6/1H ,'SIGMA Z CHARACTERISTIC
     2 =',F12.6/1H ,'SIGMA R CHARACTERISTIC =',F12.6/
     31H ,'SIGMA T CHARACTERISTIC =',F12.6/1H ,
     4 'SIGMA RZ CHARACTERISTIC =',F12.6// )
C
C  READ AND WRITE MATERIAL PROPERTIES
C
      WRITE(6,2005)
      DO 10 M=1,NUMAT
      READ(5,1010) ER(M),ET(M),EZ(M),PRRT(M),PRRZ(M),
     1PRTZ(M),RO(M),ISODIM(M)
   10 WRITE(6,2010) M,ER(M),ET(M),EZ(M),PRRT(M),PRRZ(M),
     1PRTZ(M),RO(M),ISODIM(M)
C
C  READ AND WRITE NODAL DATA AND GENERATE INTERMEDIATE
C  NODAL DATA
C
      WRITE(6,2014)
      WRITE(6,2015)
      L=1
      READ(5,1020) N,KODE(N),R(N),Z(N),U(N),V(N)
      GO TO 40
 20   READ(5,1020) N,KODE(N),R(N),Z(N),U(N),V(N)
      DN = N-L
      DR=(R(N)-R(L))/DN
```

```
      DZ=(Z(N)-Z(L))/DN
25    L=L+1
C
      IF(N-L) 50,40,30
 30   R(L)=R(L-1)+DR
      Z(L)=Z(L-1)+DZ
      KODE(L)= 0
      U(L)  = 0
      V(L)= 0
      GO TO 25
C
   40 WRITE(6,2020) N,KODE(N),R(N),Z(N),U(N),V(N)
      IF(NUMNP-N) 50,60,20
C
50    WRITE (6,2025) N
      CALL EXIT
C
   60 WRITE(6,2016)
      WRITE(6,2015)
      WRITE (6,2020)   (N,KODE(N),R(N),Z(N),U(N),V(N),
     1N=1,NUMNP)
C
C  READ AND WRITE ELEMENT DATA
C
      WRITE(6,2031)
      WRITE(6,2030)
      ML=0
51    IF (ML.GE.NUMEL)  GO TO 70
      READ(5,1035) M,NP(1,M),NP(2,M),NP(3,M),NP(4,M),
     1MAT(M)
      WRITE(6,2035)M,NP(1,M),NP(2,M),NP(3,M),NP(4,M),
     1MAT(M)
      MM=ML+1
      IF (MM.EQ.M)  GO TO 65
C
      MM1=M-1
      DO 63 I=MM,MM1
      DO 62 J=1,4
   62 NP(J,I)=NP(J,I-1)+1
      MAT(I)=MAT(I-1)
   63 CONTINUE
C
65    ML=M
      GO TO 51
70    CONTINUE
      WRITE(6,2032)
      WRITE(6,2030)
      WRITE(6,2035)  (M,(NP(J,M),J=1,4),MAT(M),
     1M=1,NUMEL)
C
C     DETERMINE BAND WIDTH AND NUMBER OF EQUATIONS
C
      L=0
      DO 80 M=1,NUMEL
```

```
      DO 80 I=1,3
      II=I+1
      DO 80 J=II,4
      K= IABS(NP(I,M)-NP(J,M))
      IF (K.GT.L)   L=K
80    CONTINUE
C
      MBAND = 2*(L+1)
      NEQ= 2*NUMNP
C
      WRITE(6,2040)MBAND,NEQ
      IF (MBAND.LE. 80.AND.NEQ.LE.800) GO TO 90
      WRITE(6,2050)
      CALL EXIT
C
90    WRITE(6,3000)
3000  FORMAT(  '  READIN COMPLETED ' ///)
      RETURN
C
C  FORMAT STATEMENTS
1000  FORMAT(18A4/ 3I6)
2000  FORMAT(1H1,10X,18A4,////
     1 1H ,     26H NUMBER OF NODAL POINTS = ,I6/
     2 1H ,     26H NUMBER OF ELEMENTS     = ,I6/
     3 1H ,     26H NUMBER OF MATERIALS    = ,I6)
2005  FORMAT(///,1H ,10X, 21H  MATERIAL PROPERTIES //
     11X,8HMAT.NO. ,4X,13HMODULOUS E(R),6X,4HE(T),6X,4
     2HE(Z),4X,21HPOISSONS RATIO PR(RT),5X,6HPR(ZR),
     35X,6HPR(ZT),4X,11HUNIT WEIGHT,4X,6HISODIM ,//)
 1010 FORMAT(3F12.0,4F6.0,I6)
2010  FORMAT(1H ,I5,F20.0,2F10.0,F24.3,2F11.3,F15.2,4X
     1,I6)
2014  FORMAT( '1',  5X, 'OUTPUT OF INPUT NODAL DATA ')
2015  FORMAT(///,10X,19H NODAL POINT OUTPUT,///
     11H ,' NODE   KODE     R CORD      Z COORD      R F
     2ORCE      Z FORCE'//)
 2016 FORMAT('1',5X,'OUTPUT OF COMPLETE NODAL DATA')
1020  FORMAT(2I6,4F12.0)
 2020 FORMAT (I4,I6,F13.6,3F12.6)
2025  FORMAT(1H0,28H ERROR IN NODAL DATA,NODE = ,I4)
2030  FORMAT(///,10X, 13H ELEMENT DATA ///,
     1' ELEM     I      J      K      L    MAT. NO.'//)
2031  FORMAT('1',5X, 'OUTPUT OF INPUT ELEMENT DATA' )
 2032 FORMAT('1',5X,'OUTPUT OF COMPLETE ELEMENT DATA')
 2035 FORMAT(I4,5I6)
 1035 FORMAT(6I6)
2040  FORMAT (///10X, 22H BAND WIDTH          = ,I6/
     1              10X, 22H NUMBER OF EQUATIONS = ,I6)
 2050 FORMAT(///10X,'PROBLEM EXCEEDS SPECIFIED LIMITS')
C
      END
```

```
      SUBROUTINE ASTIF
C
C  THIS SUBROUTINE TAKES EACH ELEMENT IN TURN AND
C  FORMS THE ELEMENT STIFFNESS MATRIX (BY CALLING
C  ELSTIF). IT ASSEMBLES THE ELEMENT STIFFNESSES INTO
C  STIF, ASSEMBLES THE APPLIED LOAD VECTOR (AP), AND
C  MODIFIES THE ASSEMBLAGES FOR DISPLACEMENT
C  BOUNDARY CONDITIONS (BY CALLING MODIFY)
C
      COMMON ER(8),ET(8),EZ(8),PRRT(8),PRRZ(8),PRTZ(8),
     1 Z(400),U(400),V(400),ISODIM(8),STIF(800,80)
      COMMON ECM(4,4),EBM(4,8),ESM(4,8),WT,NUMNP,NUMEL,
     1 NP(4,400),MAT(400),NEQ,MBAND,M,LM(8)
      COMMON RCHAR,ZCHAR,SZCHAR,SRCHAR,STCHAR,TUCHAR,
     1 RR(400),ZR(400),SIGZO(400),SIGRO(400),SIGTO(400)
      COMMON RO(8),R(400),AP(800),ESTIF(8,8),
     1NUMAT,KODE(400),SIGRZO(400)
      COMMON/SLOP/WP(800),NCW
C
C   INITIALIZE APPLIED LOAD VECTOR AND MASTER
C   STIFFNESS MATRIX AND ECM
C
      DO 10 I=1,NEQ
      WP(I)=0.0
      AP(I)=0.0
      DO 10 J=1,MBAND
10     STIF(I,J)=0.0
      DO 20 I=1,4
      DO 21 J=1,8
   21 EBM(I,J)=0.0
      DO 20 J=1,4
20    ECM(I,J)=0.0
C   FORM ELEMENT CONSTITUTIVE MATRIX (ECM) IF NUMAT=1)
C
      IF(NUMAT.NE.1) GO TO 30
      IF(ISODIM(1).NE.1) GO TO 22
      PR=PRRT(1)
      COM=ER(1)*(1.-PR)/((1.+PR)*(1.-2.*PR))
      COM1=PR/(1.-PR)
      ECM(1,1)=COM
      ECM(1,2)=COM1*COM
      ECM(1,3)=COM1*COM
      ECM(2,1)=COM1*COM
      ECM(2,2)=COM
      ECM(2,3)=COM1*COM
      ECM(3,1)=COM1*COM
      ECM(3,2)=COM1*COM
      ECM(3,3)=COM
      ECM(4,4)=COM*(1.-2.*PR)/(2.*(1.-PR))
      GO TO 30
C         ANISOTROPIC  CASE
   22 EPRRT=PRRT(1)
      EPRZT=PRTZ(1)
      EPRZR=PRRZ(1)
```

```
      VET=ET(1)
      VER=ER(1)
      VEZ=EZ(1)
      ERZ=VER/VEZ
      ETR=VET/VER
      ETZ=VET/VEZ
      COM=1./(1.-EPRRT**2*ETR-EPRZR**2*ERZ-EPRZT**2
     1*ETZ-2.*EPRZR*EPRZT*EPRRT*ETZ)
      G=VEZ/2.*(1.+EPRZR)
      ECM(1,1)=VEZ*(1.-EPRRT**2*ETR)*COM
      ECM(1,2)=(EPRZR*VER+EPRRT*EPRZT*VET)*COM
      ECM(1,3)=VET*(EPRZR*EPRRT+EPRZT)*COM
      ECM(2,2)=VER*(1.-EPRZT**2*ETZ)*COM
      ECM(2,3)=VET*(EPRRT+EPRZR*EPRZT*ERZ)*COM
      ECM(3,3)=VET*(1.-EPRZR**2*ERZ)*COM
      ECM(4,4)=G
      ECM(2,1)=ECM(1,2)
      ECM(3,1)=ECM(1,3)
      ECM(3,2)=ECM(2,3)
C
30    DO 45 M=1,NUMEL
C
      CALL ELSTIF
C
C   ASSEMBLE ELSTIF INTO MASTER STIFFNESS MATRIX
C
      DO 35 I=1,4
      I2=2*I
      LM(I2)=2*NP(I,M)
35    LM(I2-1)=LM(I2)-1
C
C
      DO 40 I=1,8
      II=LM(I)
      I1=I+3*(I/2)+4*(-I/7+I/6-I/5-I/3)
      DO 40 J=1,8
      JJ=LM(J)-II+1
      J1=J+3*(J/2)+4*(-J/7+J/6-J/5-J/3)
      IF (JJ.LE.0) GO TO 40
      STIF(II,JJ)=STIF(II,JJ)+ESTIF(I1,J1)
40    CONTINUE
C
C   ADD GRAVITY LOADS INTO WP VECTOR
C
      DO 45 I=2,8,2
      II=LM(I)
      WP(II)=WP(II)-WT
45    CONTINUE
C
C   MULTIPLY NODAL LOADS BY 2*PI*R  AND
C   ADD NODAL LOADS & GRAVITY LOADS INTO AP VECTOR
C
      DO 50 N=1,NUMNP
      IF(KODE(N)-1)46,47,48
```

```
46     V(N)=V(N)*2.*3.1416*ABS(R(N))
47     U(N)=U(N)*2.*3.1416*ABS(R(N))
   48 CONTINUE
      IF(KODE(N)-10) 51,49,51
49     V(N)=V(N)*2.*3.1416*ABS(R(N))
   51 N2=2*N
      AP(N2)=WP(N2)+V(N)
50     AP(N2-1)=AP(N2-1)+U(N)
C
C   MODIFY STIFFNESS AND LOAD VECTOR FOR DISPLACEMENT
C   BOUNDARY CONDITIONS
C
      NCW=0
      DO 102 N=1,NUMNP
      N2=2*N
      II=N2-1
      IF (KODE(N)-1) 100,80,60
   60 CALL MODIFY (II,N)
      IF (KODE(N).NE.11) GO TO 100
   80 CALL MODIFY (N2,N)
      NCW=NCW+1
      GO TO 102
  100 WP(N2)=0.0
  102 CONTINUE
C
      RETURN
      END
```

```
      SUBROUTINE ELSTIF
C  THIS SUBROUTINE FORMS THE ELEMENT STIFFNESS MATRIX
C  (ESTIF) FCR LINEAR STRAIN TRAPEZOID
C
      COMMON ER(8),ET(8),EZ(8),PRRT(8),PRRZ(8),PRTZ(8),
     1 Z(400),U(400),V(400),ISODIM(8),STIF(800,80)
      COMMON ECM(4,4),EBM(4,8),ESM(4,8),WT,NUMNP,NUMEL,
     1 NP(4,400),MAT(400),NEQ,MBAND,M,LM(8)
      COMMON RCHAR,ZCHAR,SZCHAR,SRCHAR,STCHAR,TUCHAR,
     1 RR(400),ZR(400),SIGZO(400),SIGRO(400),SIGTO(400)
      COMMON RO(8),R(400),AP(800),ESTIF(8,8),
     1NUMAT,KODE(400),SIGRZO(400)
      COMMON/BETTER/ RT(4),ZT(4),FIJ(4,4),DJ,RAD,
     1ESMRC(4,8)
C
C
      GP = 1.0/SQRT(3.0)
C
C  ACCUMULATES ELEMENT COORDINATE LOCATIONS
C
      DO 20 I=1,4
      J=NP(I,M)
      RT(I)=R(J)
   20 ZT(I)=Z(J)
C
C   FORM CONSTITUTIVE MATRIX
      NM=1
      IF (NUMAT.EQ.1) GO TO 30
      NM=MAT(M)
      IF(ISODIM(NM).NE.1) GO TO 22
      PR=PRRT(NM)
      COM=ER(NM)*(1.-PR)/((1.+PR)*(1.-2.*PR))
      COM1=PR/(1.-PR)
      ECM(1,1)=COM
      ECM(1,2)=COM1*COM
      ECM(1,3)=COM1*COM
      ECM(2,1)=COM1*COM
      ECM(2,2)=COM
      ECM(2,3)=COM1*COM
      ECM(3,1)=COM1*COM
      ECM(3,2)=COM1*COM
      ECM(3,3)=COM
      ECM(4,4)=COM*(1.-2.*PR)/(2.*(1.-PR))
      GO TO 30
C          ANISOTROPIC  CASE
   22 EPRRT=PRRT(NM)
      EPRZT=PRTZ(NM)
      EPRZR=PRRZ(NM)
      VET=ET(NM)
      VER=ER(NM)
      VEZ=EZ(NM)
      ERZ=VER/VEZ
      ETR=VET/VER
      ETZ=VET/VEZ
```

```
      COM=1./(1.-EPRRT**2*ETR-EPRZR**2*ERZ-EPRZT**2
     1*ETZ-2.*EPRZR*EPRZT*EPRRT*ETZ)
      G=VEZ/2.*(1.+EPRZR)
      ECM(1,1)=VEZ*(1.-EPRRT**2*ETR)*COM
      ECM(1,2)=(EPRZR*VER+EPRRT*EPRZT*VET)*COM
      ECM(1,3)=VET*(EPRZR*EPRRT+EPRZT)*COM
      ECM(2,2)=VER*(1.-EPRZT**2*ETZ)*COM
      ECM(2,3)=VET*(EPRRT+EPRZR*EPRZT*ERZ)*COM
      ECM(3,3)=VET*(1.-EPRZR**2*ERZ)*COM
      ECM(4,4)=G
      ECM(2,1)=ECM(1,2)
      ECM(3,1)=ECM(1,3)
      ECM(3,2)=ECM(2,3)
C       ZERO'S STIFFNESS MATRIX
   30 DO 19 I=1,8
      DO 19 J=1,8
   19 ESTIF (I,J)=0.0
      VOL=0.0
C
C     FORM ELEMENT STIFFNESS MATRIX (ESTIF)
C    DOES INTEGRATION QUADRANT BY QUADRANT
C    USING GAUSSE LEGENDRE QUADRATURE
C
      DO 28 K=1,4
      K1=-1+2*(K/2-2*(K/4))
      K2=-1+2*(K/3)
      EPS= FLOAT (K1)*GP
      PNU= FLOAT (K2)*GP
C
      CALL BETA(EPS,PNU)
      VOL=VOL+DJ
      DO 28 I=1,8
      DO 28 J=1,8
      DO 28 L=1,4
   28 ESTIF(I,J)=ESTIF(I,J)+EBM(L,I)*ESMRC(L,J)
      WT=VOL*3.1416*RAD*RO(NM)/2.0
      RETURN
C
C
C
      END
```

```
      SUBROUTINE BETA(EPS,PNU)
      COMMON ER(8),ET(8),EZ(8),PRRT(8),PRRZ(8),PRTZ(8),
     1 Z(400),U(400),V(400),ISODIM(8),STIF(800,80)
      COMMON ECM(4,4),EBM(4,8),ESM(4,8),WT,NUMNP,NUMEL,
     1 NP(4,400),MAT(400),NEQ,MBAND,M,LM(8)
      COMMON RCHAR,ZCHAR,SZCHAR,SRCHAR,STCHAR,TUCHAR,
     1 RR(400),ZR(400),SIGZO(400),SIGRO(400),SIGTO(400)
      COMMON RO(8),R(400),AP(800),ESTIF(8,8),
     1NUMAT,KODE(400),SIGRZO(400)
      COMMON/BETTER/ RT(4),ZT(4),FIJ(4,4),DJ,RAD,
     1ESMRC(4,8)
      R42=RT(4)-RT(2)
      Z42=ZT(4)-ZT(2)
      R31=RT(3)-RT(1)
      Z31=ZT(3)-ZT(1)
      RE34=(RT(3)-RT(4))*EPS
      ZE34=(ZT(3)-ZT(4))*EPS
      RE12=(RT(1)-RT(2))*EPS
      ZE12=(ZT(1)-ZT(2))*EPS
      RN41=(RT(4)-RT(1))*PNU
      ZN41=(ZT(4)-ZT(1))*PNU
      RN23=(RT(2)-RT(3))*PNU
      ZN23=(ZT(2)-ZT(3))*PNU
      EBM(1,5)=(R42+RE34+RN23)/8.0
      EBM(1,6)=(RN41-R31-RE34)/8.0
      EBM(1,7)=(R42+RE12+RN41)/(-8.0)
      EBM(1,8)=(R31+RE12-RN23)/8.0
      EBM(2,1)=-(Z42+ZE34+ZN23)/8.0
      EBM(2,2)=(Z31+ZE34-ZN41)/8.0
      EBM(2,3)=(Z42+ZE12+ZN41)/8.0
      EBM(2,4)=(ZN23-Z31-ZE12)/8.0
      DJ=0.
C
C   FORM ELEMENT B MATRIX (EBM)
C
      DO 25 I=1,4
      DJ=DJ+EBM(1,I+4)*ZT(I)
      EBM(4,I)=EBM(1,I+4)
   25 EBM(4,I+4)=EBM(2,I)
      IF (DJ.LE.0.) GO TO 75
      RAD=.25*((1.-EPS)*(1.-PNU)*RT(1)+(1.+EPS)*
     1(1.-PNU)*RT(2)+(1.+EPS)*(1.+PNU)*RT(3)+
     2(1.-EPS)*(1.+PNU)*RT(4))
      RAD=ABS(RAD)
      EBM(3,1)=DJ*(.25*(1.-EPS)*(1.-PNU))/RAD
      EBM(3,2)=DJ*(.25*(1.+EPS)*(1.-PNU))/RAD
      EBM(3,3)=DJ*(.25*(1.+EPS)*(1.+PNU))/RAD
      EBM(3,4)=DJ*(.25*(1.-EPS)*(1.+PNU))/RAD
C
C   FORM ELEMENT STRESS MATRIX (ESM)
C
      DO 27 I=1,4
      DO 27 J=1,8
      ESM(I,J)=0.0
```

```
      DO 26 L=1,4
   26 ESM(I,J)=ESM(I,J)+ECM(I,L)*EBM(L,J)
      ESM(I,J)=ESM(I,J)/DJ
   27 ESMRC(I,J)=ESM(I,J)*2.*3.1416*RAD
      RETURN
75    WRITE(6,1000) M
 1000 FORMAT(1H1,'VOLUME OF ELEMENT',I4,'IS LE
     1SS THAN ZERO')
      CALL EXIT
80    RETURN
      END
```

```
      SUBROUTINE BAND1
C
C  THIS SUBROUTINE SOLVES FOR DISPLACEMENTS USING A
C  GAUSSIAN ELIMINATION TECHNIQUE FOR SYMMETRIC
C  BANDED MATRICES STORED IN CORE
C
      COMMON ER(8),ET(8),EZ(8),PRRT(8),PRRZ(8),PRTZ(8),
     1 Z(400),U(400),V(400),ISODIM(8),   A(800,80)
      COMMON ECM(4,4),EBM(4,8),ESM(4,8),WT,NUMNP,NUMEL,
     1 NP(4,400),MAT(400),NN,MM,M,LM(8)
      COMMON RCHAR,ZCHAR,SZCHAR,SRCHAR,STCHAR,TUCHAR,
     1 RR(400),ZR(400),SIGZO(400),SIGRO(400),SIGTO(400)
      COMMON RO(8),R(400), B(800),ESTIF(8,8),
     1NUMAT,KODE(400),SIGRZO(400)
      DIMENSION NODNO(800)
C
C TRIANGULARIZE AND REDUCE RIGHT HAND SIDE
      NL=NN-MM+1
      NM=NN-1
      MR=MM
C
      DO 100 N=1,NM
      IF (A(N,1).LE.0.) GO TO 700
      BN=B(N)
      B(N)=BN/A(N,1)
      IF (N.GT.NL) MR=NN-N+1
C
      DO 100 L=2,MR
      IF (A(N,L).EQ.0.)GO TO 100
      C= A(N,L)/A(N,1)
      I= N+L-1
      J= 0
      DO 50 K=L,MR
      J=J+1
50    A(I,J)= A(I,J)-C*A(N,K)
      B(I)=B(I)-C*BN
      A(N,L)=C
100   CONTINUE
C
C   BACK SUBSTITUTE
C
      I=NN
C
      B(NN)=B(NN)/A(NN,1)
      DO 600 N=1,NM
      I=I-1
      IF (N.LT.MM)      MR= N+1
      DO 600 J=2,MR
      K=I+J-1
600   B(I) =B(I)- A(I,J)*B(K)
      DO 650 N=1,NN
  650 NODNO(N)=1+(N-1)/2
      WRITE(6,2001)  (NODNO(I),B(I),I=1,NN)
 2001 FORMAT('1',  '  NODAL DISPLACEMENTS  ' ,//
```

```
      1'   NODE',11X,'U',6X,'NODE',11X,'V'//
      22(I6,E15.5))
       RETURN
700    WRITE (6,2000) N
       CALL EXIT
 2000 FORMAT(1H0,'ZERO OR NEGATIVE ELEMENT ON MAIN DIA
      1GONAL OF TRIANGULARIZED MATRIX FOR EQUA
      2TION',I5)
C
       END
```

```
      SUBROUTINE MODIFY (I,N)
C
C  THIS SUBROUTINE MODIFIES KSTIF AND AP IF A
C  DISPLACEMENT BOUNDARY CONDITION IS IMPOSED IN
C  EQUATION I ASSOCIATED WITH NODAL POINT N
C
      COMMON ER(8),ET(8),EZ(8),PRRT(8),PRRZ(8),PRTZ(8),
     1 Z(400),U(400),V(400),ISODIM(8),STIF(800,80)
      COMMON ECM(4,4),EBM(4,8),ESM(4,8),WT,NUMNP,NUMEL,
     1 NP(4,400),MAT(400),NEQ,MBAND,M,LM(8)
      COMMON RCHAR,ZCHAR,SZCHAR,SRCHAR,STCHAR,TUCHAR,
     1 RR(400),ZR(400),SIGZO(400),SIGRO(400),SIGTO(400)
      COMMON RO(8),R(400),AP(800),ESTIF(8,8),
     1NUMAT,KODE(400),SIGRZO(400)
C
      DISP=U(N)
      IF((I-2*N).EQ.0)   DISP=V(N)
C
      DO 50 J=2,MBAND
      IL=I+J-1
      IU=I-J+1
      IF(IU.LE.0)GO TO 10
      AP(IU)=AP(IU) - STIF(IU,J)*DISP
       STIF(IU ,J)=0.0
10    IF(IL.GT.NEQ) GO TO 50
      AP(IL)= AP(IL)- STIF(I,J)*DISP
       STIF(I,J)=0.0
50    CONTINUE
      AP(I)=DISP
       STIF(I,1)=1.0
      RETURN
      END
```

```
      SUBROUTINE STRESS
C
C  THIS SUBROUTINE FORMS THE LEMENT STRESS MATRIX
C  (ESM), MUITIPLIES BY THE ELEMENT DISPLACEMENT
C  VECTOR (ELDISP) AND RECORDS THE STRESSES IN
C  SIGEL. IT THEN COMPUTES THE PRINCIPAL STRESSES
C  AND DIRECTIONS(SIGP)
C
      COMMON ER(8),ET(8),EZ(8),PRRT(8),PRRZ(8),PRTZ(8),
     1 Z(400),U(400),V(400),ISODIM(8),STIF(800,80)
      COMMON ECM(4,4),EBM(4,8),ESM(4,8),WT,NUMNP,NUMEL,
     1 NP(4,400),MAT(400),NEQ,MBAND,M,LM(8)
      COMMON ECHAR,ZCHAR,SZCHAR,SRCHAR,STCHAR,TUCHAR,
     1 RR(400),ZR(400),SIGZO(400),SIGRO(400),SIGTO(400)
      COMMON RO(8),R(400),AP(800),ESTIF(8,8),
     1NUMAT,KODE(400),SIGRZO(400)
C
      DIMENSION SIGEL(400,4),SIGP(400,7),ELDISP(8),
     1SIGA(400,4),KOUNT(400)
      COMMON/BETTER/ RT(4),ZT(4),FIJ(4,4),DJ,RAD,
     1ESMRC(4,8)
      COMMON/SLOP/WP(800),NCW
C
C   ZERO'S SIGEL,KOUNT & SIGA
C
      DO 1 I=1,NUMEL
      DO 1 J=1,4
    1 SIGEL(I,J)=0.
      DO 5 N=1,NUMNP
      KOUNT(N)=0
      DO 5 J=1,4
5     SIGA(N,J)=0.0
C
      DO  15 M=1,NUMEL
C   COMPUTE ELEMENT DISPLACEMENTS
C
      DO 10 I=1,4
      J=NP(I,M)
      ELDISP(I)=AP(2*J-1)
      ELDISP(I+4)=AP(2*J)
      KOUNT(J)=KOUNT(J)+1
      RT(I)=R(J)
   10 ZT(I)=Z(J)
      DO 15 K=1,4
      L=NP(K,M)
      EPS=FLOAT(-1+2*(K/2-2*(K/4)))
      PNU=FLOAT(-1+2*(K/3))
      CALL BETA(EPS,PNU)
      DO 15 I=1,4
C
C  ACCUMULATE FOR NODAL STRESSES
C
      DO 15 J=1,8
   15 SIGA(L,I)=SIGA(L,I)+ESM(I,J)*ELDISP(J)
```

```
C
C  FIND AVERAGE NODAL STRESSES
C
      DO 110 N=1,NUMNP
      RK=KOUNT(N)
      DO 110 I=1,4
110   SIGA(N,I)= SIGA(N,I)/RK
C
C  COMPUTE  ELEMENT STRESSES
      DO 16 M=1,NUMEL
      DO 16 K=1,4
      L=NP(K,M)
      DO 16 I=1,4
   16 SIGEL(M,I)=SIGEL(M,I)+SIGA(L,I)/4.
C
C  COMPUTE ELEMENT PRINCIPAL STRESSES  AND DIRECTIONS
C
      DO 100 M=1,NUMEL
      SIGM=(SIGEL(M,1)+SIGEL(M,2))/2.
      SIGD2=(SIGEL(M,1)-SIGEL(M,2))/2.
      RAD = SQRT(SIGD2**2 +SIGEL(M,4)**2)
      SIGP(M,1)=SIGM+RAD
      SIGP(M,2)= SIGM-RAD
      SIGP(M,3)=SIGEL(M,3)
      SIGP(M,4)=(SIGP(M,2)-SIGP(M,3))/2.
      SIGP(M,5)=(SIGP(M,1)-SIGP(M,3))/2.
      SIGP(M,6)=(SIGP(M,1)-SIGP(M,2))/2.
      SIGP(M,7)=0.5*57.29578*ATAN2(SIGEL(M,4),SIGD2)
100   CONTINUE
C
C
C   FIND  MAXIMUM  ELEMENT STRESSES
C
      SIG1=SIGP(1,1)
      SIG2=SIGP(1,2)
      SIG3=SIGP(1,3)
      SIG4=SIGP(1,4)
      SIG5=SIGP(1,5)
      SIG6=SIGP(1,6)
      M1=0
      M2=0
      M3=0
      M4=0
      M5=0
      M6=0
      DO 145 M=1,NUMEL
      IF (SIGP(M,1).LT.SIG1) GO TO 115
      SIG1=SIGP(M,1)
      M1=M
115   IF (SIGP(M,2).GT.SIG2) GO TO 120
      SIG2=SIGP(M,2)
      M2=M
120   IF (SIGP(M,3).LT.SIG3) GO TO 130
      SIG3=SIGP(M,3)
```

```
      M3=M
 130  IF (SIGP(M,4).LT.SIG4) GO TO 135
      SIG4=SIGP(M,4)
      M4=M
 135  IF (SIGP(M,5).LT.SIG5) GO TO 141
      SIG5=SIGP(M,5)
      M5=M
 141  IF (SIGP(M,6).LT.SIG6) GO TO 145
      SIG6=SIGP(M,6)
      M6=M
  145 CONTINUE
C  FIND CHARACTERISTIC NODAL VALUES
      DO 300 N=1,NUMNP
      RR(N)=R(N)/RCHAR
      ZR(N)=Z(N)/ZCHAR
      SIGZO(N)=SIGA(N,1)/SZCHAR
      SIGRO(N)=SIGA(N,2)/SRCHAR
      SIGTO(N)=SIGA(N,3)/STCHAR
      SIGRZO(N)=SIGA(N,4)/TUCHAR
 300  CONTINUE
      WRITE(6,2000)
      WRITE(6,2010)  (M,(SIGEL(M,I)  ,I=1,4),M=1,NUMEL)
      WRITE(6,2020)
      WRITE(6,2030)  (M,(SIGP (M,I)  ,I=1,7),M=1,NUMEL)
      WRITE(6,2040)SIG1,M1,SIG2,M2,SIG3,M3,SIG4,M4,
     1SIG5,M5,SIG6,M6
      WRITE(6,2050)
      WRITE(6,2010)  (N,(SIGA(N,I),I=1,4),N=1,NUMNP)
      WRITE(6,3010)
      WRITE(6,3020)  (N,RR(N),ZR(N),SIGZO(N),SIGRO(N),
     1SIGTO(N),SIGRZO(N),N=1,NUMNP)
 3010 FORMAT(1H1, 'AVERAGE CHARACTERISTIC NODAL VALUES'
     1///1X,'NODE    R CH.       Z CH.     SIGMA Z C
     2H.   SIGMA R CH.        SIGMA T CH.    SIGMA R
     3Z CH.'//)
 3020 FORMAT (I4,6F12.6)
 2000 FORMAT(1H1,10X, 21H R-Z ELEMENT STRESSES ///
     11X,'ELEM      SIGMA Z      SIGMA R      SIGMA T
     2  SIGMA RZ'//)
 2010 FORMAT(I4,F11.6,3F12.6)
 2020 FORMAT(1H1,10X,'ELEMENT PRINCIPAL STRESSES'///
     11X,'ELEM      SIGMA I       SIGMA II      SIGMA II
     2      SIGMA III       TAU RZ      TAU RT      TAU TZ
     3      SIGMA I DEG'//)
2030  FORMAT(I4,F11.6,5F12.6, F14.3)
 2040 FORMAT(1H1,'MAXIMUM PRINCIPAL STRESSES IN RZ PL
     1ANE= ',F11.6,' AND OCCURS IN ELEM',I6//' MINIMU
     1M PRINCIPAL STRESS IN RZ PL
     2ANE= ',F11.6,' AND OCCURS IN ELEM',I6//' MAXIMU
     3M HOOP STRESS =',F11.6,' AND OCCURS IN ELEM',I6/
     4/' MAXIMUM TAU RZ =',F11.6,' AND OCCURS IN ELEM'
     5,I6//' MAXIMUM TAU RT =',F11.6,' AND OCCURS IN E
     6LEM',I6//' MAXIMUM TAU TZ =',F11.6,' AND OCCUR
     7S IN ELEM',I6//)
```

```
2050 FORMAT (1H1, 'AVERAGE NODAL STRESSES '///
    1'NODE     SIGMA Z     SIGMA R     SIGMA T     SI
    2GMA RZ'//)
     WRITE (6,2060)
2060 FORMAT ('0','REACTICN CORRECTION AT NODES DUE T
    1O WEIGHT')
     IF (NCW.EQ.0) GO TC 150
     WRITE (6,2070)
2070 FORMAT (T10,'NODE',T20,'CORRECTION',//)
     I=0
     DO 140 N=1,NUMNP
     NN=2*N
     IF (WP(NN).EQ.0.0) GO TO 140
     WRITE (6,2080)N,WP(NN)
2080 FORMAT (T11,I3,T23,F10.4)
     I=I+1
     IF (I.GE.NCW) RETURN
 140 CONTINUE
 150 WRITE (6,2090)
2090 FORMAT ('NONE')
     RETURN
     END
```